Aus der Klinik für Kieferorthopädie und Orthodontie des
Zentrums für Zahn-, Mund- und Kieferheilkunde
des Universitätsklinikums Ulm
Ärztlicher Direktor: Prof. Dr. Dr. B. Lapatki

Topographical Characterization of the Midfacial Musculature Revealed by Means of High-Density Surface Electromyography

Dissertation
Zur
Erlangung des Doktorgrades der Zahnmedizin
der Medizinischen Fakultät der Universität Ulm

Alisa Barth
geboren in Aalen

2016

Amtierender Dekan: Prof. Dr. Thomas Wirth
1. Berichterstatter: Prof. Dr. Dr. Bernd Lapatki
2. Berichterstatter: Prof. Dr. Elmar Pinkhardt
Tag der Promotion: 19.10.2017

Contents

Contents I
Abbreviations III
1 Introduction 1
1.1 Specific Characteristics of Facial Muscles 2
1.2 Functional Anatomy of Midfacial Muscles 3
1.2.1 M. orbicularis oculi 4
1.2.2 Buccolabial muscles 5
1.2.3 The Modiolus 14
1.3 High-density Surface Electromyography 16
1.4 Application of botulinum neurotoxin in the midface 19
1.5 Study Goals and Hypothesis 21
2 Materials and Methods 22
2.1 Electrode grids 22
2.2 Data acquisition 25
2.3 Recording procedure 26
2.4 Data analysis 26
2.5 Data selection 27
2.6 Location of motor end plates, fiber orientation, motor unit size 28
2.7 Normalisation 31
2.8 Assignment of decomposed MUs to certain facial muscles 33
3 Results 35
3.1 Co-activation of MUs in attempted selective muscle contractions 35
3.2 Occurrence of muscle subcomponents and muscle classification 36
3.3 Motor endplates and muscle fiber orientations of the complete midfacial musculature 38
3.4 Motor endplate location and muscle fiber direction of individual muscle subcomponents 40
3.4.1 Orbicularis oculi muscle 40
3.4.2 Zygomaticus major muscle 44
3.4.3 Zygomaticus minor muscle 48

3.4.4 Levator labii superioris muscle 53
3.4.5 Levator labii superioris alaeque nasi muscle 57
3.4.6 Buccinator muscle 61
3.4.7 Levator anguli oris 65
3.4.8 Incisivus muscle 69
3.4.9 Orbicularis oris muscle pars marginalis 73
3.4.10 Orbicularis oris muscle pars peripheralis 76
3.4.11 Orbicularis oris muscle pars tangentialis 80
3.4.12 Nasalis muscle 84
3.5 Motor unit sizes 85
4 Discussion 86
4.1 Recording technique 86
4.2 Data analysis 88
4.3 Discussion of results 89
4.4 Conclusion 96
5 Summary 97
6 Bibliography 99
Appendix 105
Curriculum vitae 121

Abbreviations

AP	Action potential
BUC	Buccinator muscle
BoNT	Botulinum neurotoxin
BoNT-A	Botulinum neurotoxin A
CKC	Convolution kernel compensation
HDsEMG	High-density surface electromyography
IED	Inter-electrode distance
INC	Incisivus muscle
LAO	Levator anguli oris muscle
LLS	Levator labii superioris muscle
LLSan	Levator labii superioris alaeque nasi muscle
NAS	Nasalis muscle
mar	Marginal part of orbicularis oris muscle
MEP	Motor endplate
MU	Motor unit
MUAP	Motor unit action potential
MVC	Maximal voluntary contraction
OOC	Orbicularis oculi muscle
OOR	Orbicularis oris muscle
OORmar	Orbicularis oris muscle pars marginalis
OORper	Orbicularis oris muscle pars peripheralis
OORtan	Orbicularis oris muscle pars tangentialis
per	Peripheral part of orbicularis oris muscle
RIS	Risorius muscle
sEMG	Surface electromyography
sMUP	Surface motor unit potential
tan	Tangential fibers of orbicularis oris muscle
ZYGmaj	Zygomaticus major muscle
ZYGmin	Zygomaticus minor muscle

1 Introduction

The facial muscles are a highly complex muscle system, in which its subcomponents are controlled independently. It not only ensures the sense organs' accurate function or contributes to speech production, but also mediates emotions and is therefore essential for social interactions. Pathological alterations that cause limitations in this sensitive area are particularly detrimental to the individual. In terms of advancing examination methods and (non-)surgical therapies, e.g. the application of botulinum neurotoxin, well-founded anatomical and neurophysiologic knowledge of the facial muscles is crucial. A motor unit is the smallest functional unit of a muscle. It is defined as a single motor neuron and its associated muscle fibers innervated by this motor neuron.

High-density surface electromyography (HDsEMG) provides a non-invasive method to gain anatomical and topographical information on a motor unit level. Placing the highly flexible multi-electrode arrays over the muscle allows obtaining temporal and spatial information such as motor endplate location, fiber orientation and motor unit size. Combining the electrophysiological results with the placement of the electrode grids allows topographical mapping and description of the anatomical information relative to facial landmarks. The method of HDsEMG has already been successfully applied to the upper, lower and midfacial musculature (Neubert 2016; Lapatki et al. 2006; Matt 2013).

This study's aim is to gain again more topographical information of the midfacial musculature on a motor unit level by the use of an altered electrode setup to cover more midfacial muscles and to map these results in mean faces. This allows critical comparison with previous HDsEMG studies, as well as anatomical and histological studies.

1.1 Specific Characteristics of Facial Muscles

The facial muscles are innervated by branches of the facial nerve which originates from the second pharyngeal arch. They are characterized as skeletal muscles, hence they are striated muscles. Yet, their organization differs from other skeletal muscles.

They are flat, straplike muscle sheets and muscle bundles in the subcutaneous adipose tissue and are neither enveloped by a fascia nor have typical muscle bellies or muscle spindles (Happak et al. 1997; May et al. 1999). Facial muscles have a non-tendinous attachment to soft tissue, i.e. the facial skin, mucosa or other muscle tissue and mostly arise from bone (Standring et al. 2008). They show interdigitation and overlap in relatively small areas and show a remarkably high inter- and intra-individual variability in both location and morphology of the muscles (Happak et al. 1997; Freilinger et al. 1990; Ito et al. 2006; Stal et al. 1990).

On a motor unit level, facial muscles' endplates are to be found in round or oval-shaped cluster-like arrangements, varying in size and therefore also referred to as 'motor zones'. They are evenly distributed over the muscle or located in eccentric position (Lapatki et al. 2006; Happak et al. 1997). A great number of facial muscle fibers were identified bearing more than one motor end plate within a distance of up to 500µm, whereas the skeletal muscles usually have one motor end plate (Standring et al. 2008; Happak et al. 1997). These characteristics resemble those of different laryngeal muscles (Happak et al. 1997; Rossi et al. 1965). Therefore, the unique innervation pattern of facial muscles appears to be common among several muscles stemming from branchial arches, i.e. here the second branchial arch.

In the following subitems, functional anatomy of those individual facial muscles investigated in this study is explained. This information is required as basis for the results and discussion sections.

1.2 Functional Anatomy of Midfacial Muscles

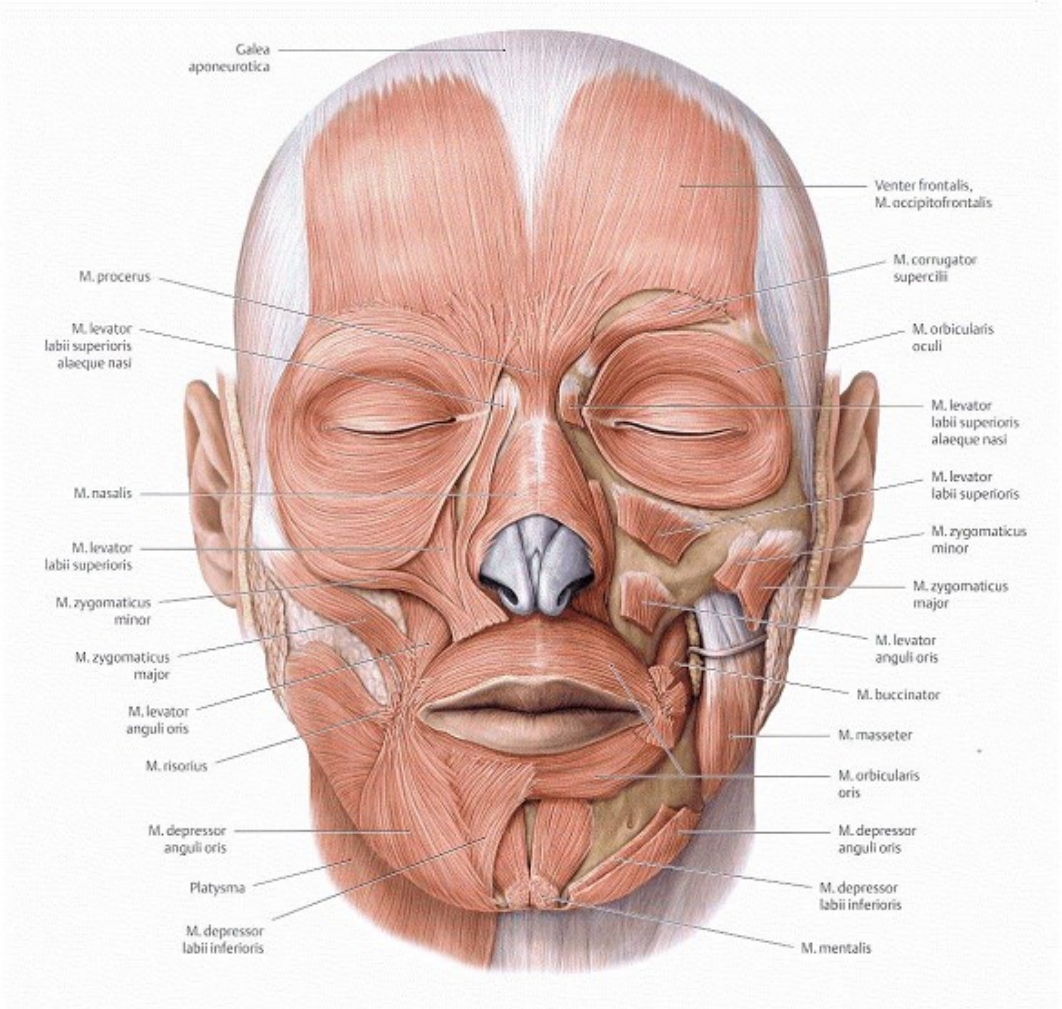


Figure 1: Frontal overview of the complete facial musulature (Reprinted from Schünke M, Schulte E, Schumacher U: 3. Sytematik der Muskulatur. Prometheus Kopf, Hals und Neuroanatomie, 2: 62-65 Copyright 2009, with permission from Thieme)

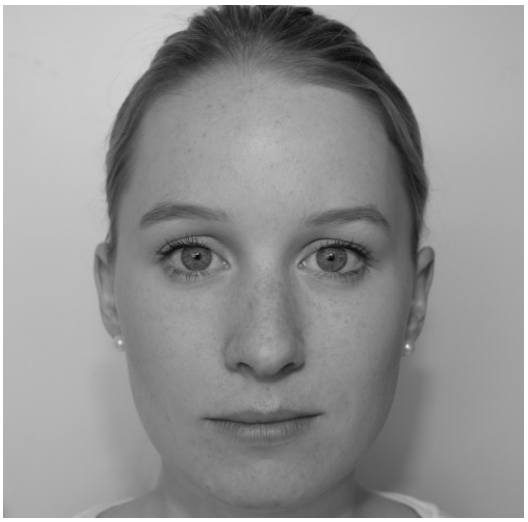


Figure 2: Face at rest.

1.2.1 M. orbicularis oculi

Orbicularis oculi (OOC) is a broad, flat, elliptical muscle that surrounds the circumference of the orbit and spreads into the adjacent region of the eyelids and surrounding skin area. It adapts to the orbit and eyelids. It has orbital, palpebral and lacrimal parts (Benninghoff et al. 2008; Standring et al. 2008).

The orbital portion arises from the anterior lacrimal crest and the medial palpebral ligament. The fibres form complete ellipses without interruption on the lateral side, where there is no bony attachment, and blend with neighbouring muscles (Benninghoff et al. 2008; Standring et al. 2008).

The palpebral portion is located under the thin, fatless skin of the eyelid. Its fibres mainly arise from the medial palpebral ligament, sweep across the eyelids, and interlace at the lateral commisure to form the lateral palpebral raphe (Benninghoff et al. 2008; Standring et al. 2008).

The lacrimal portion is seen as a small, rectangular segment of the palpebral part, also referred to as Horner's muscle. Its function is to aid in drainage of tears by dilatating the lacrimal sac or maintaining the thickness of tear film over the cornea (Benninghoff et al. 2008; Shinohara et al. 2001)

Orbital and palpebral parts of the OOC can be contracted separately. Contraction of the palpebral part closes the lid. However, contraction of the orbital part causes eye closure, which is mainly affected by raising the lower lid and drawing the skin of the temple, forehead and infraorbital area together with the upper and lower lids medially (Benninghoff et al. 2008; Standring et al. 2008; Aumüller et al. 2010; Lapatki 2010).

OOC is innervated by temporal, zygomatic and buccal braches of the facial nerve. The temporal branch is located under the temporoparietal fascia above the zygomatic arch and divides into two to 4 braches running into the upper OOC. The branches run horizontally along the fibres of the OOC. Zygomatic and buccal branches run into the lower OOC. Buccal branches innervate the medial portion of the lower OOC, zygomatic branches innervate the middle and lateral portion, approaching the muscle at a right angle (Hwang 2014).



Figure 3: Bilateral orbicularis oculi muscle pars orbitalis contraction

1.2.2 Buccolabial muscles

The buccolabial muscles are complexly assembled in a three-dimensional way to control the shape of the mouth and the posture of the lips. From a functional point of view, the buccolabial muscles can be divided into three groups, whereof two are located in the midface. The retractors of the upper lip are the levator labii superioris muscle (LLS), the levator labii superioris alaeque nasi muscle (LLSan) and the zygomaticus minor muscle (ZYGmin). Muscles that converge towards the corners of the mouth constitute the other group, which is made up of the levator anguli oris muscle (LAO), zygomaticus major muscle (ZYGmaj), buccinator muscle (BUC), incisivus labii superioris and inferioris muscle (INC), orbicularis oris superior and inferiors muscle (OOR) and depressor anguli oris muscle. This groups' function is to close and seal the oral commisure and causes the two-dimensional displacement of the modiolus (Standring et al. 2008; Lapatki 2010).

1.2.2.1 Zygomaticus major muscle

The zygomaticus major muscle (ZYGmaj) is a typical risible muscle and plays an important role in the facial expression. From its origin anterior to the zygomaticotemporal suture within the subzygomatic fossa, ZYGmaj passes in medio-inferior direction to the modiolus (Miller et al. 2007). There, it blends with

other muscles such as LAO, BUC, OOR, RIS and the depressor anguli oris muscle (Shim et al. 2008). ZYGmaj is usually represented as a single muscle band, however the anatomic variant of a bifid ZYGmaj is described. The bifid ZYGmaj originates from the zygomatic bone as a single muscular band and divides into superior and inferior fibers at the infrazygomatic region superficial to the buccal fat pad (Pessa et al. 1998a; Hu et al. 2008) . In case of a bifid ZYGmaj, the superior muscle fibers are described to be larger and wider than the inferior fibers and insert into the modiolar region. However, the inferior muscle fibers are described to run with the superficial or deep fibers of the depressor anguli oris muscle or tether the overlaying skin and to insert into the inferior to the modiolar region (Hu et al. 2008; Pessa et al. 1998b). ZYGmaj is innervated from its deep surface by two to four branches of the zygomatic arch of the facial nerve (Happak et al. 1997).

The ZYGmaj draws the angle of the mouth upwards and laterally, as in laughing. When contracted, in some individuals the lower portion of the upper incisors and the canine and in some cases also the buccal teeth of the corresponding side may become visible. Contraction of the ZYGmaj muscle creates a modification of the lateral portion of the nasolabial fold and also vertical, arched wrinkles on the cheek. Isolated contraction of ZYGmaj is indicated by missing evertion of the upper lip's lateral portion, which would be performed by the zygomaticus minor. It can also be demonstrated by an absence of a dimple lateral to the corner of the mouth, which would be caused by activation of BUC (Benninghoff et al. 2008; Standring et al. 2008; Lapatki 2010).



Figure 4: Right zygomaticus major muscle contraction

1.2.2.2 Zygomaticus minor muscle

The zygomaticus minor (ZYGmin) emanates from the OOC and lies medial to ZYGmaj. It arises from the lateral surface of the zygomatic bone, where it is still part of the OOC and passes downwards and medially into the muscular substance of the upper lip (Aumüller et al. 2010). It is innervated from its deep surface by two to four branches of the zygomatic arch of the facial nerve (Happak et al. 1997). ZYGmin is described to have an inconstancy in its occurrence and to be highly variable in its size (Pessa et al. 1998a; Waller et al. 2008). Contraction of the ZYGmin elevates and everts only the lateral portion of the upper lip, as well as maintains the convex curvature of the nasolabial furrow (Benninghoff et al. 2008; Standring et al. 2008; Lapatki 2010).

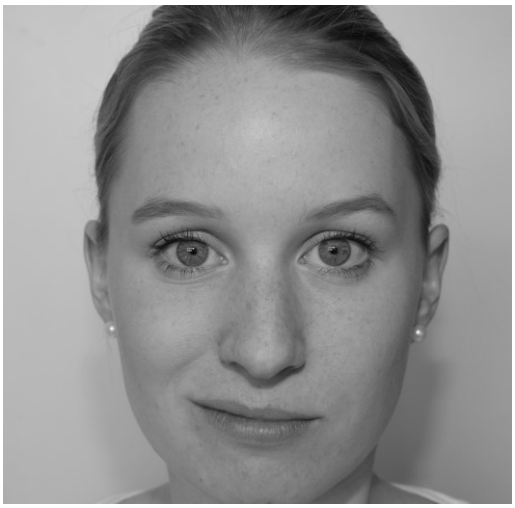


Figure 5: Right zygomaticus minor muscle contraction

1.2.2.3 Levator labii superioris and levator labii superioris alaeque nasi muscle

The levator labii superioris (LLS) muscle arises from the maxilla and zygomatic bone above the infraorbital foramen (inferior orbital margin).The levator labii superioris alaeque nasi (LLS an) muscle arises from the upper part of the frontal process of the maxilla. As both muscles' fibres pass downwards, they blend with ZYG min and converge into the muscular substance of the upper lip.

Their common action is to raise and evert the upper lip and to elevate the side of the nose. Consequently, the upper lip adopts a rectangular shape and the upper frontal teeth become visible. Furthermore, these muscles increase the curvature of the top of the nasolabial furrow and deepen both the nasolabial and inferior tarsal furrow (Standring et al. 2008; Lapatki 2010).
Due to the common insertion of ZYG min, LLS and LLS an in the upper lip, these three muscles are often referred to as one muscle, the quadratus labii superioris.
Contraction of the quadratus labii superioris usually shows co-activation of the OOR, which can be observed by absent separation of the upper and lower lips (Lapatki 2010).

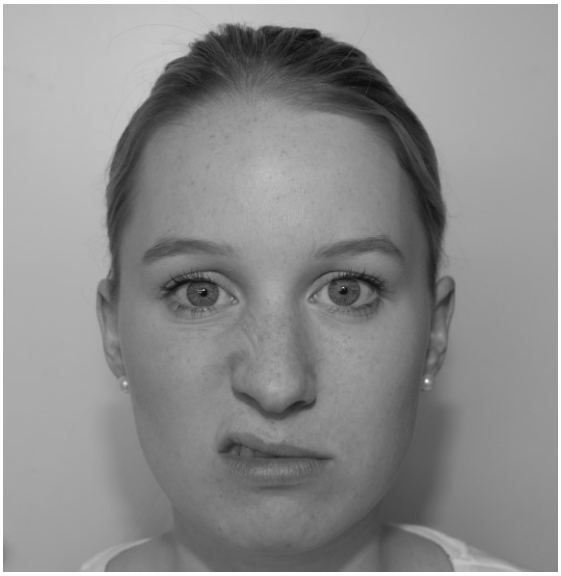


Figure 6: Right levator labii superioris and levator labii superioris alaeque nasi muscle contraction.

1.2.2.4 Levator anguli oris muscle

The relatively deeply located levator anguli oris (LAO) arises from the canine fossa of the maxilla just below the infraorbital foramen. Covered by LLS, it runs in latero-inferior direction to enter the modiolus. At the modiolus its fibers blend with fibers of ZYGmaj, OOR, RIS, BUC and the depressor anguli oris muscle. The LAO is innervated by terminal buccal branches of the facial nerve. When contracted, the angle of the mouth is slightly elevated and displaced in medial

direction. In addition, the lateral portion of the upper lip is compressed and bulges in a characteristic manner (Benninghoff et al. 2008; Lapatki 2010; Ewart et al. 2005).

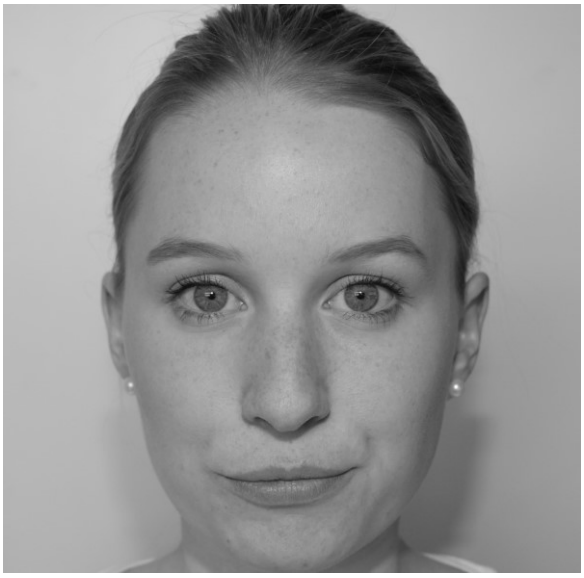


Figure 7: Bilateral levator anguli oris muscle contraction

1.2.2.5 Buccinator muscle

The buccinator muscle (BUC) is located deeply. It arises from the outer surfaces of the alveolar processes of the maxilla and mandible, respectively opposite the molar teeth. Its posterior border is attached to the anterior margin of the pterygomandibular raphe. The main part of its fibres converges to a plate towards the modiolus. Its deep, i.e. oral fibres are attached to the mucous membrane of the cheeks which can be regarded as a site of insertion for these fibres (Standring et al. 2008; Lapatki 2010). BUC is innervated by numerous buccal branches of the facial nerve from its superficial surface (Happak et al. 1997).

Contraction of BUC results in the characteristic corn-shaped dimple lateral to the corner of the mouth. Thereby, the deep portion of the modiolus and the submucosa in this area is dragged laterally. A lack of this dimple occurs if the corner of the mouth is only drawn laterally by the ZYGmaj. Isolated contraction of BUC creates an ‘artificial smile’.

Moreover, contraction is important during mastication as it compresses the cheek against the teeth and gums to assist the tongue in directing food between the teeth. As the mouth closes, the buccolabial mucosa must be retracted progressively from the occlusal surfaces. If the cheeks have been distended with air, buccinators contraction expels the air between the lips. The latter accounts for its name as ‘buccinator’ is latin and means ‘trumpeter’ (Benninghoff et al. 2008; Standring et al. 2008; Lapatki 2010).

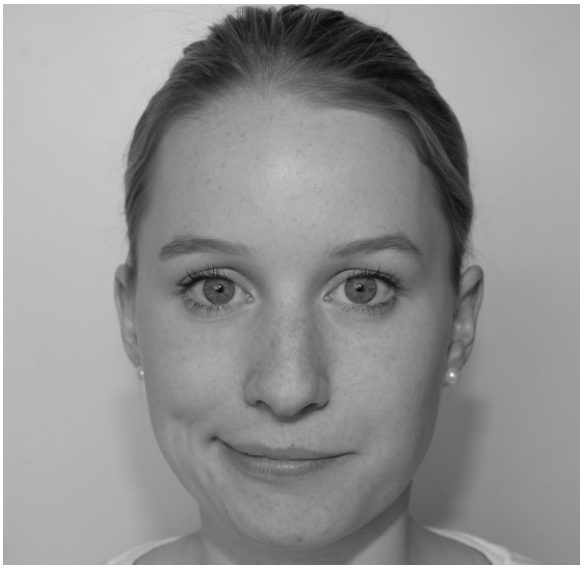


Figure 8: Right buccinator muscle contraction

1.2.2.6 Orbicularis oris muscle

The orbicularis oris muscle (OOR) is the muscular basis for the lips. It is a complex of muscles and not a real sphincter. It consists of four substantially independent quadrants (upper, lower, left and right) each of which contains a peripheral part and a marginal part. Each part is attached to the modiolus and continues similar to a fan towards the facial midline (oriented parallel to the vermilion zone). There it crosses some millimeteres into the contralateral segment. At this point the fibres from the two sides interlace on their way to their dermal insertions, creating the ridges of the philtrum on the upper lip and the less marked corresponding depression in the lower lip. OOR is innervated from its lateral side by two terminal nerve branches of the facial nerve, i.e. the lower buccal and marginal mandibular branch (Happak et al. 1997).

The peripheral parts of the upper and lower orbicularis oris muscles (OORper) reach the nasal septum and accordingly the mentolabial fold, and lie close to and parallel with the inner mucosal surface of the lip.

The marginal part (OORmar) is developed to a unique extent in human lips and closely related to speech and the production of musical tones. In every quadrant, it occupies the core of the red lip, therefore also curling outward, and even extends the vermillion zone a few millimetres (Hwang et al. 2007).

Furthermore, there are also non-horizontal, i.e. tangential, fibres (OORtan) that pass between the horizontal bundles to their submucosal attachments. The tangential fibers originate either outside the lips or attach to the hairy skin of the lips. They run diagonally trough the vermilion part of the lips from the hairy epidermis adjacent to the outer vermilion border towards the inner part of the vermilion. They probably belong to the retractors of the upper and lower lip (Blair 1986).

Contraction of OOR can cause a wide range of actions. Contraction of only OORmar closes the lips by pressing the upper and lower red lips toward each other and narrows the red-lips, too. The OORtan tightens the lips into a narrower, wedge-shaped profile as the marginal part is flattened and slightly tilted forward.

Going from this position, additional contraction of OORper can tilt the marginal lip portions partly back. Contraction of all OOR fibre groups together produces a high tonus in the whole labial area. It inverts the red-lips and presses the lips towards each other and against the frontal teeth (Benninghoff et al. 2008; Standring et al. 2008; Lapatki 2010)

A



B



C



Figure 9: Bilateral, selective contraction of the different fiber groups of the orbicularis oris muscle. Pars marginalis (A), pars tangentialis (B), pars tangentialis and peripheralis (C)

1.2.2.7 Incisivus labii superioris and inferioris muscle

The incisivus labii superioris and inferioris (INC) are mentioned rarely in literature. INC are considered as a part of the oral orbicular complex and therefore subdivided in four quadrants as OOR.

The incisivus labii superioris arises from the bony floor of the incisive fossa of the maxilla just above the eminence of the lateral incisor tooth. Initially, it lies deep to the OORper sup. In their course towards the modiolus, the fibres intermingle with and become part of the horizontal fibres of the OOR.

The incisivus labii inferioris has its osseous attachment on the floor of the incisive fossa of the mandible, lateral to mentalis and below the eminence of the lateral incisor tooth. Just as the incisivus labii superioris fibres, the fibres of the incisivus labii inferioris become part of the horizontal fibres of the OOR on their way to the modiolus (Standring et al. 2008; Lapatki 2010).

Simultaneous action of the four INC moves the corner of the mouth against each other and rounds the marginal lip portion as in whistling and is therefore the counterpart of BUC.

Differential action of the four INC allows them to change the orientation of the lip line (Lapatki 2010).

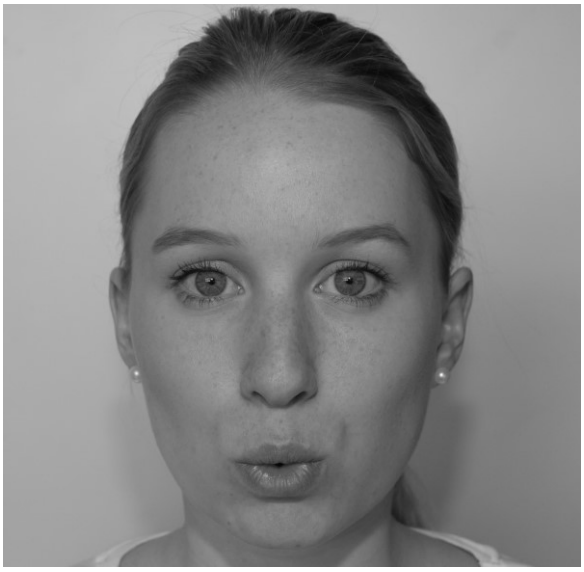


Figure 10: Bilateral incisivus muscle contraction

1.2.2.8 Risorius muscle

The risorius muscle (RIS) is a highly variable muscle. It ranges from one or more slender fascicles to a wide, thin superficial fan. RIS is only present in a small minority of individuals and is discussed to be the mere extension of the platysma (Pessa et al. 1998a; Waller et al. 2008; Ewart et al. 2005).
The pattern of RIS origination varies. RIS can originate from the superficial musculoaponeurotic system (SMAS) layer, the parotid-masseteric fascia or the masseter tendon and inserts into the modiolus (Bae et al. 2014).
Contraction of RIS pulls the corner of the mouth laterally in facial actions as grinning and laughing and creates the so-called dimples (Benninghoff et al. 2008; Standring et al. 2008)

1.2.2.9 Nasalis muscle

The nasalis muscle (NAS) consists of a transverse part and an alar part and is innervated by buccal branches of the facial nerve. The transverse part arises from the maxilla lateral to the canine and has its onset on the bridge of the nose. The alar part arises from the maxilla above the lateral incisor and continues to its onset on the ala of the nose. The transverse part pulls the tip of the nose caudally and compresses the nostrils. Its antagonist, i.e. the alar part, expands the nostrils (Aumüller et al. 2010).

1.2.3 The Modiolus

The modiolus is a muscular-tendinous node that lies just lateral the corners of the mouth. It has no precise histological boundaries as it is an irregular zone where dense, compact interlacing tissue grades into the stems of individually recognizable muscles. The modiolus has the form of a blunt cone. Its base is adjacent and adherent to the mucosa. It is kidney-shaped, with the buccal angle projecting towards the hilum. The blunt apex of the cone is located lateral to the buccal angle. At least nine muscles, depending on the classification employed,

are attached to each modiolus. Activities may be divided into three phases. At first, a particular modiolar muscle group becomes dominant over its antagonists and the modiolus is rapidly relocated. Next, the modiolus is transiently fixed in this new site by simultaneous contraction of the modiolar muscles and therefore provides a fixed base from which the main effectors, buccinators and OOR, carry out their specific actions. Modiolar movement may be bilaterally symmetrical, unilateral or asymmetrical (Standring et al. 2008).

1.3 High-density Surface Electromyography

Electromyography is a technique for evaluating and recording the electrical activity produced by the skeletal muscles. An electromyograph detects the electrical potential generated by muscle cells when these cells are electrically or neurologically activated. Surface EMG (sEMG) is a non-invasive method to measure the electrical activity of muscle fibers through the intact skin and thereby gain topographical information on a motor unit level. A motor unit is defined as a single alpha motor neuron and its associated muscle fibers. It is the smallest functional unit of a muscle.

Basic to all sEMG measurements is the determination of the voltage difference between two surface electrodes (Zwarts et al. 2004). The EMG signal is the summation of all of a MU's muscle fiber action potential, i.e. a motor unit action potential (MUAP). Different derivations or montages can be distinguished. In case of a monopolar recording, one electrode is far away from the target muscle. A classic configuration is placing two nearby electrodes over the muscle, which results in a bipolar recording. 'Higher order' derivations can be achieved when combining the activity of one electrode with that of one or several surrounding electrodes close to the muscle (Merletti et al. 1999; Disselhorst-Klug et al. 1997; Broman et al. 1985; van Vugt et al. 2001). The resulting effect is always a 'spatial high pass filtering', which gives a narrowing of the spatial view. The exact montage to be used depends on the clinical or research question. The higher the derivation's order and the smaller the inter-electrode distances (IED), the smaller becomes the recording area of the electrodes. Furthermore, bipolar or higher order montages and a short IED cause suppression of cross-talk between muscles and of far-field activity originating from the start and extinction of the action potential (Zwarts et al. 2003; Broman et al. 1985).

To gain topographical information about the distribution of the EMG activity over a muscle, the number of electrodes in sEMG (multichannel sEMG) has to be increased. When arranging several bipolar recording electrodes in line, a linear array results (Farina et al. 2000; Masuda et al. 1986). This arrangement enables the measurement of sarcolemmal propagation by comparing the time delay of the consecutive signals, if the electrodes are aligned with muscle fiber direction

(Figure 11 B). This gives access to the first spatial properties of the motor unit potential (MUP): its origin at the endplate zone, its propagation along the sarcolemma and its extinction at the tendon. In bipolar derivations the endplate zone is characterized by a phase reversal of the signal and often by low amplitude if one electrode is approximately above the endplate zone. However, in monopolar derivations the electrode with the highest amplitude indicates the endplate location.

Positioning the bipolar recording electrodes perpendicular to muscle fiber direction allows distinguishing different motor units better. As shown in Figure 11 A, the sEMG amplitude changes in medial-lateral direction and no propagation can be observed. The surface motor unit potential (sMUP) peaks from different MUs have their maximum at different medial-lateral positions, which indicates a spatial spread of MUs (Kleine et al. 2000). The center of a MU is located where the highest sMUP amplitude is detected. The potential decreases with increasing distance between the electrode and the bioelectric source (Zwarts et al. 2003).

Decomposition of HDsEMG signal allows single MU analysis in terms of MU endplate position, fiber direction and length, MU depth and firing pattern (Lapatki et al. 2006; Roeleveld et al. 2002; Lapatki et al. 2004).

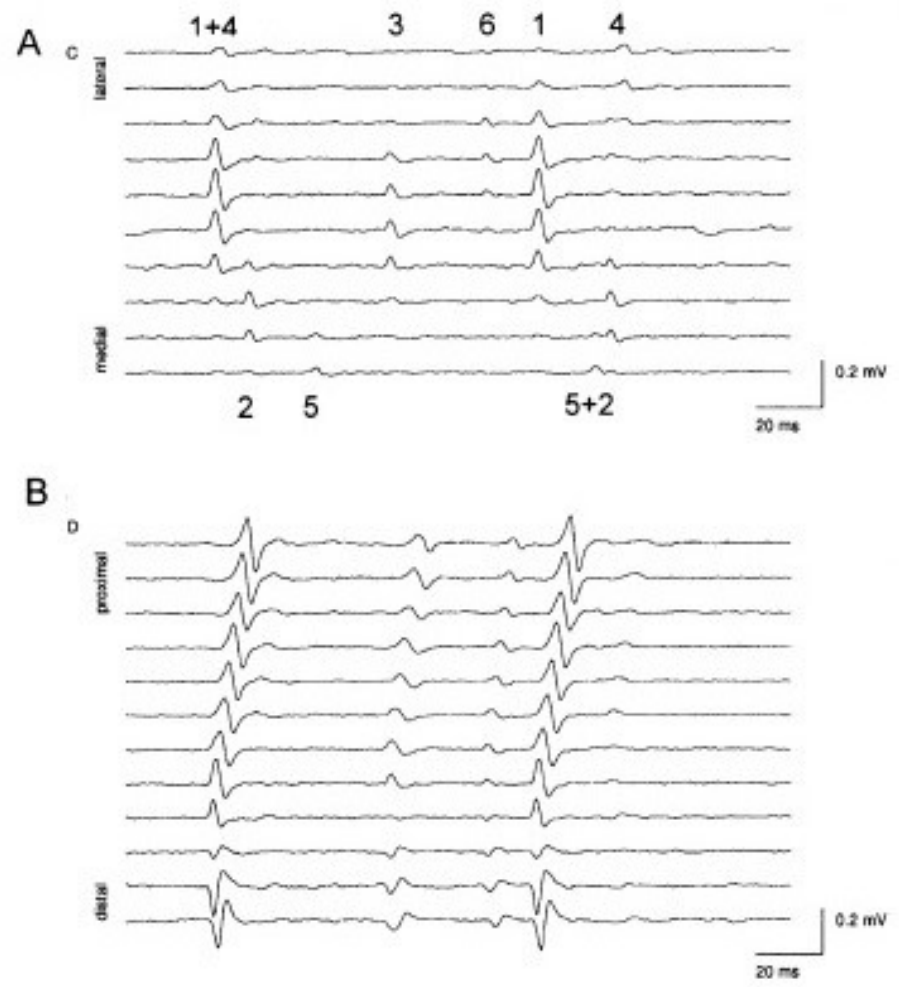


Figure 11: Surface electromyography (sEMG) patterns from a selection of electrodes from high-density electromyography grids of biceps brachii muscle.
A: Ten bipolar signals (calculated in fiber direction) presented in the direction perpendicular to the fibers show the variability of the sEMG amplitude over the muscle in medial lateral direction.
B: Twelve bipolar signals in the fiber direction from the same time segment as in part A show the position of the endplate at the third row below and the propagation of surface motor unit potentials along the muscle fiber in two directions from here with phase reversal (Reprinted from Machiel J. Zwarts,Dick F. Stegeman: Multichannel surface EMG: Basic aspects and clinical utility, Copyright 2003, with permission from John Wiley and Sons).

1.4 Application of botulinum neurotoxin in the midface

Botulinum neurotoxin (BoNT) is a metabolite of the clostridium botulinum bacterium. For medical application, only botulinum neurotoxin A (BoNT-A) is used. It inhibits the release of the neurotransmitter acetylcholine and hence blocks the excitation from nerve to muscle in the neuromuscular junction.

The S1 guidline 'aesthetic BoNT- therapy' of the german dermatologists' society defines the treatment of the glabellar region as the only on-label use, i.e. the use of pharmaceutical drugs for approved indications. However, approved off-label indications are the forehead, eyebrow lift, cow's feet, suborbital region, bunny line, perioral, corner of the mouth, chin and platysma. Seldom off-label indications are gummy smiles, cheek wrinkles, nasolabial region and tip of the nose. The average duration of a BonT-A treatment is three to five months, depending on treatment applied. The guideline offers recommendations for BoNT-A application for on-label and off-label indications in terms of injection points, BoNT-A dose and possible complications (Imhof et al. 2012).

BoNT-A is a popular method of treatment in the midface, not only for gummy smiles, but also synkinesis or rejuvenation.

Gummy smile is defined as the exposure of more than 3 mm of gingival tissue while smiling (Garber et al. 1996). Compared to surgical procedures such as lip reconstruction (Dayakar et al. 2014) or containment of the elevator muscle of the upper lip (Storrer et al. 2014), BoNT-A injection represents a low-risk and minimally invasive treatment for a neuromuscular gummy smile correction caused by hyperfunctional upper lip elevator muscles (Suber et al. 2014; Polo 2005).

Different strategies for targeting BoNT-A injections in the treatment of gummy smiles are to be found in literature. Depending on whether smiles are classified into different types or not, the methods of BoNT-A injection differ.

Hwang et al. (2009) identified a simple and reproducible injection point for BoNT-A in gummy smile treatment, called the Yonsei point. Polo (2008) recommends an injection protocol depending on anterior gingival exposure, also taking asymmetries into account. The protocol varies in dosage and the number of defined injection sites with improvements lasting three to six months (Polo 2005; Polo 2008; Polo 2013). Sucupira et al. (2012) injected BonT-A 3 to 5 mm lateral

of the nostril into the levator labii superioris alaeque nasi muscle, independent of the type of smile, though customized the dosage in case of asymmetries. Mazzuco et al. (2010) distinguished four different types of gummy smiles and applied different techniques of injection for each type. The authors recommend an identification of the gummy smile type and the muscles involved to apply the correct injection technique.

None of the above-mentioned recommendations for BoNT-A use in gummy smile therapy consider motor endplate position.

Lapatki et al. (2011) show that endplate targeted injections of a minimal effective BoNT-A dose optimize the BoNT-A's effect and thus may also decrease unwanted side effects.

1.5 Study Goals and Hypothesis

This study's goal is to gain topographical information of the midfacial musculature on a motor unit level. More specifically, motor endplate location and distribution over the muscle, fiber orientation and motor unit size should be determined and localized. The use of an altered electrode setup enables to cover midfacial muscles not only in parts as it has been possible in a previous study, but in their whole territory. Moreover, from the enlagement of the recording area we also expect to detect a greater number of midfacial muscles. The results should be mapped in mean faces that will be created on the basis of our subjects' 3D face scan data to describe the results relative to facial landmarks.

We hypothesize that facial muscle anatomy shows high inter-individual variability or even absence of midfacial muscles or muscle subcomponents. We expect the investigated facial muscles to show either endplates distributed over the muscles or endplates concentrated in centric or eccentric positions on the muscle.

2 Materials and Methods

In this study, the midfacial musculature of 16 healthy subjects was analyzed (eight men and eight women). The subjects had an average age of 25.9 years (minimum: 21; maximum 29), and no known neurological or general health disorders.

In preparation for the study the procedure of the measurements was explained to the subjects. They were specially trained to learn and improve their skills to selectively contract single muscles of the midfacial musculature, as this is a complex task and requires exercise.

The Ethics Commission of the Ulm University approved the protocol of the study (number 104/14).

2.1 Electrode grids

For the examination of the midfacial musculature, the technique of high-density surface EMG (HDsEMG) was employed (Lapatki et al. 2004).

Therefore, two HDsEMG grids (Digiraster Tetzner GmbH, Stuttgart, Germany), each consisting of 126 (9x14) chlorided silver electrodes on a highly flexible carrier material (Polyimide®, 50µm thick), were used. The HDsEMG grids have been successfully applied in studies to obtain topographical information about the lower and midfacial musculature (Lapatki et al. 2006; Matt 2013). The electrode grids were vertically displaced by one electrode row and one grid was modified by cutting out seven electrodes. This allowed subject-specific adaption of the grid to achieve an adaption to the anatomic circumstances, i.e. the ala of the nose, the best way possible. The carrier material between the two medial columns was carefully cut in to allow again higher flexibility of the grid in order to adapt to the subjects individual anatomy.

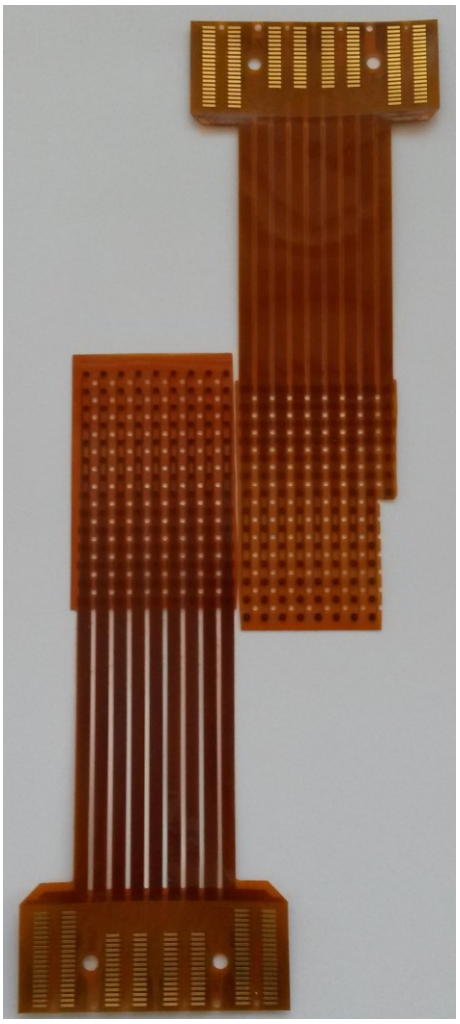


Figure 12: Two high-density surface electromyography grids (Digiraster Tetzner GmbH, Stuttgart, Germany), each of both consisting of 126 (9x14) chlorided silver electrodes. Note the modification of the right grid with 7 electrodes cut out. Department of orthodontics, Ulm University, 2014.

The electrodes were 2 mm in diameter with an inter-electrode distance (IED) of 4 mm (centre to centre) in both directions. The total thickness of these grids (electrode, carrier material, traces, protection lacquer) is 470µm in the area of the electrodes and 150µm between them. This minimal thickness and high mechanical flexibility of the grid allows EMG recording despite intense muscle exercise (Lapatki et al. 2004).

The electrode grids were positioned on the right side of the face, parallel to the bipupil line and facial midline and as close to the ala of the nose as possible. Depending on the subjects facial height, minimum the top four and maximum all seven electrodes of the medial column of the medial grid were applied for the measurement.

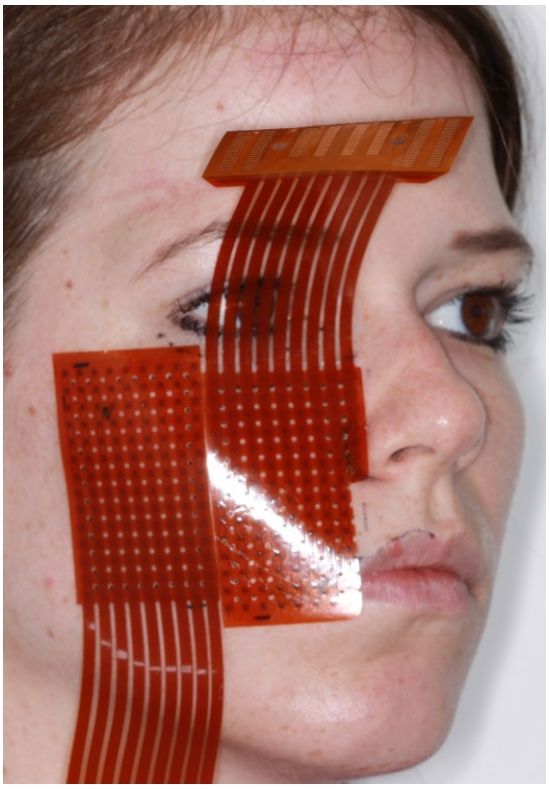


Figure 13: Two 9x14 electrode grids applied to one subject with the medial grid shifted one row caudally and seven electrodes cut out in the most medial column to adapt the grid to the ala of the nose the best way possible. Anatomical landmarks, i.e. the subzygomatic fossa, the infraorbital margin, the vermillion border and the ala of the nose, were marked. For the measurement, the lead wires of the medial grid were deflected away from the subject's eye.
High-density surface electromyography (HDsEMG) measurements of the midfacial muscles. Department of orthodontics, Ulm University, 2014.

Due to individual differences in facial height and width of the ala of the nose, different distances to the facial midline and individual coverage of the vermillion of the lip occurred.

After removal of hair and fat from the skin, i.e. shaving the skin if necessary and cleaning it with an alcohol-wetted dental cotton roll, anatomical landmarks, i.e. the subzygomatic fossa, the tragus point, the inferior orbital margin, the vermillion border and the ala of the nose, are marked. Then, the electrode grid is attached to the skin with a double-sided adhesive tape (1522 Medical double coated tape, 3M, ST. Paul, MN, USA). This double-sided adhesive tape is congruent with the grid and has two kinds of holes to accommodate the electrodes (holes of 2.2 mm in diameter to leave the electrode areas blank and holes of 1.2 mm in diameter that match the perforation of the grid). First, the double-sided adhesive tape is applied to the skin leaving the protective film on the grid-side of the tape. This allows the holes of the tape to be selectively filled with electrode cream

(Marquette-Hellige, Freiburg) to reduce skin-electrode-resistance. Surplus cream is removed using a dental cotton roll to leave only a thin layer on the skin of the blank electrode spaces. Thereafter, the protective tape is peeled off and the electrodes can be accurately placed in the electrode-cream filled holes (Lapatki et al. 2004).

For monopolar recording of the data, a reference electrode on the nasal dorsum was attached. The recording system further requires two additional electrodes: a common mode sense (CMS) placed on the nasal dorsum and a driven right leg (DRL) electrode was placed on the mastoid process (Lapatki et al. 2004).

After the measurement, the grid and adhesive tape are detached from the skin by carefully pulling the connection trails.

2.2 Data acquisition

Data were acquired monopolarly, i.e. referred to a remote reference electrode attached on the dorsum nasi, through a 256-channel amplifier (ActiveTwo, BioSemi, Amsterdam, The Netherlands). To optimize signal stability, two additional electrodes were used: a common mode sense (CMS) on the nasal dorsum and a driven right leg (DRL) electrode on the mastoid process (see (Metting van Rijn et al. 1990) for technical details).

The signals were recorded by the amplifier at a sampling rate of 4096 Hz, applying a bandpass filter to the 0-800 Hz range. The A/D converter offered a resolution of 31.25nV over an amplitude range of ±262 mV (24 bits). Signals were pre-amplified near (<10 cm) the electrodes. To enable the subjects' heads an unencumbered mobility, the lead wires to the amplifier were attached to a headset.

Data were recorded with the non-commercial data acquisition software (MyoDaq), which was developed by our study group (Blok et al. 2002) and allows monitoring output during the measurement process. The output of a specific line of column of channels can be selected for either monopolar, bipolar or higher electrode montages.

2.3 Recording procedure

After attachment of the electrode grids and the headset, subjects were again trained in performing isolated contractions. During recording the subjects performed the trained isolated contractions of midfacial muscles (BUC, INC, LAO, LLS, OOC, OORtan, OOR tan+per, OOR tan+per+mar, ZYGmaj, ZYGmin) at different contraction levels, i.e. on a level of 5%, 10%, 20%, 30% and 50% of the maximal voluntary contraction (MVC). Each contraction was held as constant as possible for 30 seconds. The subjects were supported by visual feedback to control the applied force and keep it on a constant level by displaying a bar diagram showing the root mean square value for selected channels. After each contraction a pause of about 60 seconds was introduced to prevent muscle fatigue.

2.4 Data analysis

The HDsEMG signals were filtered by a 10 Hz, high-pass, second-order Butterworth filter and decomposed using the convolution kernel compensation (CKC) technique (Holobar et al. 2007). The first step in data analysis is a visual inspection of the raw HDsEMG data's quality recorded with the non-commercial software (MyoView), which was developed by our study group (Blok et al. 2002). Selection of channels is essential as bad electrode-skin contact or a short circuit between two or more electrodes may result in "bad" channels, which need to be sorted before decomposition. CKC decomposition of high-density sEMG is fully automatic and allows the identification of complete discharge patterns of many concurrent active MUs at variable contraction levels (Holobar et al. 2009). By spike-triggered averaging, i.e. averaging the raw interference EMG signal in the vicinity of the identified discharge times, the MUAPs as detected by the corresponding electrodes can be very accurately estimated. Repetition of this procedure for every measurement point results in multichannel representation ('template'). This template, the so-called 'fingerprint of a MU', is more or less unique for every MU (Zwarts et al. 2003; Radeke et al. 2014).

A visual inspection and editing of the decomposition results made sure that the identified firing patterns were smooth and regular and that all the activity in the signal was accounted for (Marateb et al. 2011).

2.5 Data selection

For further analysis, an individual contraction level for every single muscle and again individual for every subject was chosen.

The criterion was, whether the contraction was selective for the target muscle or not. If yes, the contraction level with the highest number of selective MUs was chosen. In case of non-selective contraction, the level with the most MUs was chosen.

Table 1: Contraction level of selective muscle contractions in % of the maximal voluntary contraction. Contracted muscle in the second row, subjects in the first column (Buccinator (BUC), incisivus (INC), levator anguli oris (LAO), orbicularis oculi (OOC), orbicularis oris pars marginalis (OORmar)/ pars peripheralis (OORper)/ pars tangentialis (OORtan), orbicularis oris pars tangentialis and peripheralis (OOR tan+per), orbicularis oris pars tangentialis and peripheralis and marginalis (OOR tan+per+mar), zygomaticus major (ZYGmaj), zygomaticus minor (ZYGmin) muscle).
High-density surface electromyography (HDsEMG) measurements of the midfacial muscles. Department of orthodontics, Ulm University, 2014.

	Contraction level of selective muscle contractions in %									
	BUC	INC	LAO	LLS	OOC	OOR tan	OOR tan +per	OOR tan +per +mar	ZYG maj	ZYG min
Subject										
1	50	5	5	20	50	5	30	5	30	5
2	30	20	30	20	5	50	20	30	50	5
3	30	5	30	20	5	5	50	30	50	5
4	20	20	20	5	5	20	50	50	30	5
5	20	5	10	5	5	5	10	5	5	50
6	50	30	30	30	10	20	10	10	30	50
7	10	30	10	5	5	30	10	5	50	50
8	30	50	5	10	10	50	30	30	30	50
9	50	5	20	30	30	20	10	30	50	30
10	10	30	5	5	50	50	30	5	50	5
11	50	50	5	5	5	5	10	30	20	5
12	50	10	50	5	10	30	5	10	5	30
13	5	5	10	5	10	5	10	5	20	30
14	10	10	20	20	50	5	20	30	50	30
15	10	5	20	20	5	20	10	20	20	50
16	30	30	30	20	5	30	20	50	20	20

2.6 Location of motor end plates, fiber orientation, motor unit size

Spatial and temporal information of averaged monopolar MUAPs reveal the anatomical properties of a MU; i.e. the motor endplate's location and the main muscle fiber orientation. It can either be depicted in a template or as sequential amplitude maps that illustrate the activity distribution within the recorded area. These amplitude maps, which were spatially interpolated by a factor 8, add up to so-called 'MUAP movies', using shades of red and blue to approximate motor unit depolarization and repolarization.

A monopolar template shows the MU's territory. The motor endplate's location (endplate zone) can either be depicted as the electrode location with the maximal amplitude in a monopolar template and 'MUAP movie' or as the position of signal phase reversal in a bipolar template. In both, the monopolar template and the 'MUAP movie', the propagating MUAP corresponds to the muscle fiber direction and its termination point to the muscle fiber's end. Displaying this as a vector from the motor endplate to the MUAP's termination point, the vector represents the MU's muscle fiber orientation (Lapatki et al. 2006; Radeke et al. 2014).

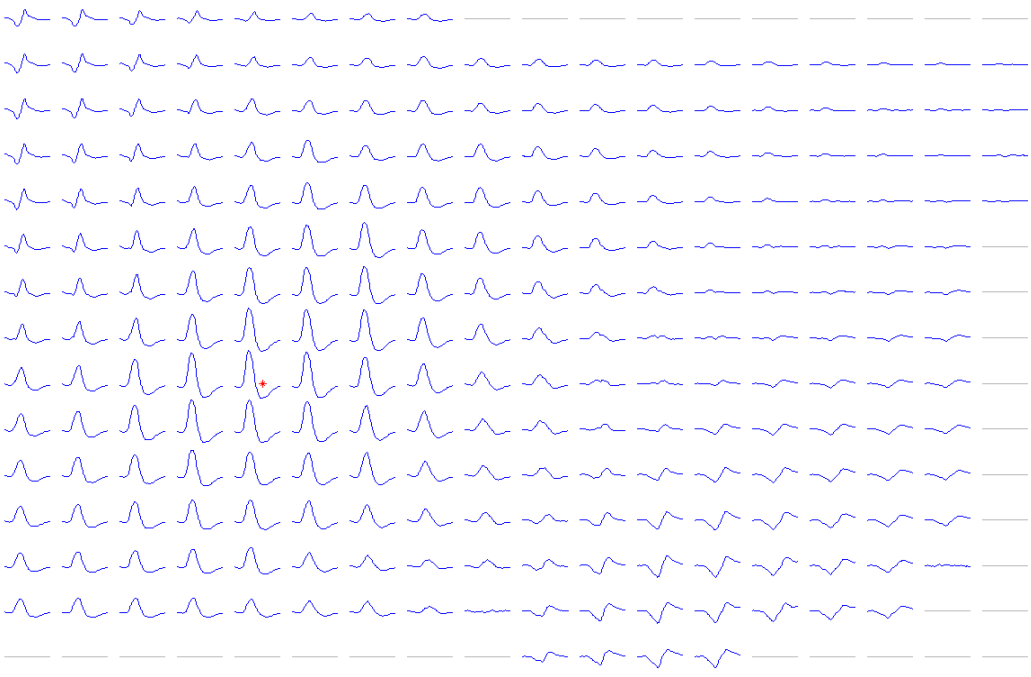


Figure 14: Example of a monopolar motor unit action potential template of zygomaticus major muscle (subject #06, motor unit (MU) #6). The red star indicates the electrode grid location with the maximal amplitude, i.e. the motor endplate location and determines the point for motor unit size measurement.
High-density surface electromyography (HDsEMG) measurements of the midfacial muscles. Department of orthodontics, Ulm University, 2014.

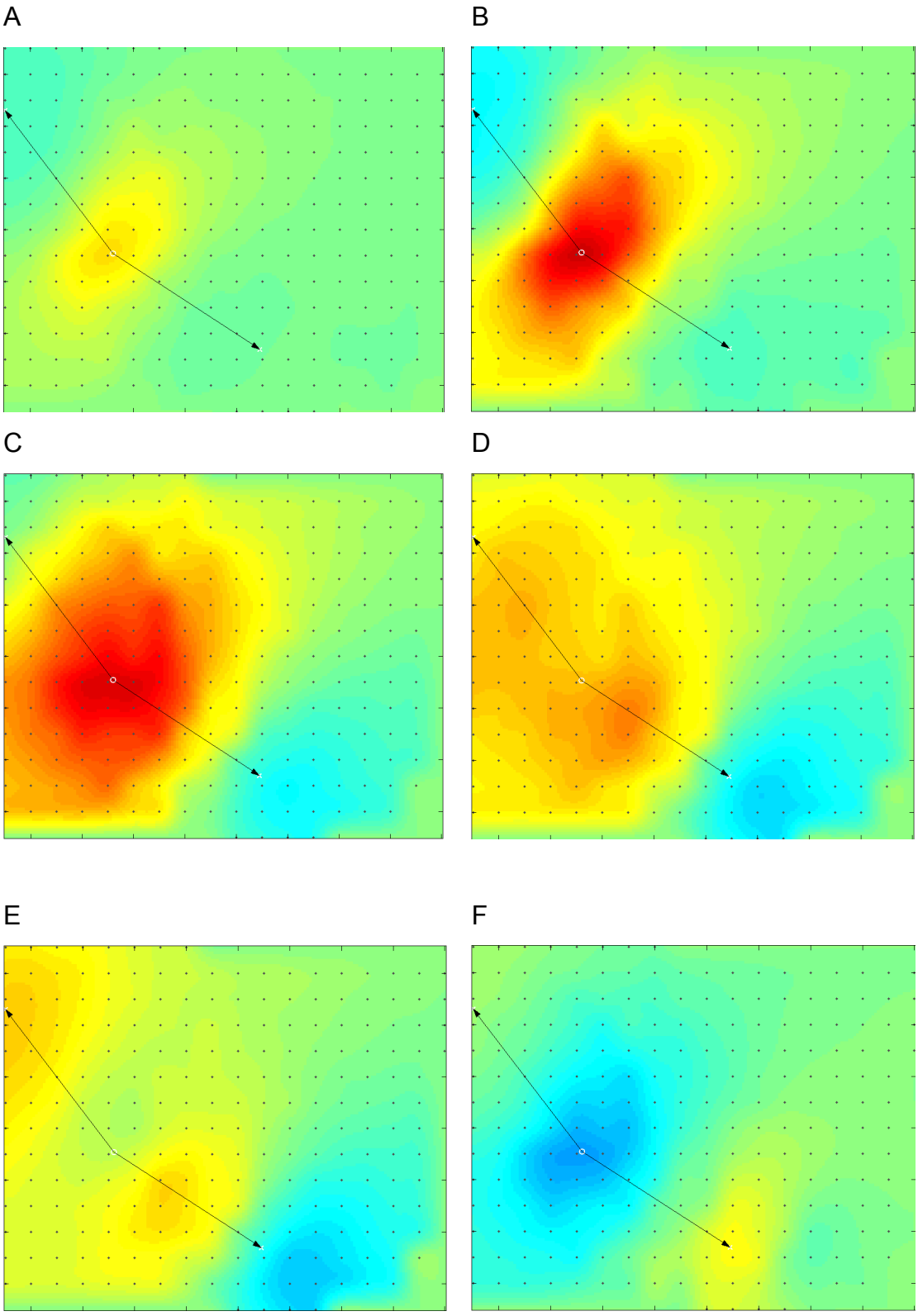


Figure 15: Six interpolated amplitude maps (A-F) of a zygomaticus major muscle motor unit (subject #06, motor unit #6) that add up to the 'motor unit action potential movie' ('MUAP movie'). Shades of red and blue approximate the motor unit depolarization and repolarization respectively.
High-density surface electromyography (HDsEMG) measurements of the midfacial muscles. Department of orthodontics, Ulm University, 2014.

A MU's electrical size is estimated by the amplitude of the largest surface MUAP in a monopolar template (Roeleveld et al. 1997a). The electrical size of the MU is proportional to the number of muscle fibers within the MU. However, due to volume conduction properties of the tissues surrounding the MU, MU depth influences the MUAP amplitude and wave shape. Hence, superficial MUs will have larger amplitudes as deep MUs. To correct for this phenomenon the spatial information provided by the high-density electrodes can be used. Superficial MUs give fast decline in amplitude with increasing distance from the MU, whereas deep MUs show much less relative amplitude decline circumferentially (Roeleveld et al. 1998). Using these differences in spatial characteristics, the depth of a MU can be estimated. For the biceps brachii muscle, this 'depth correction' of the MUAP amplitude has proven good correlation coefficients when compared to macro-EMG needle (Zwarts et al. 2003). For the facial musculature this has not yet been validated. Hence, in this study MU size is estimated without a correction for MU depth, which may be valid for superficial muscles as the facial musculature.

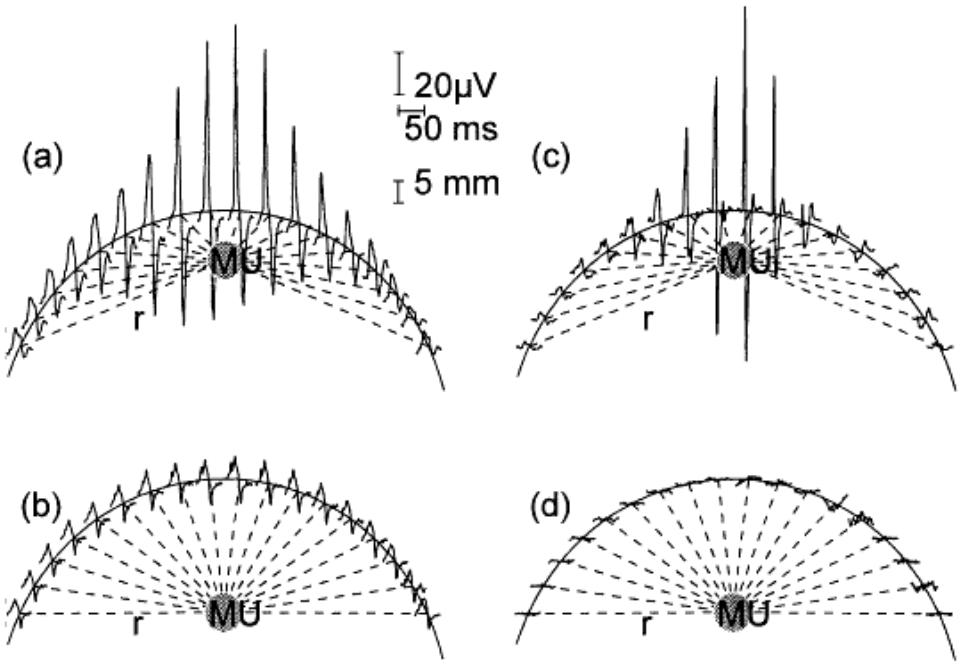


Figure 16: The location of a motor unit at different depths. Monopolar (a,b) and bipolar (c,d) motor unit action potentials. (Reprinted from Roeleveld K, Stegeman D, Vingerhoets H, Van O, A.: The motor unit potential distribution over the skin surface and its use in estimating the motor unit location. Acta Physiol Scand, 161: 465-472 (1997) with permission from John Wiley and Sons, Inc.)

2.7 Normalisation

Previous to the removal of the electrode grid, photographs and a 3D face scan (optoTOP-HE, Breuckmann GmBH, Meersburg, Germany) were taken of every subject (
Figure 17).

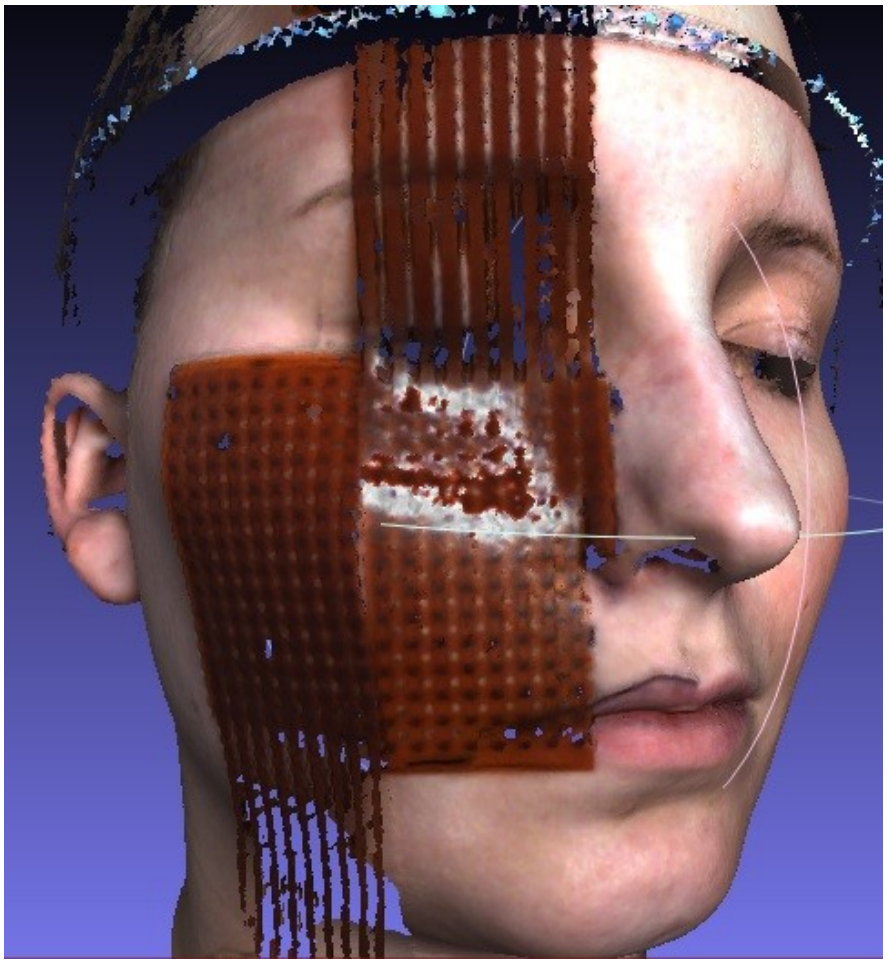


Figure 17: 3D face scan with electrode grids of a subject.
High-density surface electromyography (HDsEMG) measurements of the midfacial muscles. Department of orthodontics, Ulm University, 2014.

The 3D scan's immanent coordinates allowed measuring each subject's individual facial dimensions on the basis of anatomical landmarks. These data were used to generate the 2D normalized face and scaling factors for every subject. Thus, individual topographical results could be projected into the normalized face and individual subjects' grid positions could be reproduced.

Separately for each subject, a linear spatial scaling of the data was applied to account for the different sizes and shapes of the subjects' faces. The distance of the lateral corner of the eye and the distance of the corners of the mouth were used for an upper and lower horizontal scaling parameter respectively. For a vertical scaling, the facial height was measured from the lateral corner of the eye perpendicular to the connection line of the corners of the mouth.
For the electrode grid's position the distance of the right corner of the mouth to the most medial electrode in the bottom row of the medial grid was measured and a spatial scaling was applied as well.
The coordinates for the corners of the eye and corners of the mouth in the normalized face were calculated with the data of the 3D face scan coordinates. However, the representation of the lip closure line, the nose and the vermillion border is schematic (Figure 18).

The MUs' normalized topographical data were used to gain mean values of the examined muscles both for each subject as well as overall mean values for all subjects. This data was automatically conducted via Matlab (The Mathworks, Natick, MA) and projected in the normalized faces.

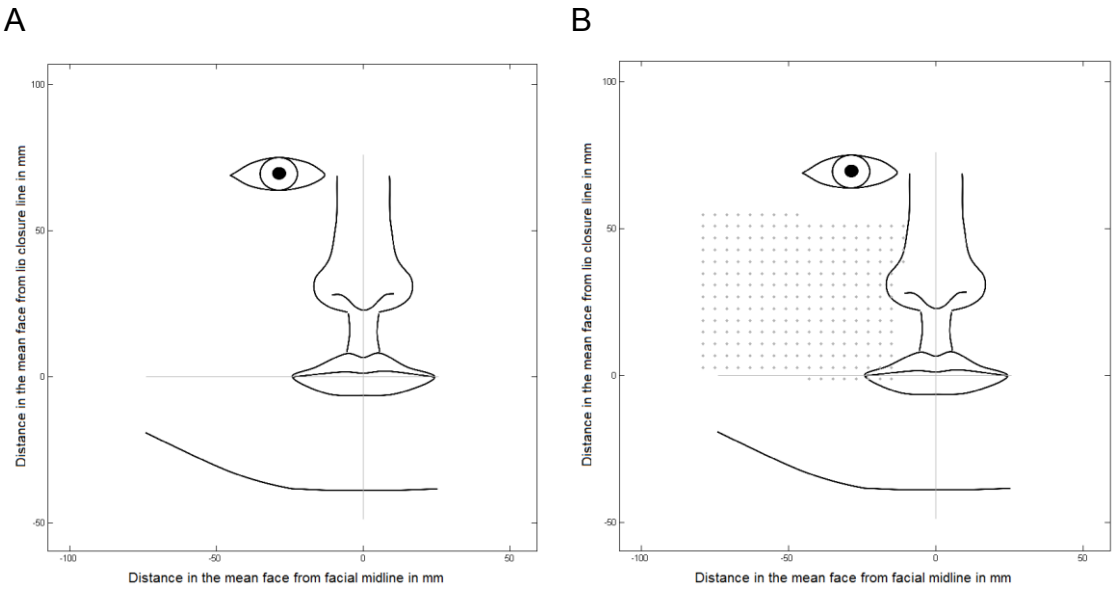


Figure 18: The normalized face without (A) and with (B) grid projection on.
High-density surface electromyography (HDsEMG) measurements of the midfacial muscles. Department of orthodontics, Ulm University, 2014.

2.8 Assignment of decomposed MUs to certain facial muscles

As all midfacial muscles converge towards the modiolus or are part of the complex arrangement of the OOR, clear criteria are needed not only to differentiate these muscles, but also for the MUs' assignment.

The topographical localization of a MU's endplate and its corresponding fibers were main criteria for the assignment. Photographs, 3D face scans and the normalized face were used to double-check the assignment.

However, all specific topographical characteristics of the amplitude wave forms were used to assign the MUs correctly to the individual facial muscle subcomponents.

OOC's MUs show a sharp waveform and fast decline of amplitude in monopolar montage due to their superficial location. The fiber orientation and topographical localization of OOC's MUs around the orbit represent outstanding criteria.

Criteria to identify BUC MUs are its deep location, which reflects in its broad waveform in monopolar montage and the topographical anatomy, i.e. the localization of BUC MUs and its fibers. The main part of fibers runs straightly towards the modiolus. A minor part of its fibers runs in latero-cranial direction, however, clearly distinguishing from ZYGmaj and ZYGmin by the MUs location more caudally.

ZYGmaj MUs can be identified by its topographical location and its fibers running in opposite directions, i.e. in latero-cranial direction towards the subzygomatic fossa and medio-caudally towards the modiolus respectively. In monopolar montage ZYGmaj's templates show a flat decline of amplitude.

ZYGmin's MUs are characterized by a more medial localization than ZYGmaj and a broad waveform in monopolar montage. Superior fibers run in latero-cranial direction; inferior fibers approach towards LLS on their way to the upper lip.

Criteria for the assignment of LLS MUs are the topography and the orientation of their superior fibers in latero-cranial direction. LLS shows a broad waveform in monopolar montage, whereas LLSan shows the characteristic sharp waveform of superficial MUs. LLSan differs from LLS in the orientation of their superior fibers, i.e. in medio-cranial direction onto the bridge of the nose, whereas the inferior fibers show a curve on their way around the nose towards the upper lip.

NAS can be identified by its topography, i.e. its potentials' orientations, which show a deviation around the ala of the nose before running onto the bridge of the nose.

Besides its anatomical topography LAO MUs are characterized by their deep location and thus flat decline of amplitude in monopolar templates.

As the fibers of the OOR complex intermingle, the fiber orientation of its composing parts and the location of their corresponding endplates were main criteria to distinguish OORmar, OORper and OORtan as well as INC.

OORtan MUs can be identified by their fast decline in amplitude and their fiber direction perpendicular to the vermillion border. OORmar MUs show a fast decline of amplitude in monopolar montage. Its short fibers run parallel to the vermillion border and are located in the area of the vermillion border and lip red.

OORper shows a more flat decline in amplitude in monopolar montage than OORmar. Its fibers are orientated parallel to the vermillion border and longer than OORmar fibers. Their endplates are either located close to the modiolus with fibers running towards the facial midline or located more medial showing fibers running in opposite direction parallel to the vermillion border.

INC shows the flattest decline of amplitude in monopolar montage of the OOR complex, which emphasizes its deep location. Its endplates are located on the medial edge of the medial grid with long fibers running parallel to the vermillion border towards the modiolus.

3 Results

3.1 Co-activation of MUs in attempted selective muscle contractions

A total of 957 MUs were found and assigned to all midfacial muscles covered by the grid setup.

Table 2: Number of motor units (MUs) found in attempted selective muscle contractions (Buccinator (BUC), incisivus (INC), levator anguli oris (LAO), orbicularis oculi (OOC), orbicularis oris pars marginalis (OORmar)/ pars peripheralis (OORper)/ pars tangentialis (OORtan), orbicularis oris pars marginalis and peripheralis and tangentialis (OOR mar+per+tan), orbicularis oris pars peripheralis and tangentialis (OOR per+tan), zygomaticus major (ZYGmaj), zygomaticus minor (ZYGmin) muscle). Contracted muscles are listed in the second row. Assigned muscles are listed in the second column. The column on the right shows the sum of identified motor units of one muscle with the total sum of analyzed motor units at the bottom.
High-density surface electromyography (HDsEMG) measurements of the midfacial muscles. Department of orthodontics, Ulm University, 2014.

		Attempted selective contraction of										
		BUC	INC	LAO	LLS	OOC	OOR mar+ per+ tan	OOR per+ tan	OOR tan	ZYG maj	ZYG min	SUM
Assignment of MUs to	BUC	25	0	3	2	1	2	0	0	6	3	42
	INC	3	15	9	1	3	4	3	11	0	1	50
	LAO	36	6	28	3	11	4	3	9	14	5	119
	LLS	2	4	5	16	3	1	4	3	4	14	56
	LLSan	0	0	2	30	1	0	0	0	6	13	52
	OOC	10	3	9	18	66	4	4	3	21	22	160
	OORmar	2	12	5	3	3	12	9	5	0	2	53
	OORper	14	36	26	14	9	42	48	39	9	13	250
	OORtan	4	10	4	4	2	12	20	18	0	3	77
	ZYGmaj	8	1	2	1	2	3	1	0	47	6	71
	ZYGmin	1	0	0	2	0	0	1	0	1	5	10
	NAS	2	1	1	0	1	3	4	3	0	2	17
											Total	957

3.2 Occurrence of muscle subcomponents and muscle classification

Table 3: Overview of all found motor units (MUs) shows the occurrence, i.e. absence and presence of muscle subcomponents in the individual subjects (1-16) (Buccinator (BUC), incisivus (INC), levator anguli oris (LAO), orbicularis oculi (OOC), orbicularis oris pars marginalis (OORmar)/ pars peripheralis (OORper)/ pars tangentialis (OORtan), zygomaticus major (ZYGmaj), zygomaticus minor (ZYGmin) muscle). The bottom row shows the total number of motor units found per subject (MUs total). The far right column shows the number of subjects in which the corresponding muscle subcomponent occurred (occurrence total (OT)).
High-density surface electromyography (HDsEMG) measurements of the midfacial muscles. Department of orthodontics, Ulm University, 2014.

Occurrence of muscle subcomponents																	
Subject	1	2	3	4	5	6	7	8	9	10	11	12	13	14	15	16	**OT**
BUC	2	3	1	3	4	3	3	1	6	3	2	4	4	0	1	2	15
INC	8	0	0	0	0	0	15	1	1	5	2	1	8	8	1	0	10
LAO	4	4	9	3	2	9	14	6	11	8	25	2	8	4	2	8	16
LLS	0	6	0	14	8	1	1	4	13	1	0	1	5	0	1	1	12
LLSan	3	5	6	0	7	0	6	5	0	4	2	3	1	6	3	1	13
OOC	23	26	11	7	25	6	9	5	2	2	8	7	16	3	2	8	16
OORmar	4	0	3	0	3	0	1	4	6	0	1	3	9	8	11	0	11
OORper	7	12	18	7	16	19	28	14	20	13	13	18	16	19	13	17	16
OORtan	5	15	7	14	1	2	2	9	2	10	1	3	0	0	6	0	13
ZYGmaj	5	10	1	8	6	2	4	9	2	3	0	5	3	12	0	1	14
ZYGmin	0	1	2	3	0	0	0	0	0	0	0	4	0	0	0	0	4
NAS	4	0	0	0	5	0	0	1	0	1	2	0	2	0	2	0	7
MUs total	65	82	58	59	77	42	83	59	63	50	56	51	72	60	42	38	

Despite subjects' individual training to selectively contract the midfacial muscles and their subcomponents, not all muscles and their subcomponents were found in every subject. LAO, OOC and OORper were the only muscles or muscle subcomponents to be found in every subject.

Regarding endplate distribution, the midfacial muscles subcomponents can be classified in class A-C for an overview (see Table 4 and Table 5). The detailed results for every muscle or its subcomponents are carried out in the individual muscles' results (see 3.4).

Table 4: Muscle classification (I) according to endplate distribution: Class A-C with definition and correspondent muscles (Buccinator (BUC), incisivus (INC), levator anguli oris (LAO), orbicularis oculi (OOC), orbicularis oris pars marginalis (OORmar)/ pars peripheralis (OORper)/ pars tangentialis (OORtan), zygomaticus major (ZYGmaj), zygomaticus minor (ZYGmin) muscle). Note that nasalis muscle (NAS) does not appear in this classification as no endplates were determined for NAS.
High-density surface electromyography (HDsEMG) measurements of the midfacial muscles. Department of orthodontics, Ulm University, 2014.

Muscle classification (I)	
Class	**Definition and correspondent muscles**
A	Widely distributed endplates on the muscle within individuals OOC, OORmar
B	Clustering of endplates (at least to a certain extent) within individuals, but great variation of the location of clusters between individuals BUC, LAO, OORper, OORtan, ZYGmin
C	Clustering of endplates with similar cluster locations among individuals INC, LLS, LLSan, ZYGmaj

Table 5: Muscle classification (II): Overview of the muscles and the correspondent class A-C (Buccinator (BUC), incisivus (INC), levator anguli oris (LAO), orbicularis oculi (OOC), orbicularis oris pars marginalis (OORmar)/ pars peripheralis (OORper)/ pars tangentialis (OORtan), zygomaticus major (ZYGmaj), zygomaticus minor (ZYGmin) muscle).
High-density surface electromyography (HDsEMG) measurements of the midfacial muscles. Department of orthodontics, Ulm University, 2014.

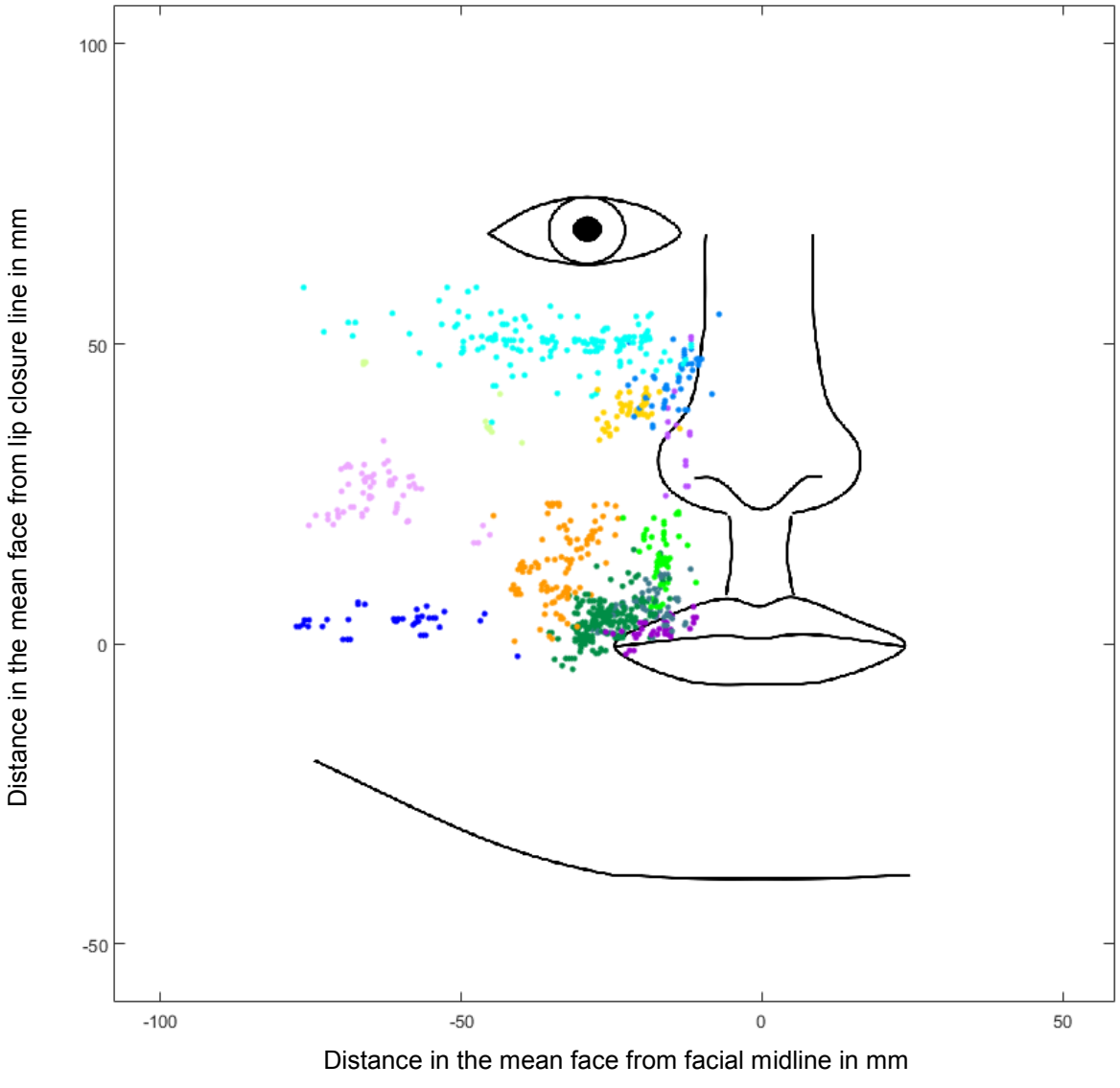
Muscle classification (II)	
BUC	B
INC	C
LAO	B
LLS	C
LLSan	C
OOC	A
OORmar	A
OORper	B
OORtan	B
ZYGmaj	C
ZYGmin	B

3.3 Motor endplates and muscle fiber orientations of the complete midfacial musculature

The motor endplates and muscle fiber orientations are presented in form of amplitude templates and in form of projections on normalized faces.

In case of the template illustration, both monopolar and bipolar montages will be shown. Thereby the circle indicates the motor end plate's position derived from the bipolar template. The lines emanating from the circle indicate the MU's muscle fiber orientations. For the projection in normalized faces, the subjects' data are standardized by individual scaling factors.

A



B

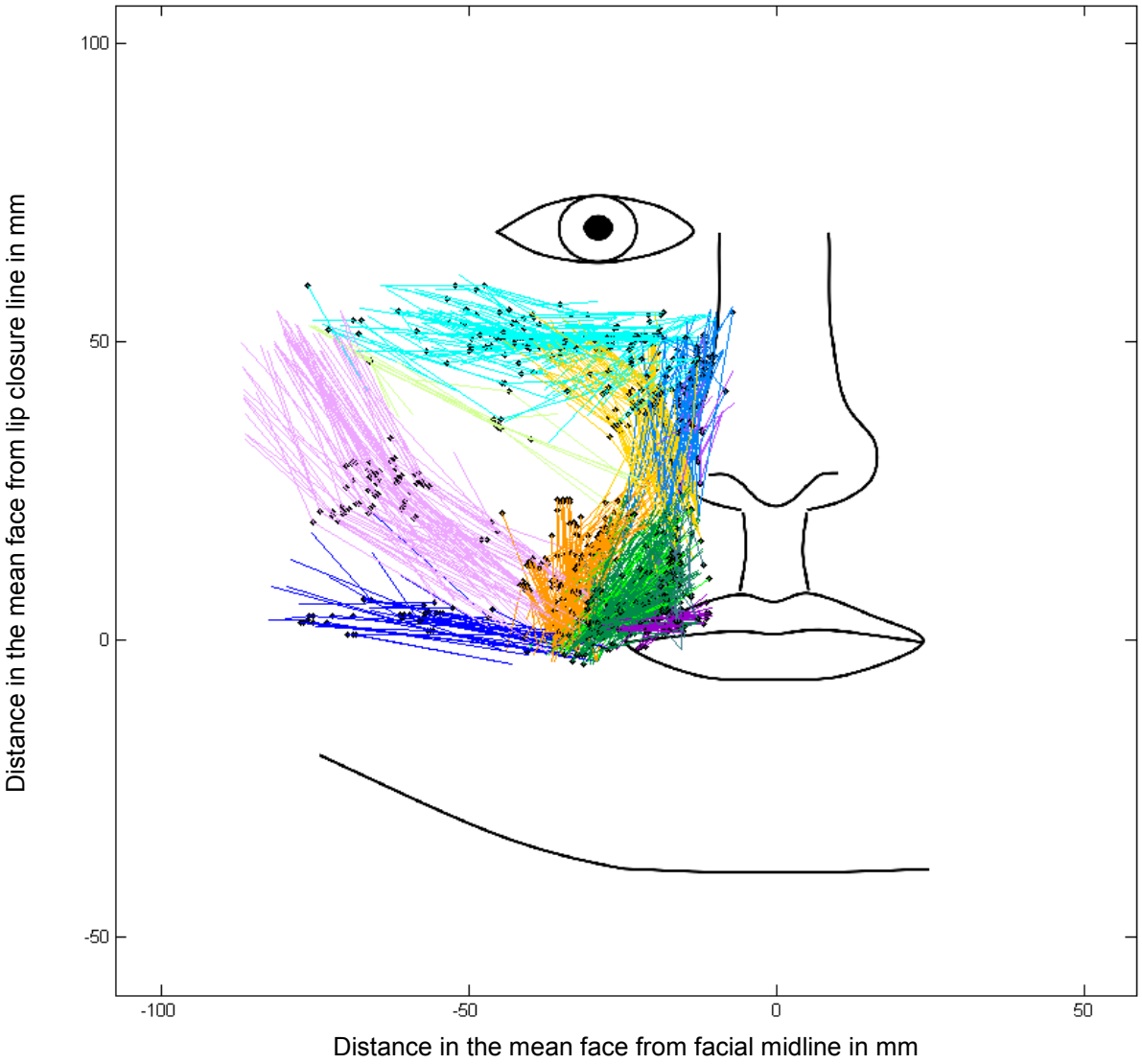


Figure 19: All subjects normalized motor units (n =957) without (A) and with (B) fiber orientation projected on the averaged face: OOC (turquois), ZYGmaj (light purple), ZYGmin (light green), BUC (dark blue), LAO (orange), LLS (yellow), LLSan (light blue), OORper (dark green), OORmar (dark purple), OORtan (grey), INC (light green) and NAS (pink).
High-density surface electromyography (HDsEMG) measurements of the midfacial muscles. Department of orthodontics, Ulm University, 2014.

3.4 Motor endplate location and muscle fiber direction of individual muscle subcomponents

3.4.1 Orbicularis oculi muscle

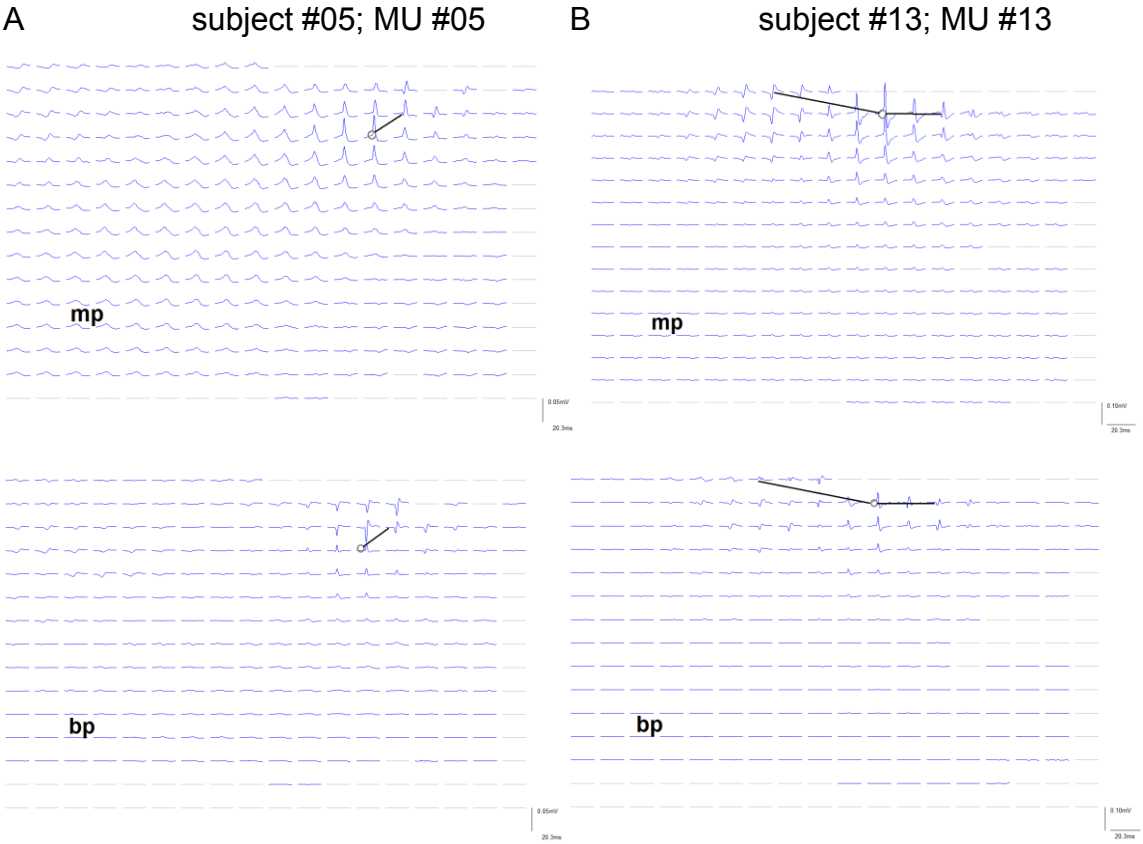


Figure 20: Two representative templates of orbicularis oculi muscle motor units (A, B) in monopolar (mp) and bipolar-vertical (bp) montage. The relatively fast decline in amplitude in the monopolar templates illustrates the superficial location of both motor units. Opposite signal polarity in bipolar montage displays the motor endplates' location. The lack of motor unit action potentials in the most inferior row refers to channels with bad connection that are omitted. Motor units with short fibers in A, motor unit with opposite fiber orientation showing short fibers in one direction and long fibers in the other in B.
High-density surface electromyography (HDsEMG) measurements of the midfacial muscles. Department of orthodontics, Ulm University, 2014.

OOC MUs were found in all subjects. All kinds of attempted selective contractions showed co-contraction of OOC MUs, however 41.5 % of all OOC MUs were actually found in selective OOC contraction (Table 2). Due to inter-individual differences in facial height and electrode grid positioning criteria, i.e. to put the grid as close to the ala of the nose as possible, differently large coverage of the lower OOC occurred in different subjects. OOC was often located on the cranial margin

of both grids and MUAP propagation was limited by the grid's location. Figure 20 shows two representative OOC MUs in monopolar and bipolar-vertical montage. The relatively fast decline in amplitude in the monopolar template indicates the MUs' superficial location. The opposite signal polarity of adjacent wave forms in the bipolar template depicts the motor endplate location. The lack of motor unit action potentials refers to channels with bad connection that are omitted. The bad channels are displayed as blank spaces in all muscles' results.

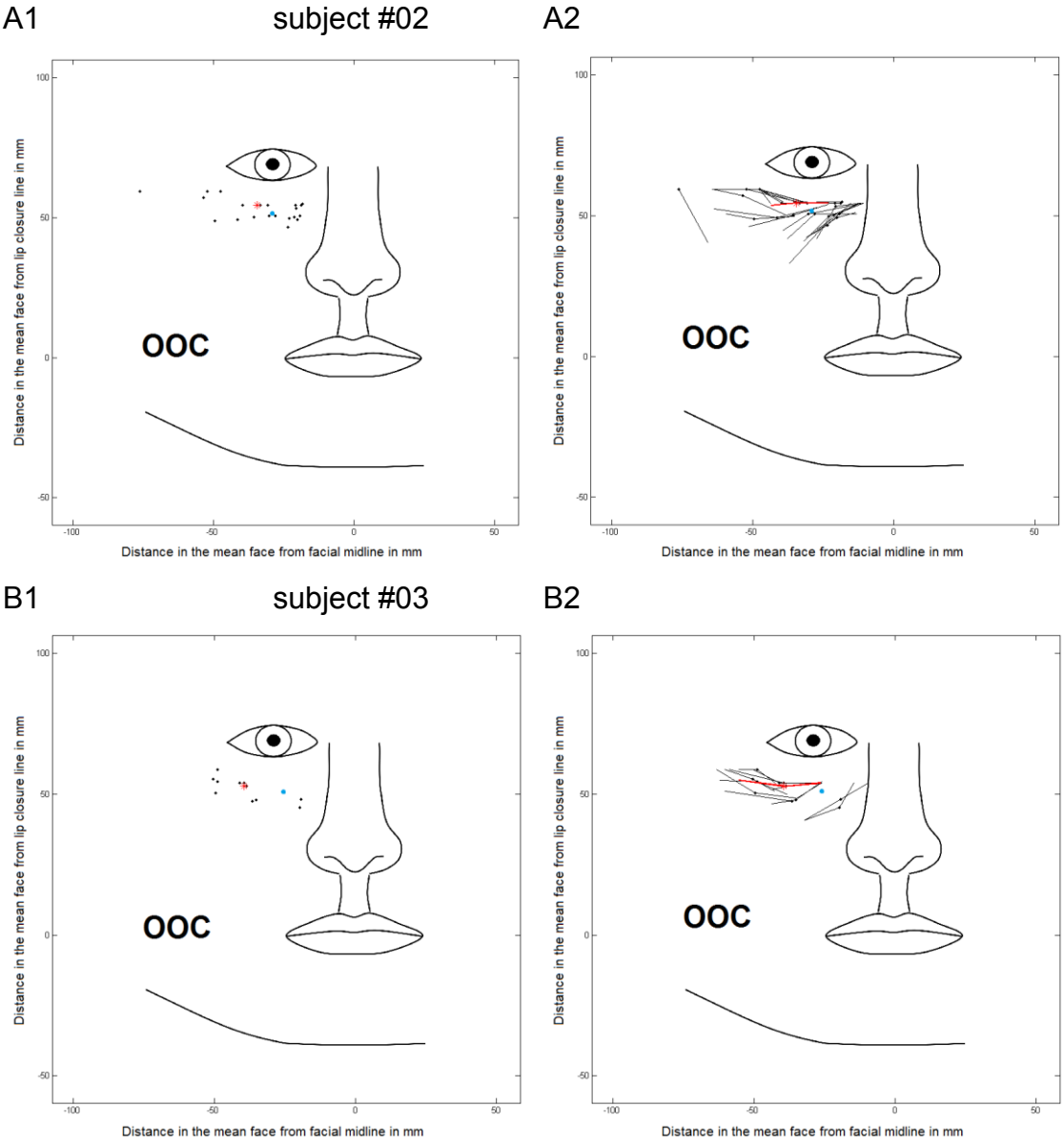


Figure 21: Representative subjects' total orbicularis oculi muscle (OOC) motor units (black) and their median (red) in the average face with (A2, B2) and without (A1, B1) fiber orientation. The blue point indicates the subjects' individual inferior margin of the orbit. The very lateral motor unit in A1 and A2 could be distinguished from ZYGmin due to endplate topography. High-density surface electromyography (HDsEMG) measurements of the midfacial muscles. Department of orthodontics, Ulm University, 2014.

Two subjects' OOC MUs in Figure 21 exemplify the high inter-individual differences in motor endplate distribution. In general, OOC endplates show a large-area distribution over the muscle and only barely a clustered distribution. Both, MUs with one or two signal propagation vectors were found. A MU's fiber orientation depends on its topographic location, as the fibers are arranged to form ellipses around the orbit. More specifically, endplates located more lateral show fibers running in latero-cranial and medio-caudal direction, whereas endplates in the area of the orbit's inferior margin show fibers running towards the corners of the eye. Endplates located the farthest medial showed fibers in both lateral and latero-caudal direction, however no fibers towards the medial palpebral ligament. The latter might be due to the limited coverage of OOC by the electrode grid. As fibers are depicted as linear vectors in one extraction algorithm, it was not possible to illustrate their elliptic course around the orbit as seen in the MUAP movies. However, these fiber orientations proved to be an outstanding distinguishing feature to identify OOC.

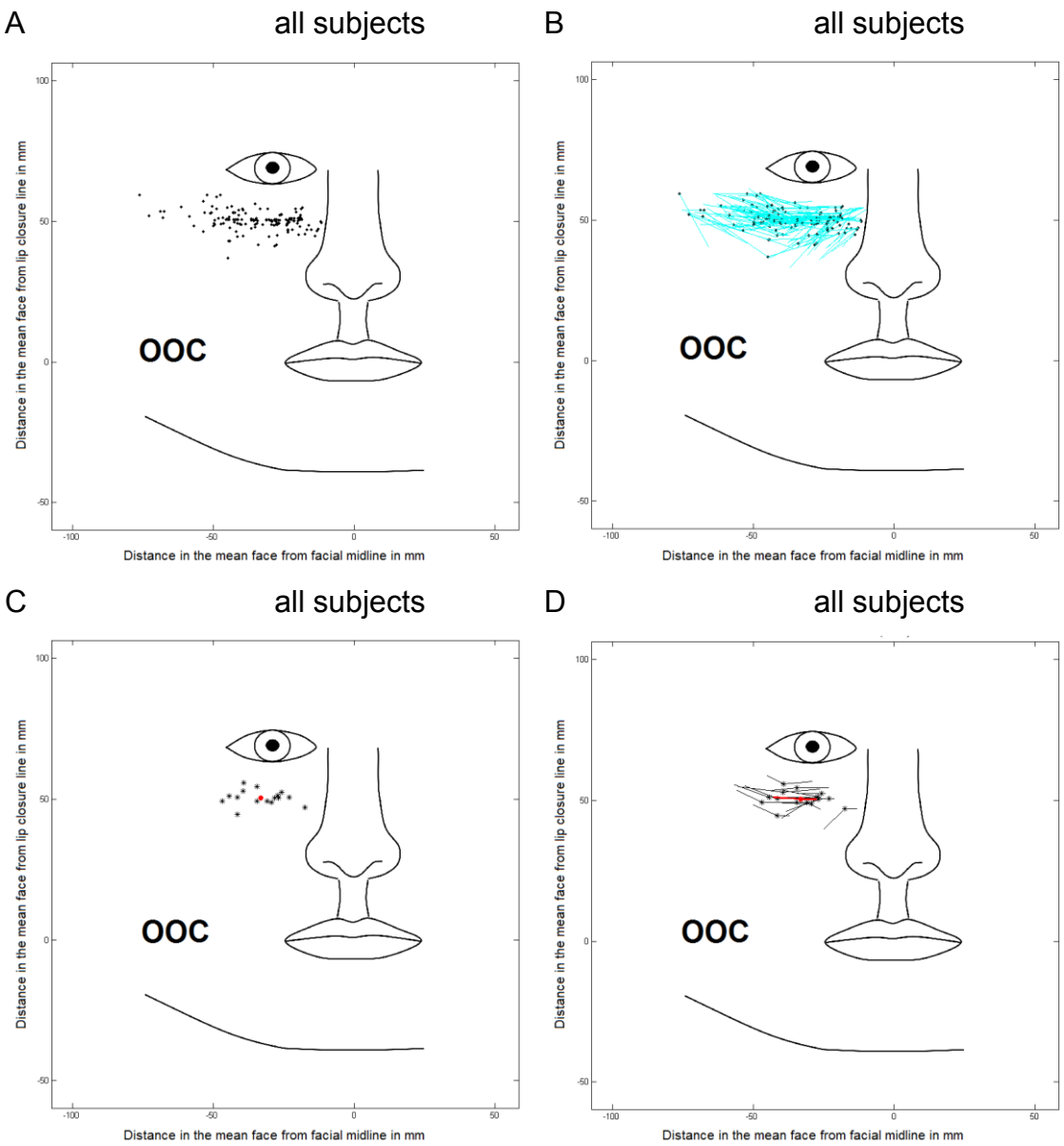


Figure 22: All subjects' orbicularis oculi muscle (OOC) motor units without (A) and with (B) fiber orientation. All median orbicularis oculi muscle (OOC) motor units (*) and mean of the median values (red) in the normalized face without (C) and with (D) fiber orientation. Farthest medial median motor unit (C, D), which belongs to subject # 16, could be surely assigned to OOC.
High-density surface electromyography (HDsEMG) measurements of the midfacial muscles. Department of orthodontics, Ulm University, 2014.

3.4.2 Zygomaticus major muscle

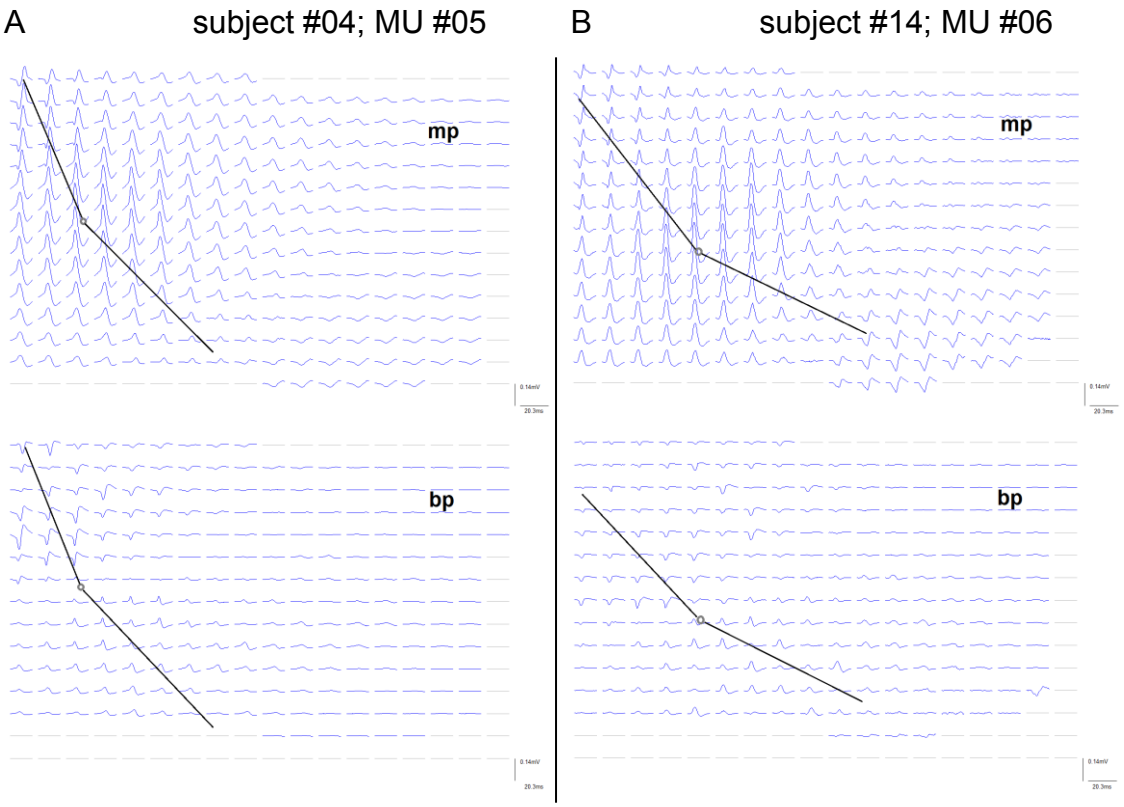


Figure 23: Characteristic templates for two motor units (A, B) of zygomaticus major muscle in monopolar (mp) and bipolar-vertical montage (bp). The motor endplates are located lateral to the center of the lateral grid (A) and slightly below the center of the lateral grid (B) as revealed by the signal phase reversal in bipolar montage. In both subjects, the motor unit action potentials propagate in two directions, i.e. in latero-cranial direction towards the subzygomatic fossa and in medio-caudal direction towards the modiolus. The lack of motor unit action potentials in the first and second row from the bottom refers to channels with bad connection that are omitted.
High-density surface electromyography (HDsEMG) measurements of the midfacial muscles. Department of orthodontics, Ulm University, 2014.

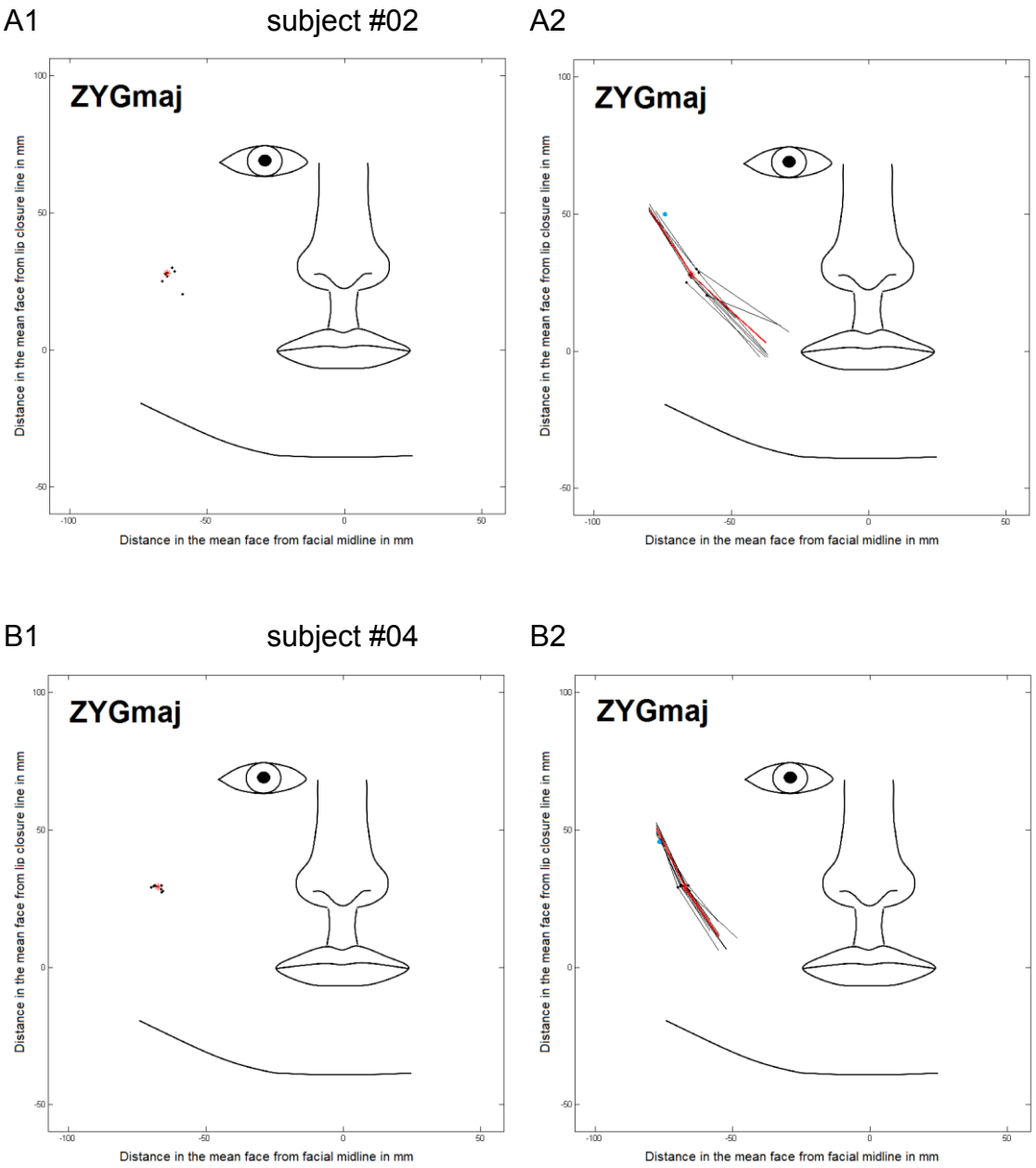


Figure 24: Two subjects' (A, B) zygomaticus major muscle (ZYGmaj) motor units (black) and their median (red) in the normalized face without (A1, B1) and with (A2, B2) fiber orientation. The blue dot in A2 and B2 indicates the subject's individual subzygomatic fossa. Motor endplates are either arranged in a cluster (B) or in a narrow band (A) and may show additional discrete endplates medio-caudally to the main endplate location.
High-density surface electromyography (HDsEMG) measurements of the midfacial muscles. Department of orthodontics, Ulm University, 2014.

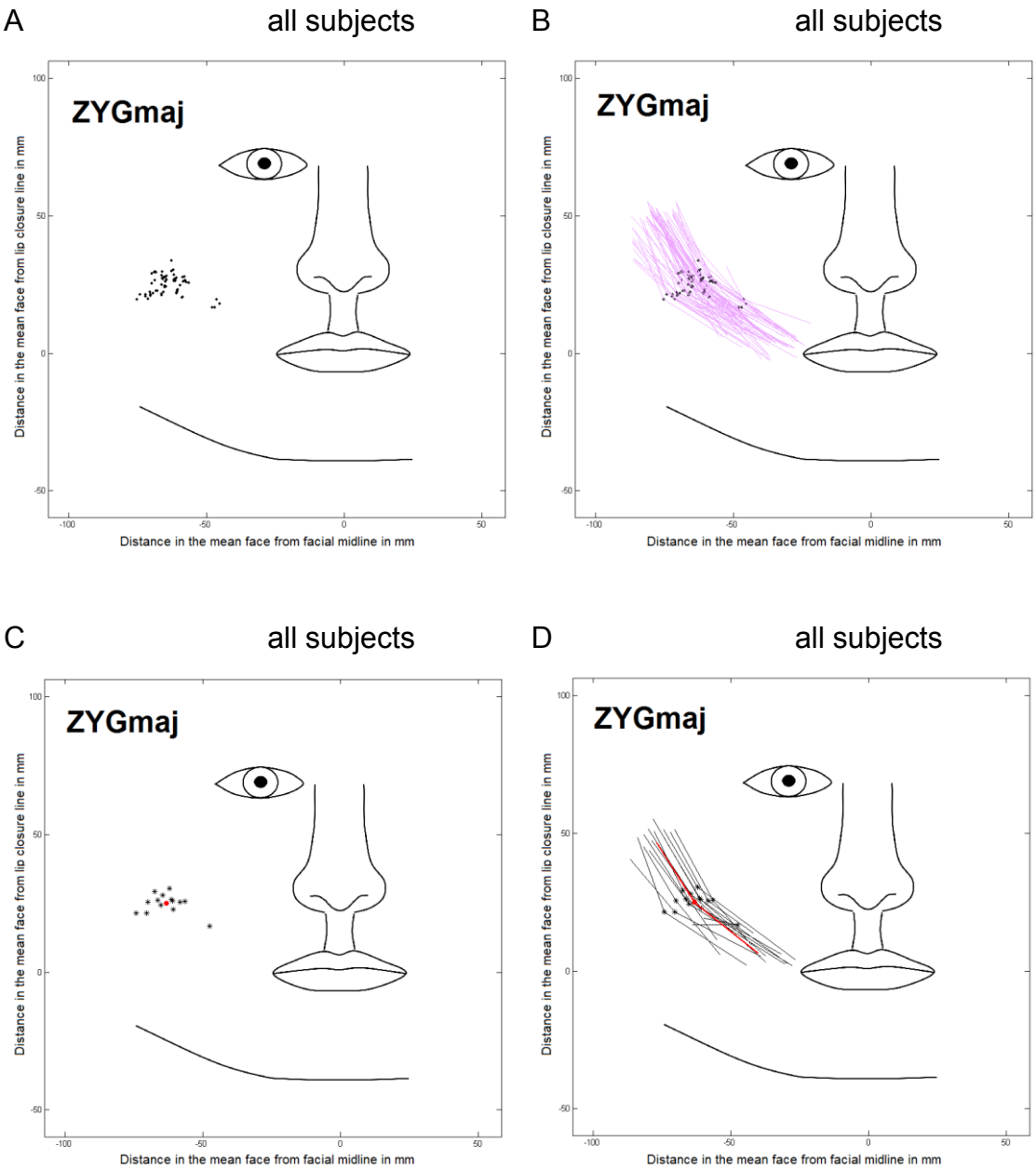


Figure 25: All subjects' zygomaticus major muscle (ZYGmaj) motor units without (A) and with (B) fiber orientation. All zygomaticus major muscle (ZYGmaj) median values (*) and mean of the median values (red) in the normalized face without (C) and with (D) fiber orientation. The endplates appear clustered and may have additional discrete endplates medio-caudally to the main cluster. The reverse appearing median fiber orientation in (D) emerges as subject 9 only shows one fiber orientation in lateral direction.
High-density surface electromyography (HDsEMG) measurements of the midfacial muscles. Department of orthodontics, Ulm University, 2014.

ZYGmaj's MUs were found in 14 of the 16 subjects. Most of them (66.2 %) were found in selective ZYGmaj contraction (Table 2). Figure 23 shows two characteristic templates of ZYGmaj MUs in monopolar (mp) and bipolar-vertical montages (bp). The flat decline of amplitude in monopolar montage indicates ZYGmaj's deep location. The opposite signal polarity in the bipolar templates

illustrate the motor endplates' locations. ZYGmaj endplates were mainly found in one cluster or a narrow band lateral to the center of the lateral grid or slightly below as shown in Figure 24 A and B. However, two subjects (#02 and #05) showed additional discrete endplates located in medio-caudal direction to the main endplate cluster (see Figure 24 A). In relation to anatomical landmarks, the endplates are located latero-caudally to the point that divides the connection line from the corner of the mouth to the subzygomatic fossa at a ratio of 2:1 whereas the one third is going from the subzygomatic fossa. Except for one subject (#9), who shows only one fiber orientation in lateral direction, all subjects show two opposite directions of signal propagation originating from the motor endplate. The superior fibers run in latero-cranial direction towards the subzygomatic fossa and the inferior fibers run in medio-caudal direction towards to modiolus. For 12 subjects, the superior fibers exceeded the electrode grid. In these cases, MUAP extinction is displayed at the border of the electrode grid.

3.4.3 Zygomaticus minor muscle

A subject #12; MU #06

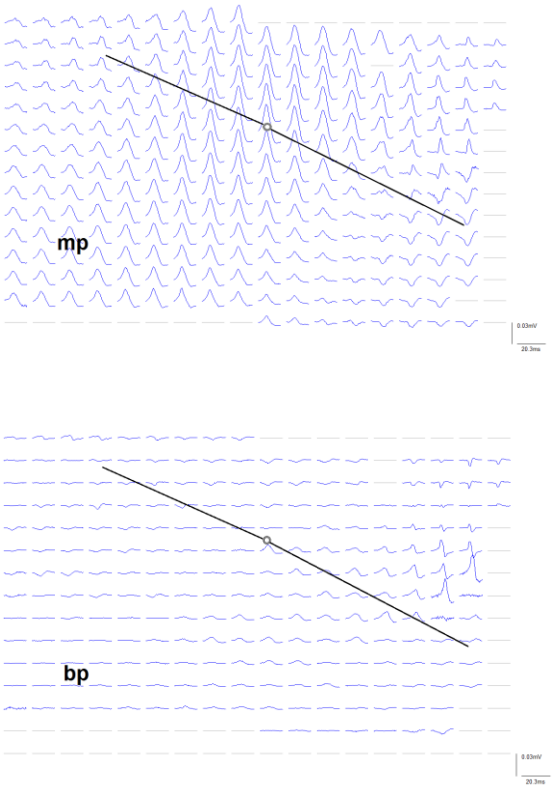


Figure 26: Representative template of a zygomaticus minor muscle motor unit in monopolar (mp) and bipolar (bp) montage. The circle indicates the endplate located under the lateral corner of the eye on a level slightly above the ala of the nose. Zygomaticus minor's superior fibers run in latero-cranial direction towards the subzygomatic fossa, its inferior fibers run in medio-caudal direction towards muscular substance of the upper lip. High-density surface electromyography (HDsEMG) measurements of the midfacial muscles. Department of orthodontics, Ulm University, 2014.

MUs of ZYGmin were found in four subjects, each of which also shows MUs of ZYGmaj. MUs of ZYGmin were found in contraction of BUC, LLS, OORper, ZYGmaj and ZYGmin (Table 2). Figure 26 shows a MU of ZYGmin in monopolar and bipolar-vertical montage. The flat decline of amplitude in the monopolar template illustrates the muscle's deep location under the fat tissue of the cheek.

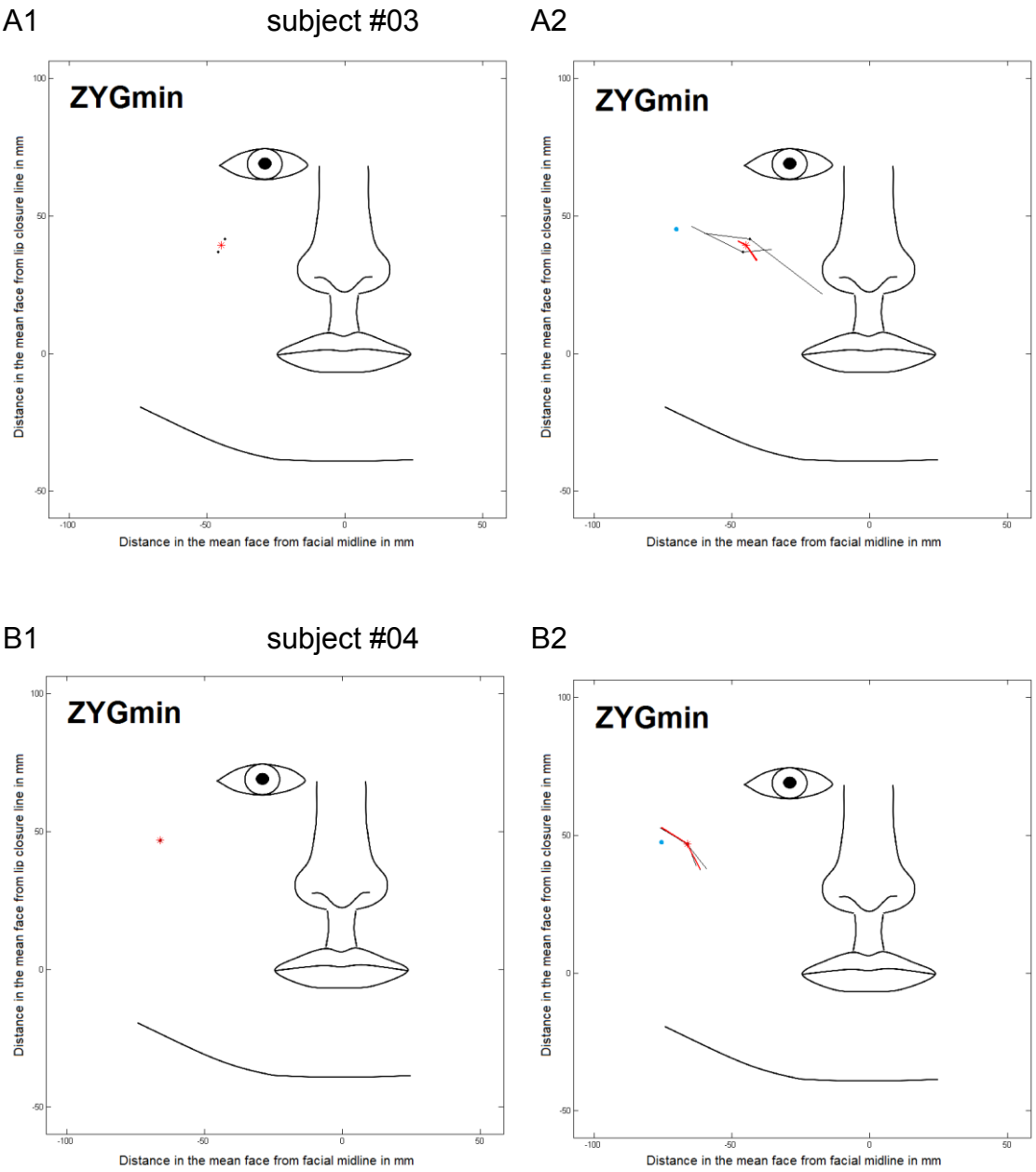


Figure 27: Individual results of zygomaticus minor muscle motor units (black) and median (red) motor units of two subjects (A, B) in the normalized face without (A1, B1) and with (A2, B2) fiber orientation. High inter-individual differences in endplate positions, fiber orientations and fiber lengths.
High-density surface electromyography (HDsEMG) measurements of the midfacial muscles. Department of orthodontics, Ulm University, 2014.

Figure 27 shows two subjects' MUs of ZYGmin. Endplates are found clustered at two sites. Three out of four subjects show clustered endplates at the lateral canthus at a level slightly above the ala of the nose (see Figure 27 A), which corresponds to the muscle's cranial third. These MUs show similar topography as those of ZYGmaj, i.e. superior fibers running in latero-cranial direction towards the

subzygomatic fossa. The inferior fibers run in medio-caudal direction towards the upper lip and end latero-caudal to the ala of the nose.

Due to the fibers' illustration as linear vectors it is not possible to illustrate the fibers' curved course. The inferior fibers show a curve to the facial the midline. One subject (Figure 27 B) showed endplates in the area of the subzygomatic fossa. These MUs show very short fibers in latero-cranial direction going beyond the subzygomatic fossa and fibers in medio-caudal direction.

Figure 28 again states ZYGmins high variability in both endplate location and fiber orientation.

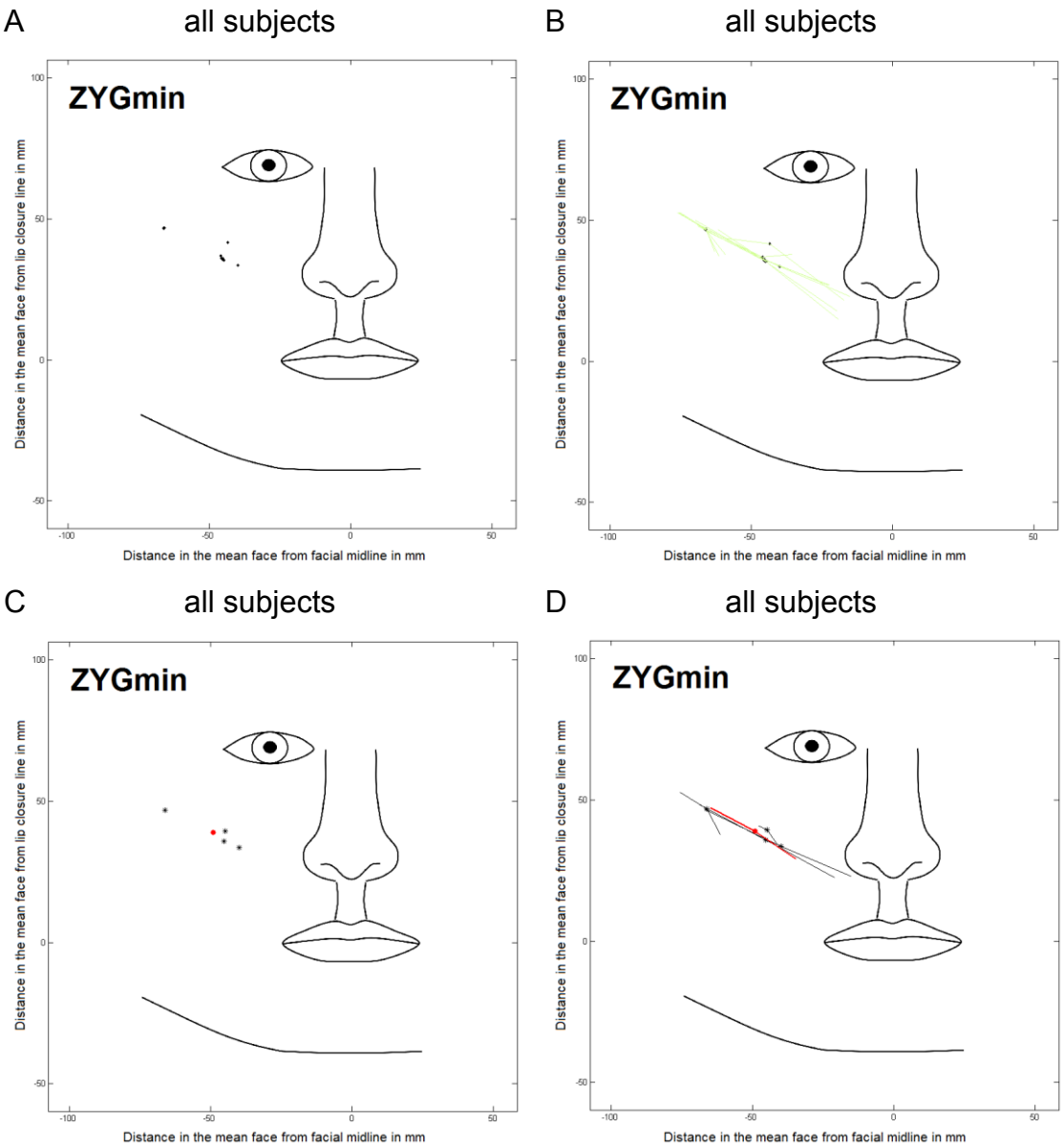


Figure 28: All found motor endplates of zygomaticus minor muscle without (A) and with (B) fiber orientations in the normalized face. Endplates are either located clustered under the lateral corner of the eye on a level slightly above the ala of the nose or in the area of the subzygomatic fossa. Both kinds of endplate locations show superior fibers in latero-cranial direction and inferior fibers in medio-caudal direction. All median zygomaticus minor muscle (ZYGmin) motor units (*) and mean of the median values (red) in the normalized face without (C) and with (D) fiber orientation.
High-density surface electromyography (HDsEMG) measurements of the midfacial muscles. Department of orthodontics, Ulm University, 2014.

For demarcation of ZYGmin from ZYGmaj, the endplate topography was a main criterion, as endplates and hence fibers of ZYGmaj were found latero-caudally to ZYGmin. For demarcation from OOC, the fiber orientations emerged to be reliable distinguishing features: ZYGmin's inferior fibers are oriented towards the upper lip, whereas OOC fibers are oriented to form parts of an ellipse around the orbit (see Figure 29).

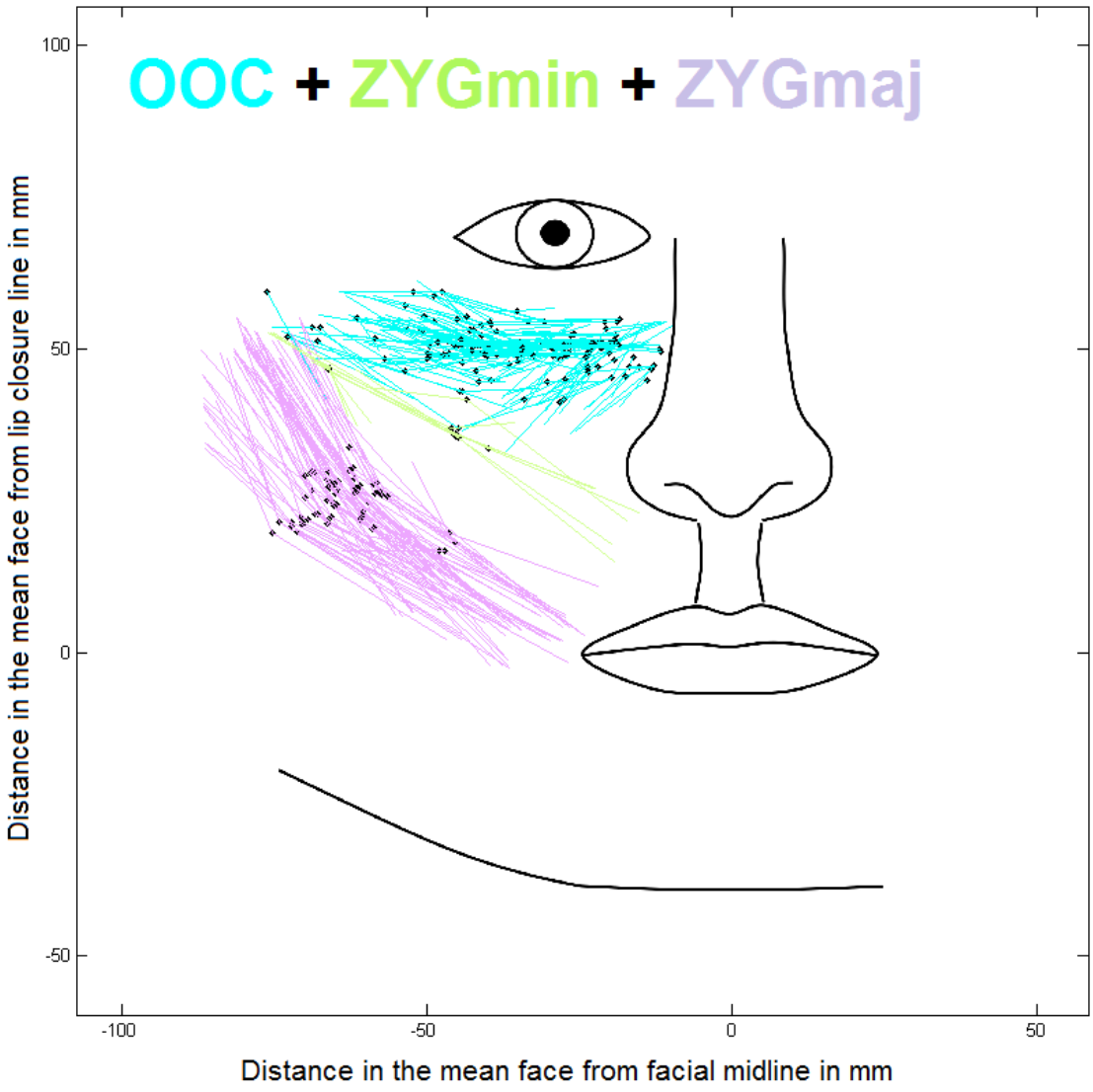


Figure 29: All subjects' motor units of orbicularis oris muscle (OOC), zygomaticus minor muscle (ZYGmin) and zygomaticus major muscle (ZYGmaj). Clarification of the assignment of MUs to midfacial muscles and demarcation of nearby midfacial muscles. High-density surface electromyography (HDsEMG) measurements of the midfacial muscles. Department of orthodontics, Ulm University, 2014.

3.4.4 Levator labii superioris muscle

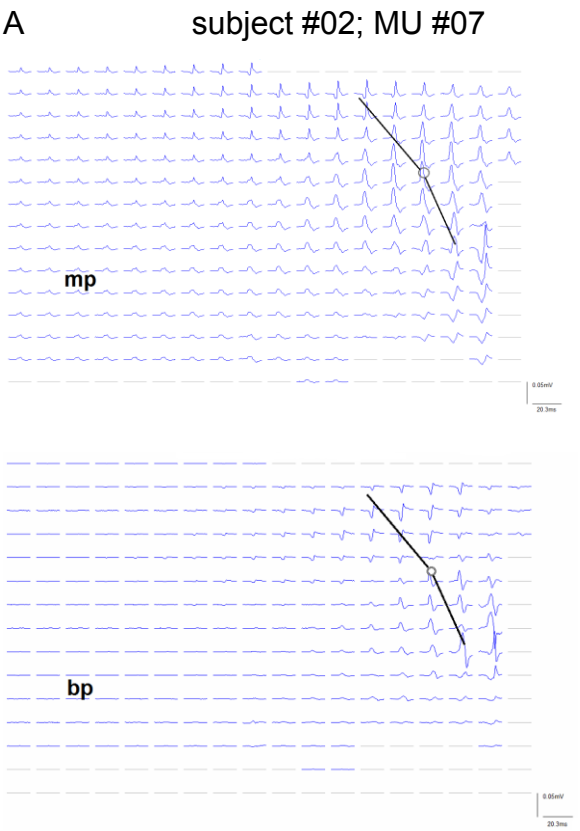


Figure 30: Exemplary template of a levator labii superioris muscle motor unit in monopolar (mp) and bipolar-vertical (bp) montage. The motor unit action potential propagates in opposite directions, i.e. latero-cranially towards the inferior margin of the orbit and medio-caudally towards the upper lip. The lack of motor unit action potentials in the first and second row from the bottom refers to channels with bad connection that are omitted.
High-density surface electromyography (HDsEMG) measurements of the midfacial muscles. Department of orthodontics, Ulm University, 2014.

LLS MUs were found in 12 subjects and in attempted selective contractions of all muscles investigated (Table 2). The occurrence of LLS was not necessarily associated with the occurrence of LLSan, i.e. sole LLS or LLSan or both appeared within one subject.

Figure 30 shows a characteristic LLS MU in monopolar and bipolar montage. The flat decline in amplitude in monopolar montage illustrates the muscle's upper part's location under OOC.

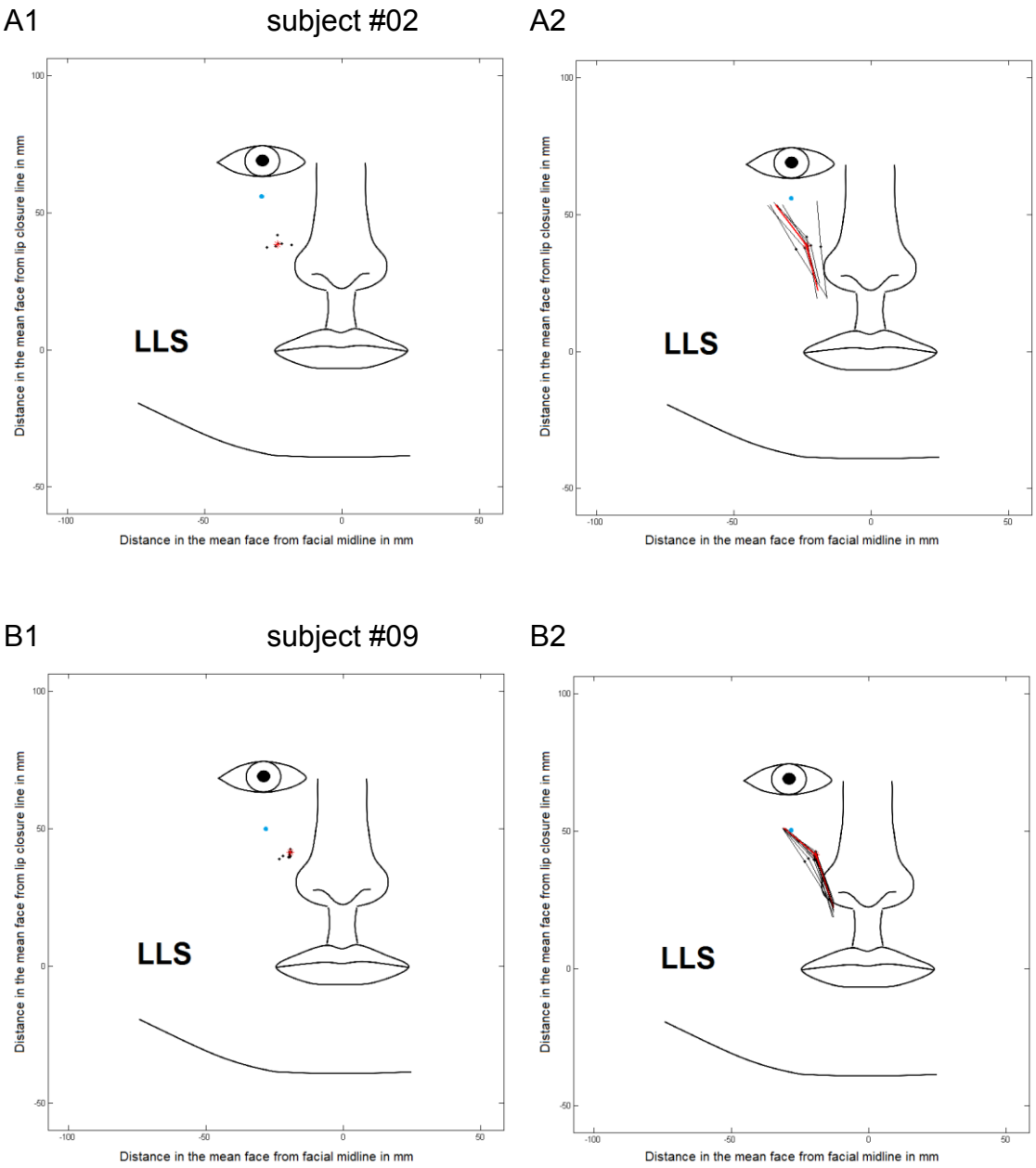


Figure 31: Representative levator labii superioris muscle (LLS) motor units and median motor units (red) of two subjects (A, B) in the normalized face without (A1, B1) and with (A2, B2) fiber orientation. The blue dot illustrates the subjects' individual inferior margin of the orbit. Note the endplate distribution in a band perpendicular to the fiber orientation.
High-density surface electromyography (HDsEMG) measurements of the midfacial muscles. Department of orthodontics, Ulm University, 2014.

LLS endplates appear as clusters in the muscle's cranial half or are arranged in a band perpendicular to the fiber orientation, i.e. similar cluster locations among individuals. They are located lateral to the endplates of LLSan, i.e. further lateral to the nose at half height of the nose. As an example,

Figure 31 B shows a subject's LLS in the normalized face with the endplates arranged in a line perpendicular to the fiber orientation. LLS MUs generally show

two MUAPs propagating in opposite directions from the endplate. The superior fibers run straight cranial or in latero-cranial direction to a point lateral to the inferior margin of the orbit. The inferior fibers run in medio-caudal direction towards the upper lip and end at a level with the nose base.

LLS MUs were distinguished from OOC by the appearance of the rather vertical fiber orientations compared to OOC, which is especially true for the appearance of inferior fibers converging towards OOR. To distinguish LLS from LLSan, the orientation of the superior LLS fibers from in a straight cranial or cranial direction, compared to the medio-cranial direction of the LLSan fibers, was the crucial factor.

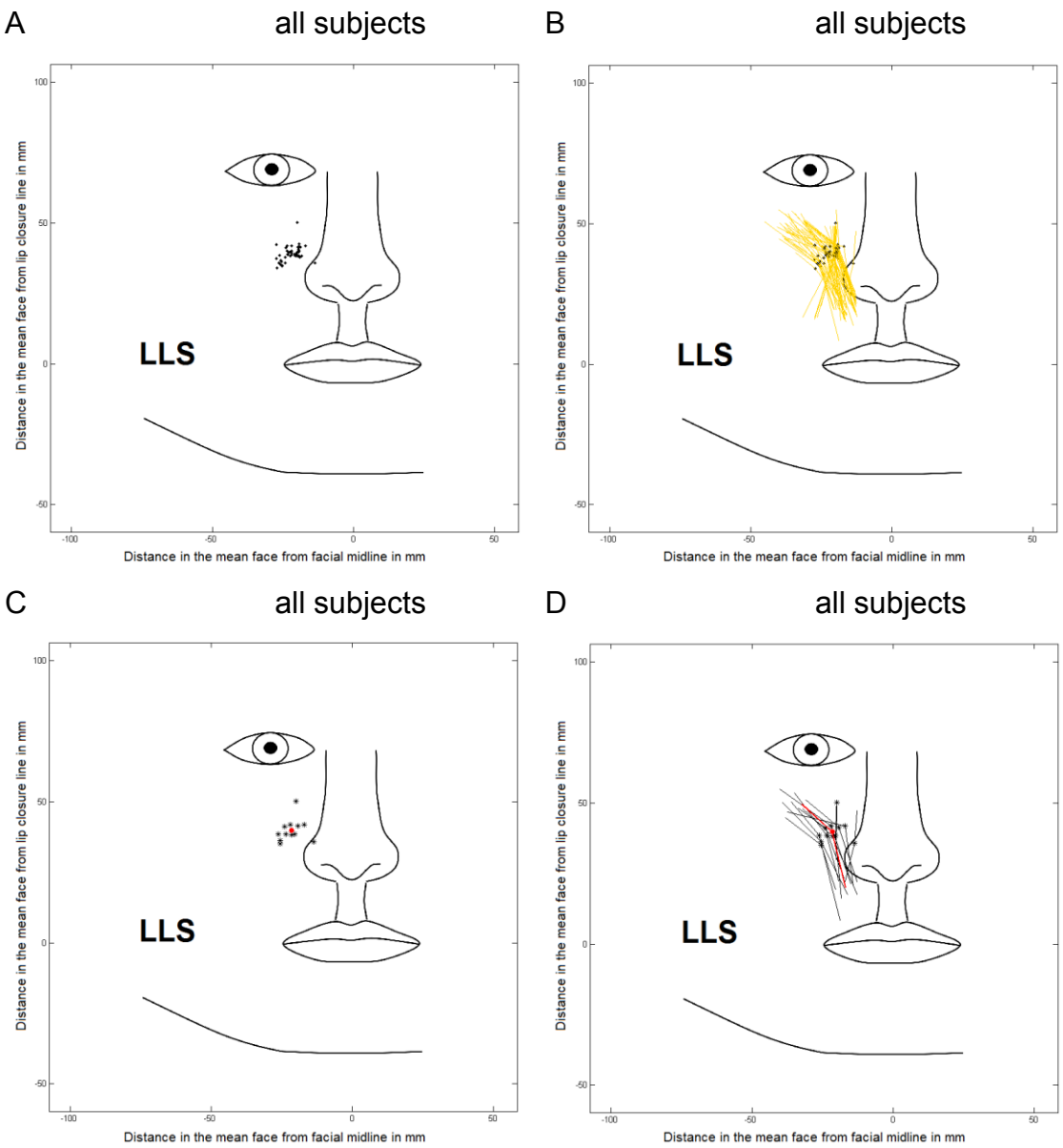


Figure 32: All levator labii superioris (LLS) motor units in the normalized face: endplates without (A) and with (B) fiber orientation. All median levator labii superioris motor units (*) and mean of the median values (red) in the normalized face without (C) and with (D) fiber orientation. The illustration of a motor unit on the ala of the nose (A-D) occurs due to schematic illustration of the nose and the 2D display of this area.
High-density surface electromyography (HDsEMG) measurements of the midfacial muscles. Department of orthodontics, Ulm University, 2014.

3.4.5 Levator labii superioris alaeque nasi muscle

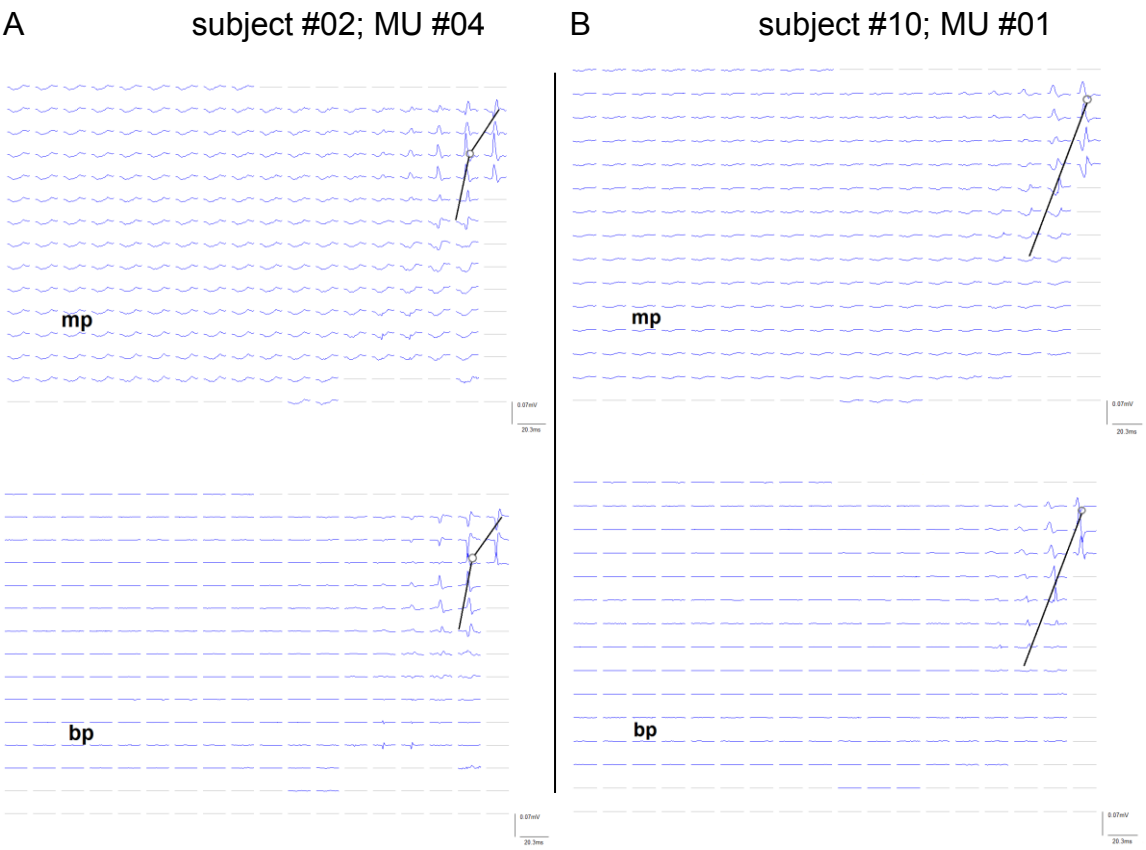


Figure 33: Two representative levator labii superiors alaeque nasi muscle (LLSan) motor units (A, B) in monopolar (mp) and bipolar-vertical (bp) montage. Note that the motor unit action potential could only be traced to the medial border of the electrode grid.
High-density surface electromyography (HDsEMG) measurements of the midfacial muscles. Department of orthodontics, Ulm University, 2014.

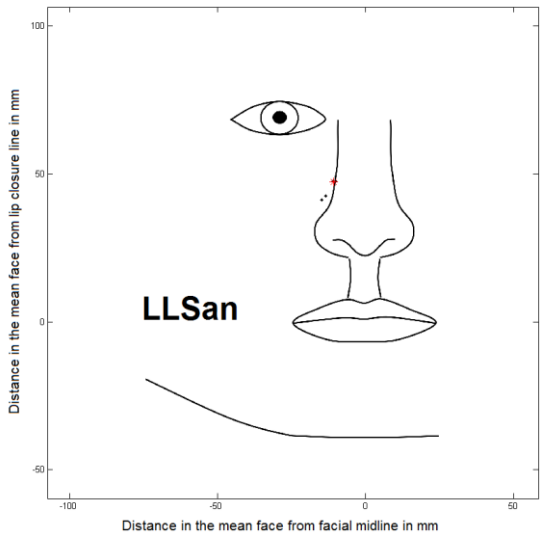
LLSan MUs were found in thirteen subjects. The vast majority of these were found in attempted contraction of LLS (Table 2). Contraction of LAO, OOC, ZYGmaj and ZYGmin, however, involved LLSan as well.

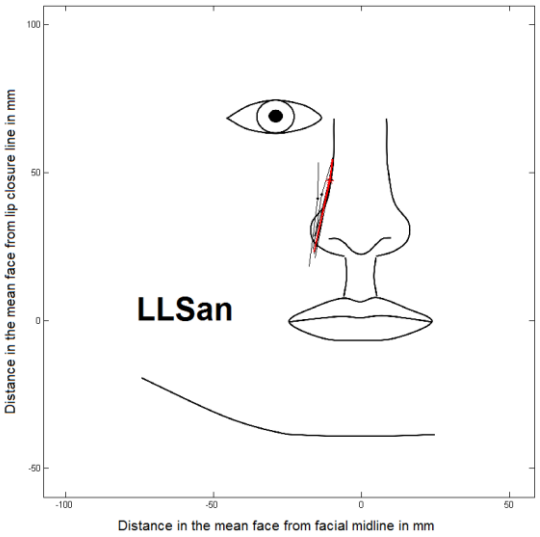
Figure 33 shows two characteristic MUs of LLSan with sharp waveforms in monopolar montage indicating LLSan's superficial location. The bipolar templates illustrate the motor endplate's location. In subject #02 (

Figure 33 A), the MUAPs propagate in two directions and represent the relatively vertical fiber orientation in medio-cranial and latero-caudal direction. In contrast, subject #10 (

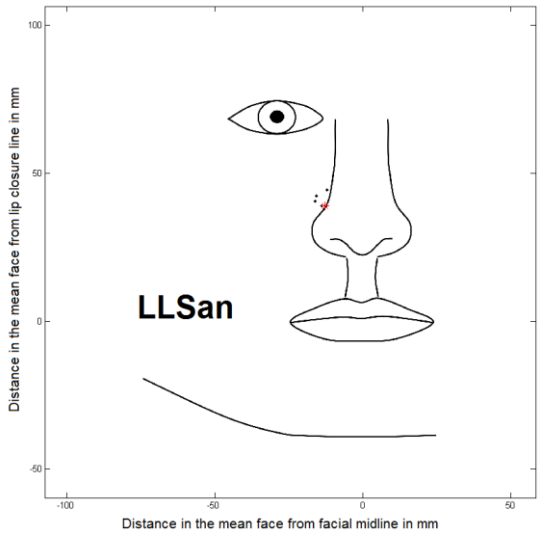
Figure 33 B) shows one MUAP propagating in latero-caudal direction.

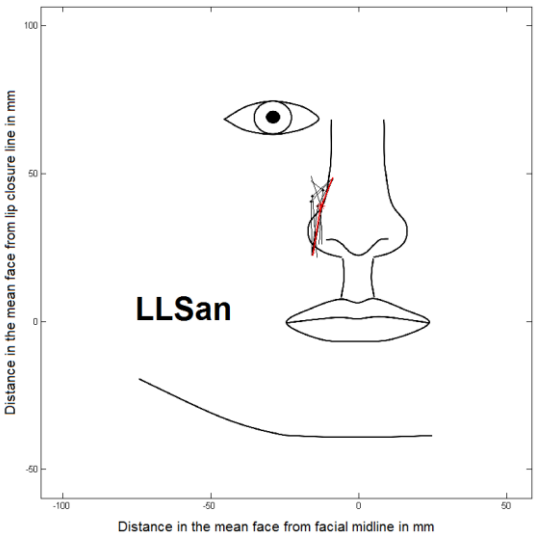
A1 subject #03 A2





B1 subject #05 B2





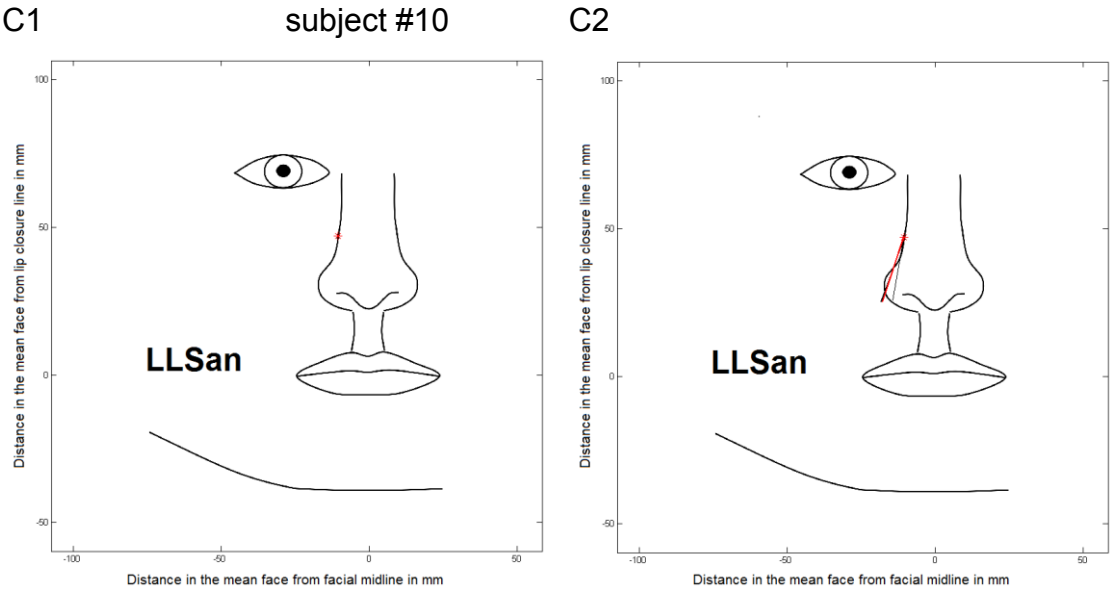


Figure 34: Individual subjects levator labii superioris alaeque nasi muscle (LLSan) motor units (black) and median motor units (red) in the normalized face: endplates without (A1, B1, C1) and with (A2, B2, C2) fiber orientation.
High-density surface electromyography (HDsEMG) measurements of the midfacial muscles. Department of orthodontics, Ulm University, 2014.

LLSan endplates are located directly lateral to the nose above the nasal wing. Most endplates show propagation in two opposite directions. The superior fiber part runs in medio-cranial direction onto the bridge of the nose, which was decisive to distinguish LLSan from LLS. The inferior fiber part runs in latero-caudal direction along the ala of the nose to the upper lip and is generally at least twice as long as the superior fiber part. Three subjects showed mere propagation in latero-caudal direction (e.g. see
Figure 34 C). The latero-caudally directed fibers' end is located on the level of the nose base. The fibers showed a curved course around the ala of the nose on their way to the upper lip.

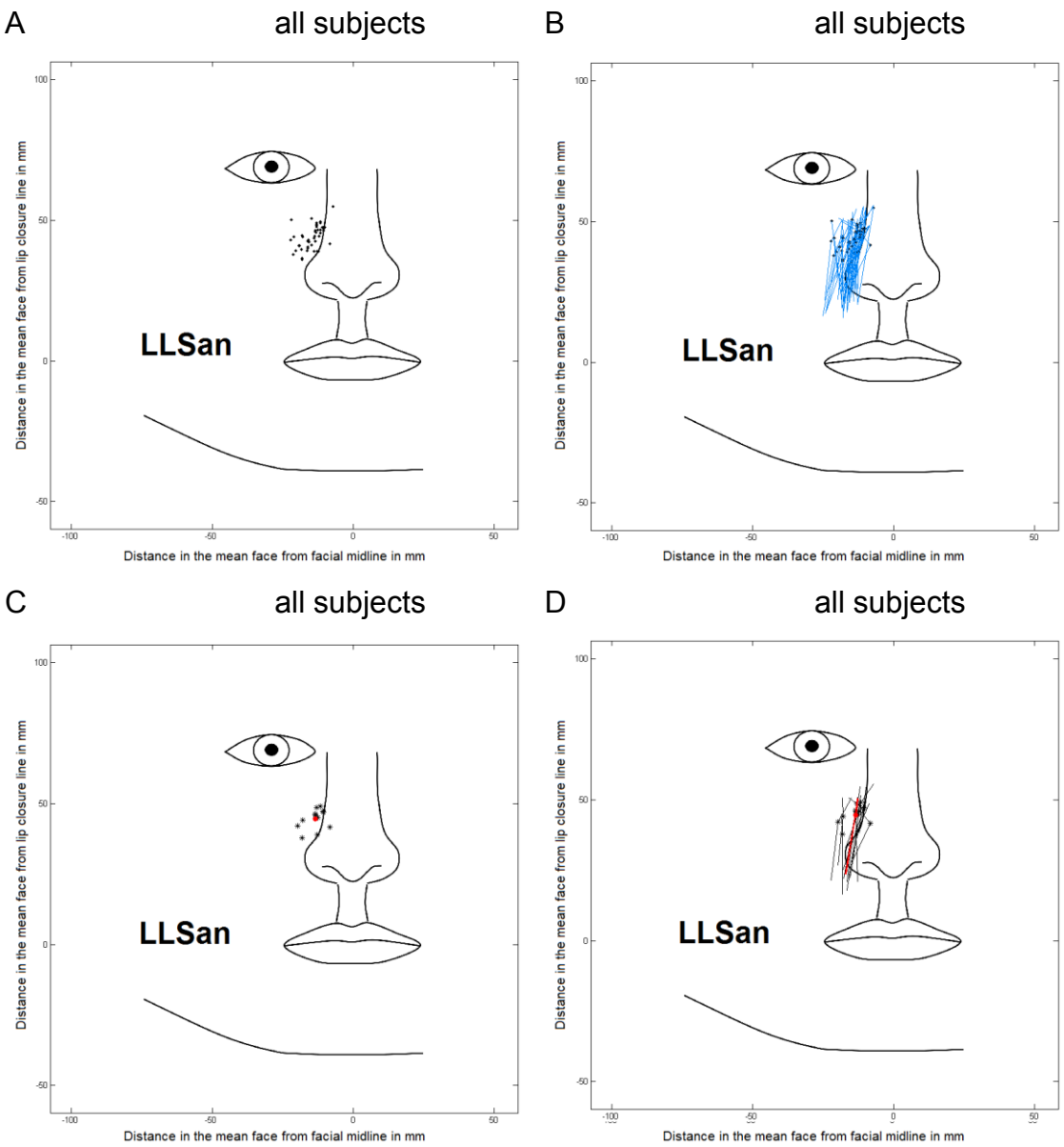


Figure 35: All subjects' levator labii superioris aleque nasi muscle (LLSan) motor units in the normalized face without (A) and with (B) fiber orientation. All levator labii superioris aleque nasi muscle median motor units (*) and mean of the median values (red) in the normalized face without (C) and with (D) fiber orientation.
High-density surface electromyography (HDsEMG) measurements of the midfacial muscles. Department of orthodontics, Ulm University, 2014.

3.4.6 Buccinator muscle

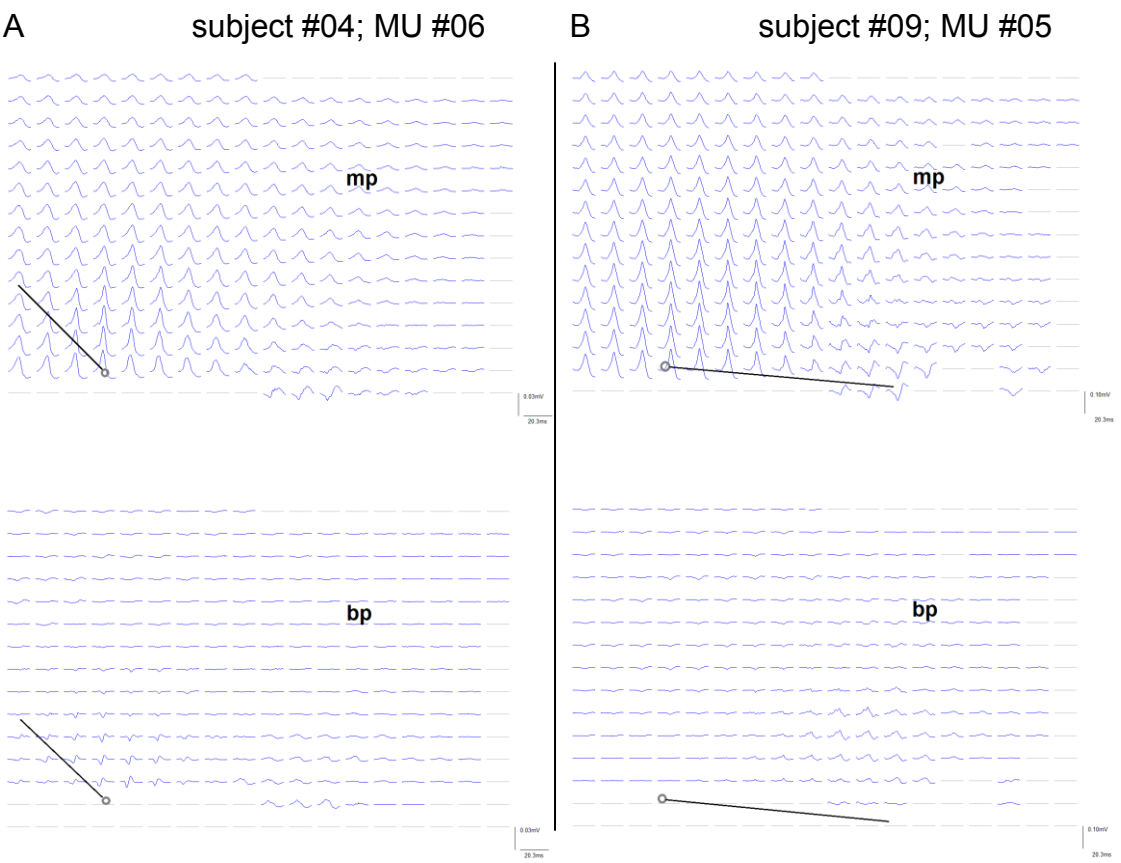


Figure 36: Characteristic templates of two subjects (A, B) representing motor unit action potentials of the buccinator muscle in monopolar (mp) and bipolar-vertical montage (bp). Both templates show similar endplate locations and characteristic flat declines in amplitude in monopolar montage. Fibers are orientated either in latero-cranial (A) or medio-caudal direction towards the modiolus (B). Due to endplate location at the caudal border of the grid, the signal phase reversal in bipolar montage could not be detected.
High-density surface electromyography (HDsEMG) measurements of the midfacial muscles. Department of orthodontics, Ulm University, 2014.

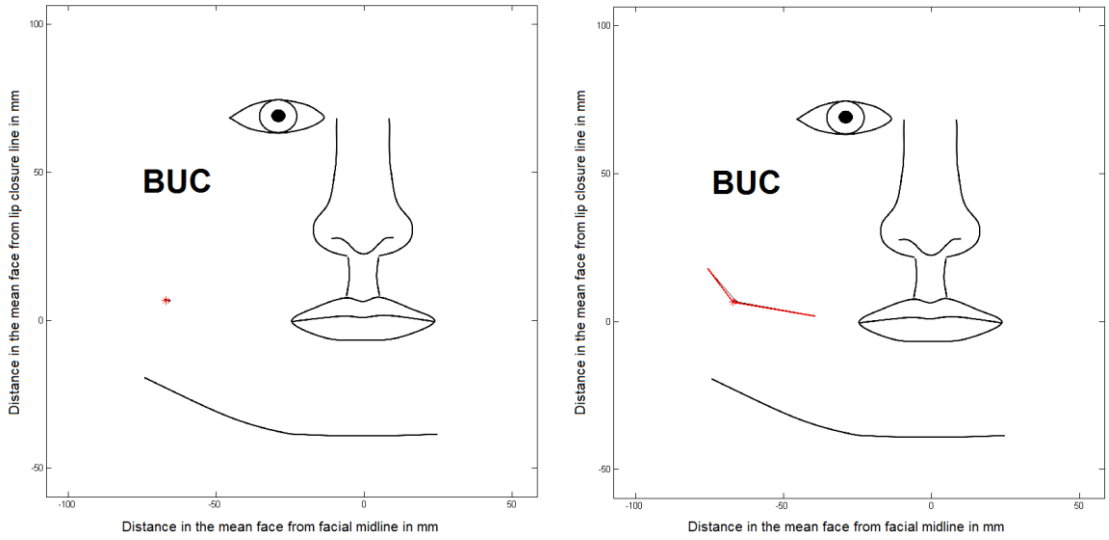
In fifteen out of sixteen subjects BUC MUs could be identified; most of them during selective contraction of BUC (59.9 %) and on the caudal border or the lateral grid. Further BUC MUs were found in contractions of LAO, LLS, OOC, OOR, ZYGmaj and ZYGmin (Table 2).

Figure 36 shows two representative templates of BUC MUs in monopolar and bipolar-vertical montage of two subjects (A and B). The flat decline in amplitude in monopolar montage illustrates BUCs deep anatomic location under the cheek's fat tissue. Both templates show similar endplate location but different fiber topography.

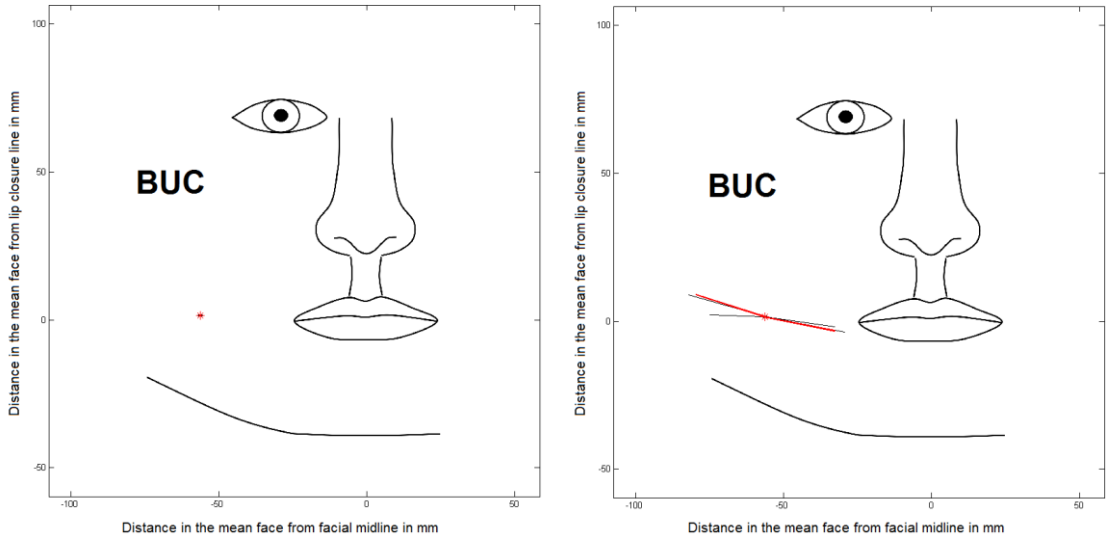
Figure 36 A is an example for a latero-cranial fiber orientation;

Figure 36 B shows fibers in medio-caudal direction that run towards the modiolus.

A1 subject #04 A2



B1 subject #07 B2



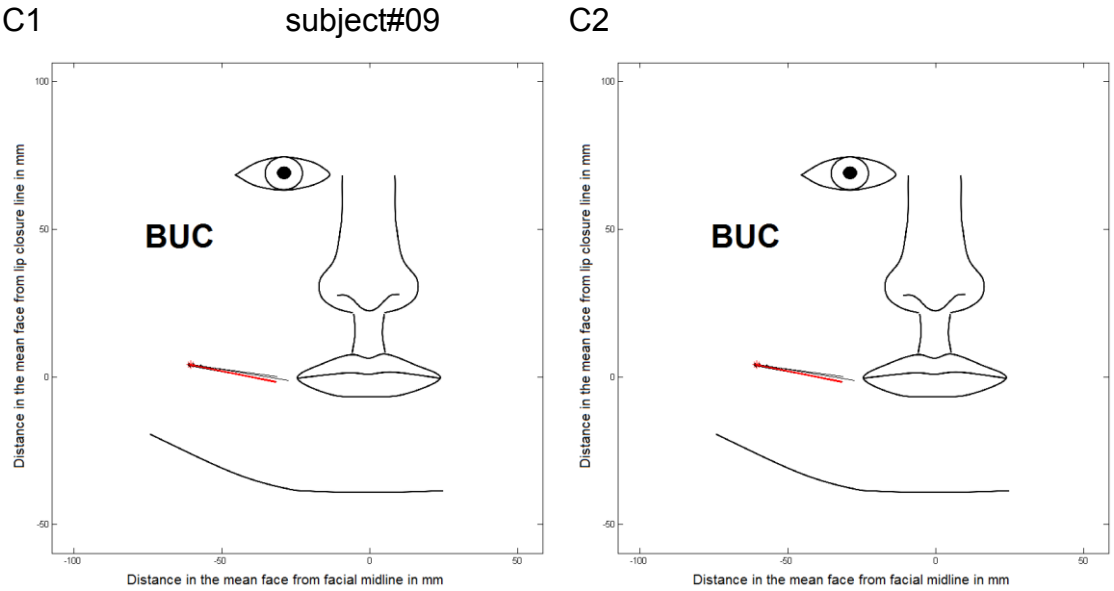


Figure 37: Representative subjects' total buccinator muscle (BUC) motor units (black) and median motor units (red) in the normalized face with (A2, B2, C2) and without (A1, B1, C1) fiber orientation. They show similar endplate locations but different kinds of fiber orientation. The endplates are located with a distance of several centimetres from the mouth corner slightly above the connecting line of the corners of the mouth.
High-density surface electromyography (HDsEMG) measurements of the midfacial muscles. Department of orthodontics, Ulm University, 2014.

In subjects' individual results, BUCs endplates appear clustered. However, all subjects' data (

Figure 38) reveal variable medio-lateral cluster location among subjects along the caudal border of the lateral electrode grid. Their medio-lateral location corresponds to an area distanced about one width of the oral fissure and in a vertical dimension between the corner of the mouth and the philtrum (

Figure 38 A). Overall results and subjects' individual results (

Figure 37) both illustrate BUCs variations in fiber orientation. The vast majority of BUC MUs show one propagation direction running almost horizontally towards the modiolus (

Figure 37 C). Four subjects (#2,#3#10,#16) show one latero-cranial MUAP direction that varies in angulations from almost horizontally to steeply rising (

Figure 37 A).

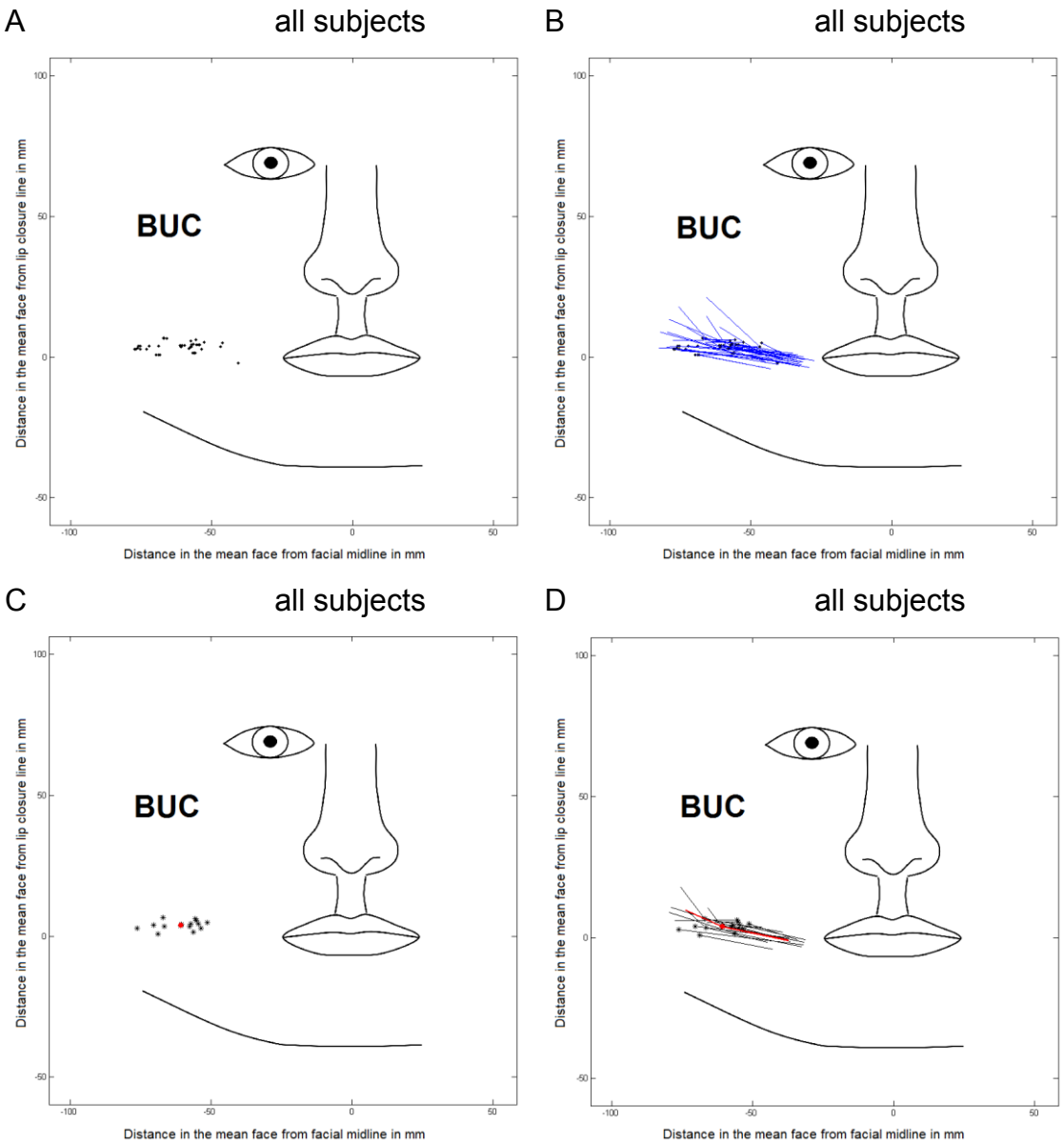


Figure 38: All subjects' buccinator muscle (BUC) motor units without (A) and with (B) fiber orientation. All median buccinator muscle motor units (*) and mean of the median values (red) in the normalized face without (C) and with (D) fiber orientation.
High-density surface electromyography (HDsEMG) measurements of the midfacial muscles. Department of orthodontics, Ulm University, 2014.

BUC MUs were distinguished from ZYGmaj MUs by endplate topography as BUC MUs are located more caudal than ZYGmaj MUs close to or on the caudal border of the lateral electrode grid.

3.4.7 Levator anguli oris

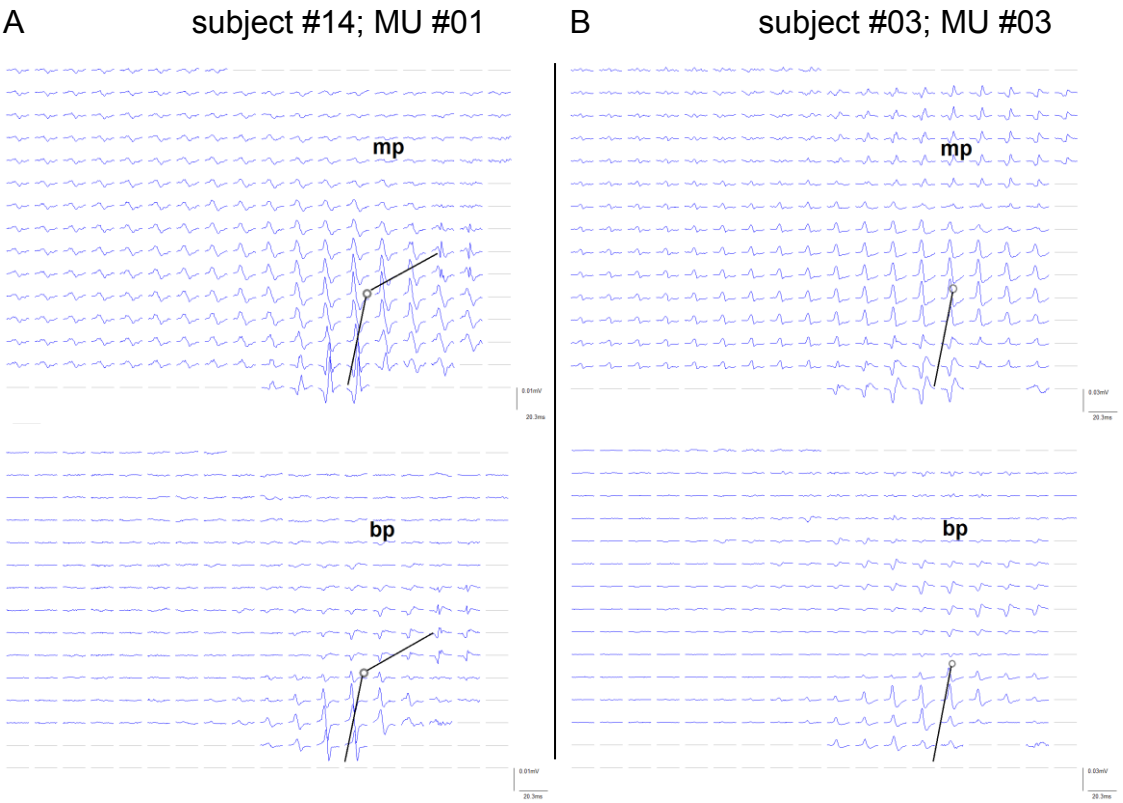
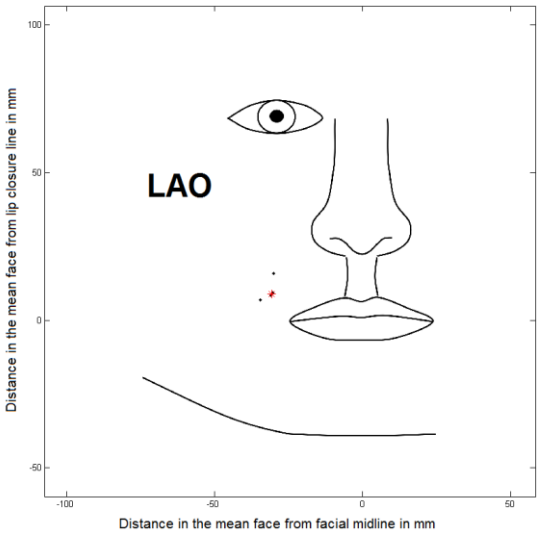
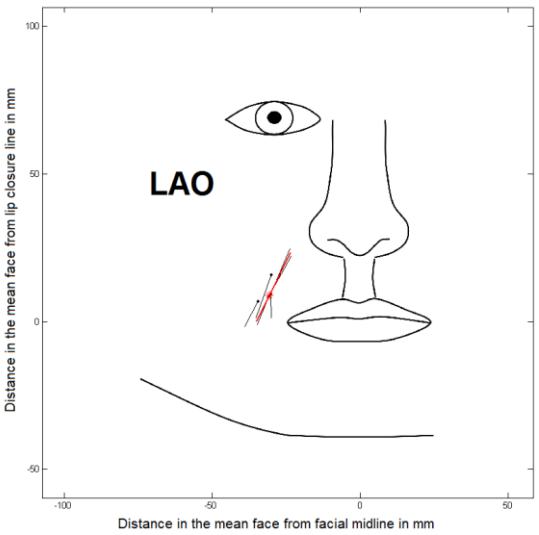


Figure 39: Two representative levator anguli oris motor units from two subjects in monopolar (mp) and bipolar-vertical (bp) montage. The opposite signal polarity in the bipolar templates illustrates the motor endplates' location. The motor unit action potential propagates in one (B) or two (A) directions. The lack of motor unit action potentials in the first and second row (A and B) from the bottom refers to channels with bad connection that are omitted.
High-density surface electromyography (HDsEMG) measurements of the midfacial muscles. Department of orthodontics, Ulm University, 2014.

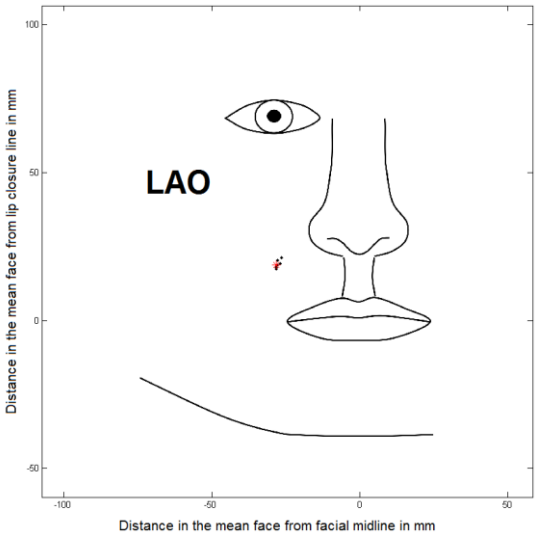
All subjects showed MUs of LAO, whereat 23.5% of LAOs total MUs were found in attempted selective contraction of this muscle (Table 2). All kind of attempted selective contractions showed LAO MUs, yet most of them were found in task for contraction of BUC (30.2%). Figure 39: spells out the flat decline in amplitude in monopolar montage of two representative MUs indicating LAOs deep location. The opposite signal polarity in bipolar montage illustrates motor endplate locations.

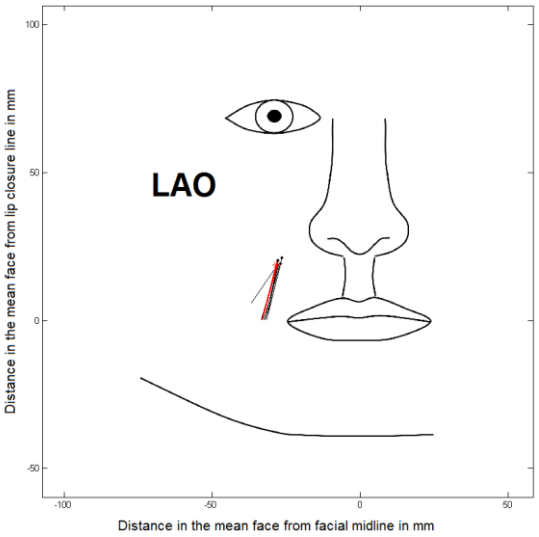
A1 subject #01 A2





B1 subject #03 B2





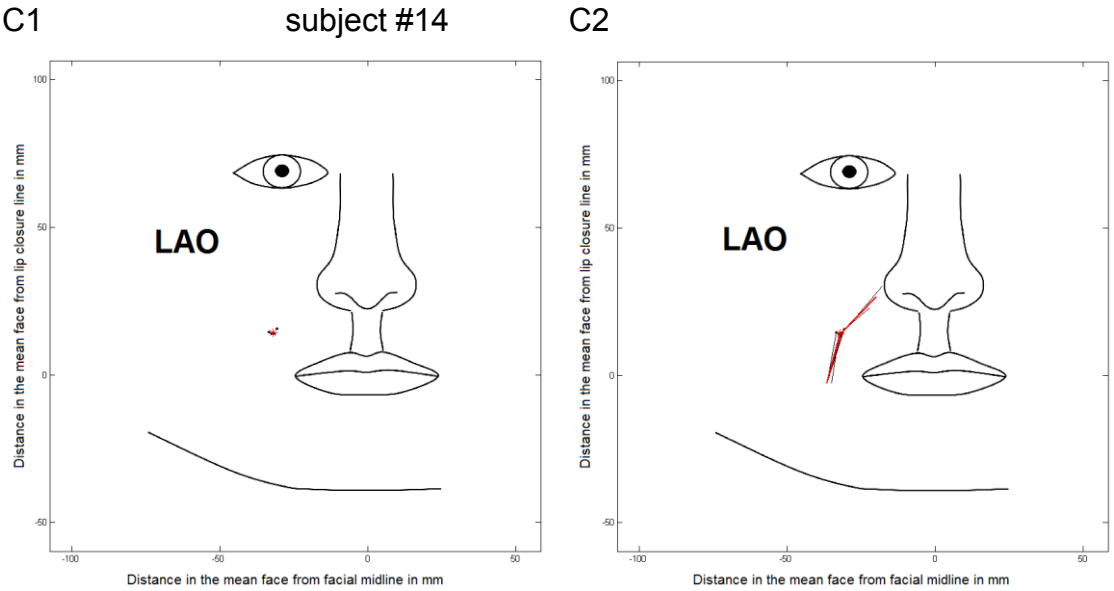


Figure 40: Representative subjects' total levator anguli oris muscle (LAO) motor units (black) and median motor units (red) in the normalized face with (A2, B2,C2) and without (A1, B1,C1) fiber orientation.
High-density surface electromyography (HDsEMG) measurements of the midfacial muscles. Department of orthodontics, Ulm University, 2014.

LAO showed multiple types of endplate distributions and fiber orientations. All in all, in horizontal dimension, the endplates were breadthways distributed between the outer canthus and the pupil, and in a vertical dimension from the modiolus up to the level of the nose base. Examining the individual subjects, endplates were either clustered latero-cranial to the corner of the mouth (cf.
Figure 40 B and C) or loosely distributed over the muscle (
Figure 40 A) or appeared in a combination of clustered endplates and additional eccentric endplates. Concerning fiber orientation, the individuals showed high inter-individual variability. The majority of MUs show one propagation direction in latero-caudal or medio-caudal direction towards the modiolus. Due to lack of muscle coverage in the area of the modiolus, the MUAP could only be traced to the electrode grids caudal border. Further MUs show fibers running in medio-cranial direction towards the ala of the nose or two fiber directions, whereof one is directed to the ala of the nose and the other one towards the modiolus.

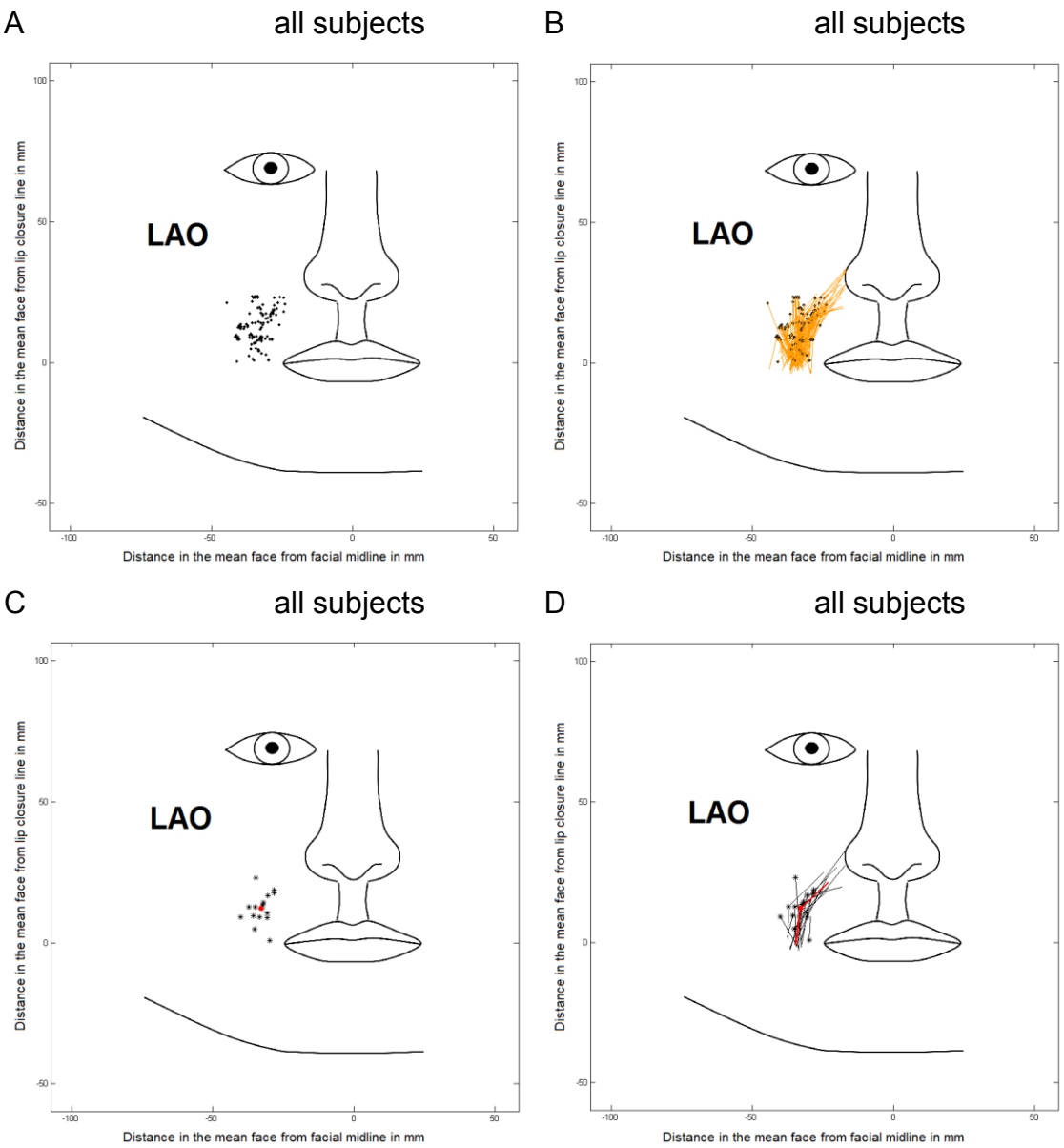


Figure 41: All subjects' levator anguli oris muscle (LAO) motor units without (A) and with (B) fiber orientation. All median levator anguli oris muscle motor units (*) and mean of the median values (red) in the normalized face without (C) and with (D) fiber orientation.
High-density surface electromyography (HDsEMG) measurements of the midfacial muscles. Department of orthodontics, Ulm University, 2014.

LAO MUs were distinguished from OORper MUs by endplate topography and fiber orientation. LAO MUs are located more latero-cranially than OORper MUs with its fibers oriented towards the modiolus or ala of the nose. In contrast, OORper endplates are located closer to the modiolus and their fibers are found more medially and often parallel to the vermillion border.

3.4.8 Incisivus muscle

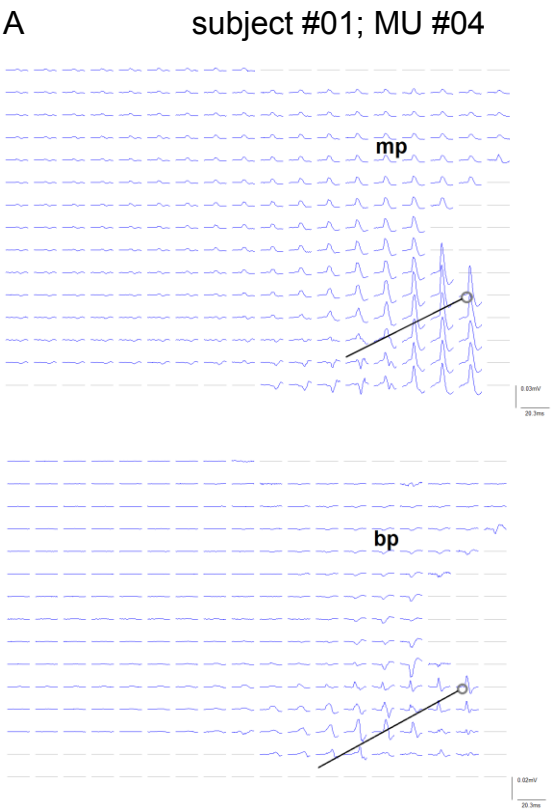


Figure 42: Representative template of an incisivus muscle motor unit in monopolar (mp) and bipolar-vertical (bp) montage. Note the endplate location at the medial border of the electrode grid. The lack of motor unit action potentials in the second and third column from the right refers to channels with bad connection that are omitted.
High-density surface electromyography (HDsEMG) measurements of the midfacial muscles. Department of orthodontics, Ulm University, 2014.

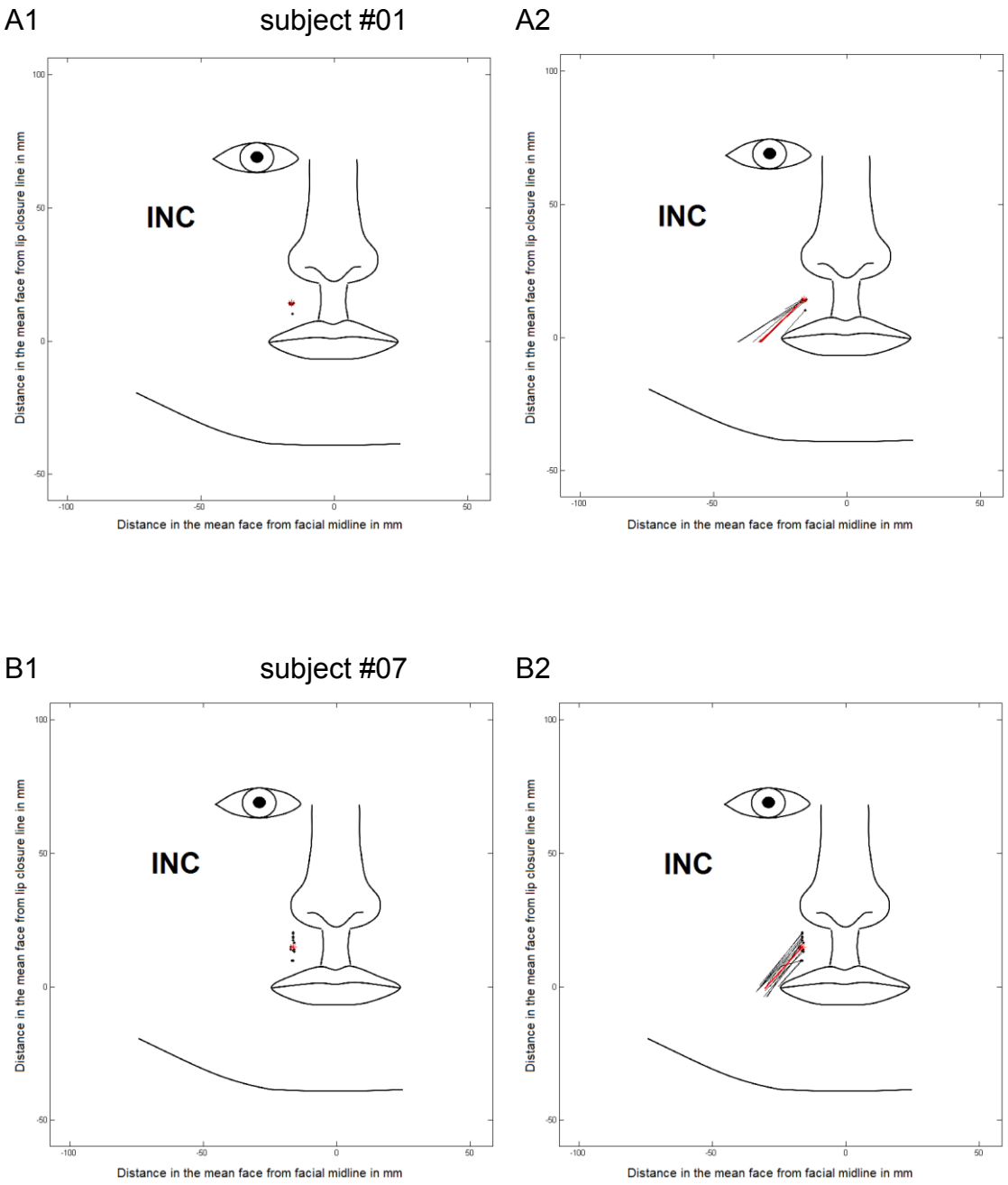


Figure 43: Representative subjects' total incisivus muscle (INC) motor units (black) and median motor units (red) in the normalized face with (A2, B2) and without (A1, B1) fiber orientation.
High-density surface electromyography (HDsEMG) measurements of the midfacial muscles. Department of orthodontics, Ulm University, 2014.

INC was found in ten subjects. Except for ZYGmaj, INC MUs were found in tasks for all muscles, however most often in tasks for INC, OORtan and LAO (Table 2).

Figure 42 shows a MU of INC in monopolar and bipolar-vertical montage. The flat decline in amplitude in the monopolar template identifies the deep location. The

circle indicates the endplate location. The MUAP runs in latero-caudal direction towards the modiolus.

Figure 43 displays two representative subjects' INC MUs in the normalized face. The endplates are identified at the medial border of the grid under the ala of the nose. They appear in a vertical line from the ala of the nose to the upper lip. The fibers are long and oriented in latero-caudal direction towards the modiolus, however often extinct at the caudal border of the grid due to insufficient coverage of the modiolus.

INC MUs were distinguished from OOR MUs, especially from OORper MUs, by their endplate locations at the medial border of the electrode grid and their fiber directions oriented towards the modiolus, which appear not only longer but also inversely oriented when compared to OORper.

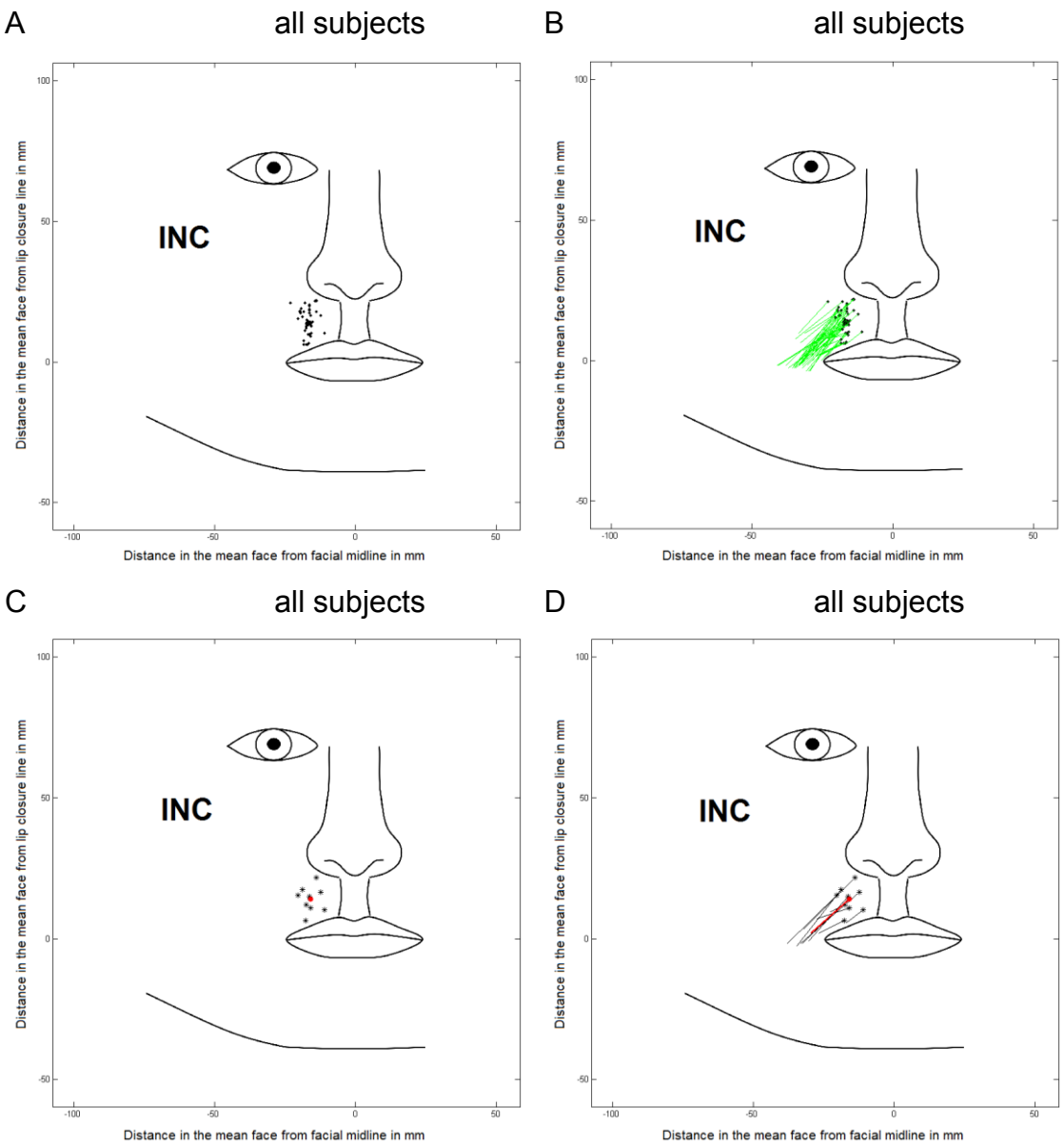


Figure 44: All subjects' incisivus muscle (INC) motor units without (A) and with (B) fiber orientation. All median incisivus muscle motor units (*) and mean of the median values (red) in the normalized face without (C) and with (D) fiber orientation. Note the endplate distribution appearing as a vertical line at the medial border of the electrode grid and the fiber orientation towards the modiolus.
High-density surface electromyography (HDsEMG) measurements of the midfacial muscles. Department of orthodontics, Ulm University, 2014.

3.4.9 Orbicularis oris muscle pars marginalis

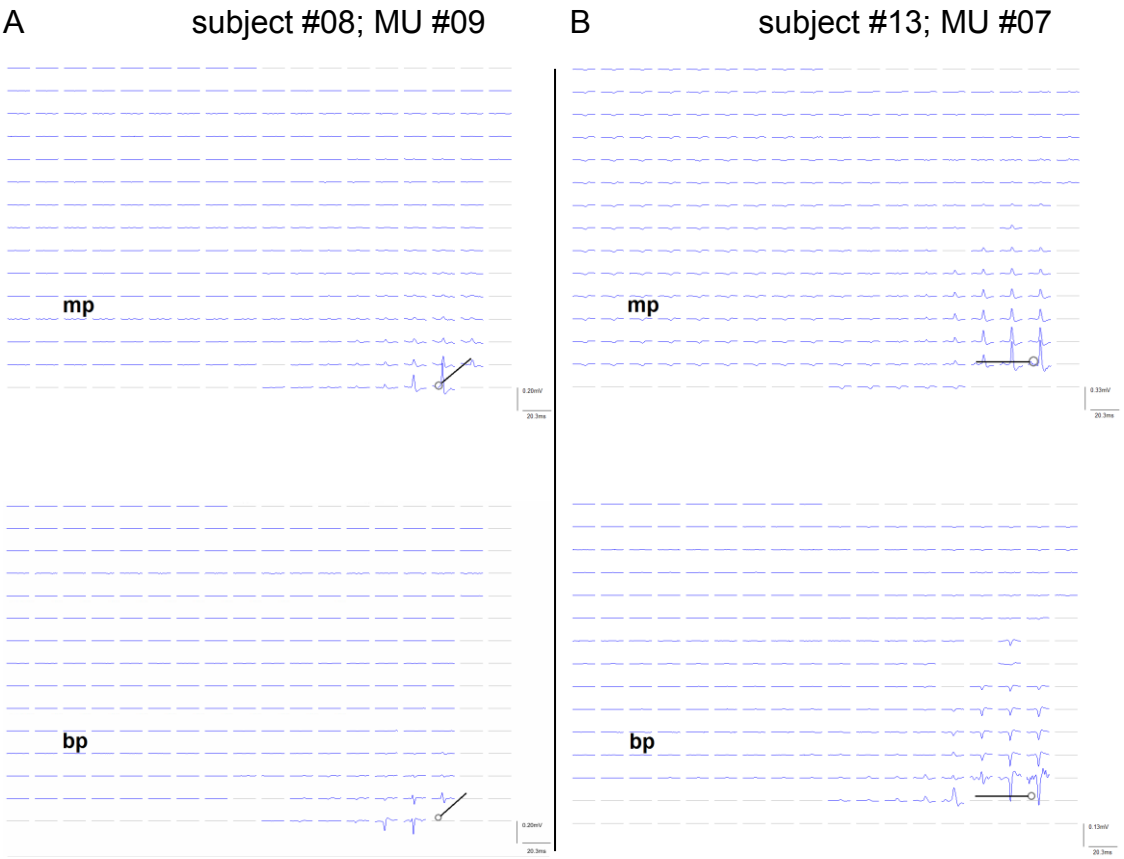


Figure 45: Characteristic templates of two subjects (A, B) for a motor unit of the orbicularis oris muscle pars marginalis (OORmar) in monopolar (mp) and bipolar-horizontal(A) or bipolar-vertical (B) montage (bp). Endplates located in the lower medial corner of the electrode grid. The characteristic fast decline in amplitude in monopolar montage reveals the motor units' superficial location. Fibers orientated in medio-cranial (A) or lateral direction towards the modiolus (B). Due to incomplete coverage of OORmar the signal phase reversal in bipolar montage could not be detected. The lack of motor unit action potentials in the second row from the bottom in (A) and the bottom row in (B) refer to channels with bad connection that are omitted.
High-density surface electromyography (HDsEMG) measurements of the midfacial muscles. Department of orthodontics, Ulm University, 2014.

OORmar MUs were found in eleven subjects, predominantly in contraction of OORmar+per+tan and LAO (Table 2). Figure 45 shows two representative templates of an OORmar MU in monopolar and bipolar-horizontal (A) or bipolar-vertical (B) montage. The extent of coverage of OORmar varied between subjects. The fast decline in amplitude in the monopolar template reveals the MU's superficial location. Signal phase reversal in the bipolar-vertical templates displays the endplate's location.

Figure 46 shows one subject's OORmar. Endplates are either located in the area of the modiolus.

Figure 47 presents all subjects' OORmar MUs and the broad and even distribution of MUs over the muscle. Fibers run parallel to the vermillion zone either towards the facial midline or in lateral direction or both.

A1 subject #08 A2

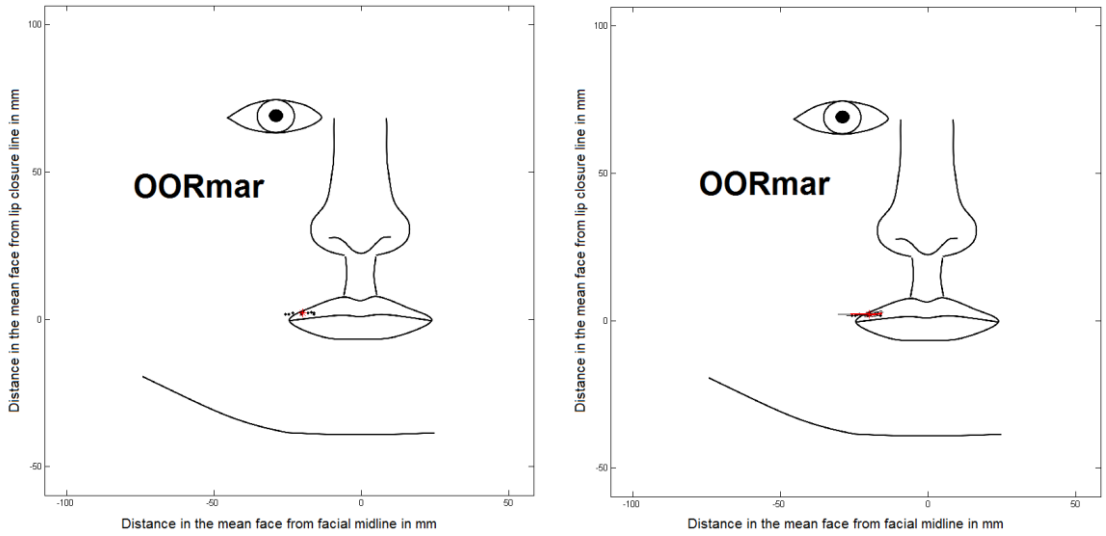


Figure 46: Representative subject's total orbicularis oris muscle pars marginalis (OORmar) motor units (black) and median motor units (red) in the normalized face without (A) and with (B) fiber orientation. The endplates are located in the area of the vermillion zone and the lip red.
High-density surface electromyography (HDsEMG) measurements of the midfacial muscles. Department of orthodontics, Ulm University, 2014.

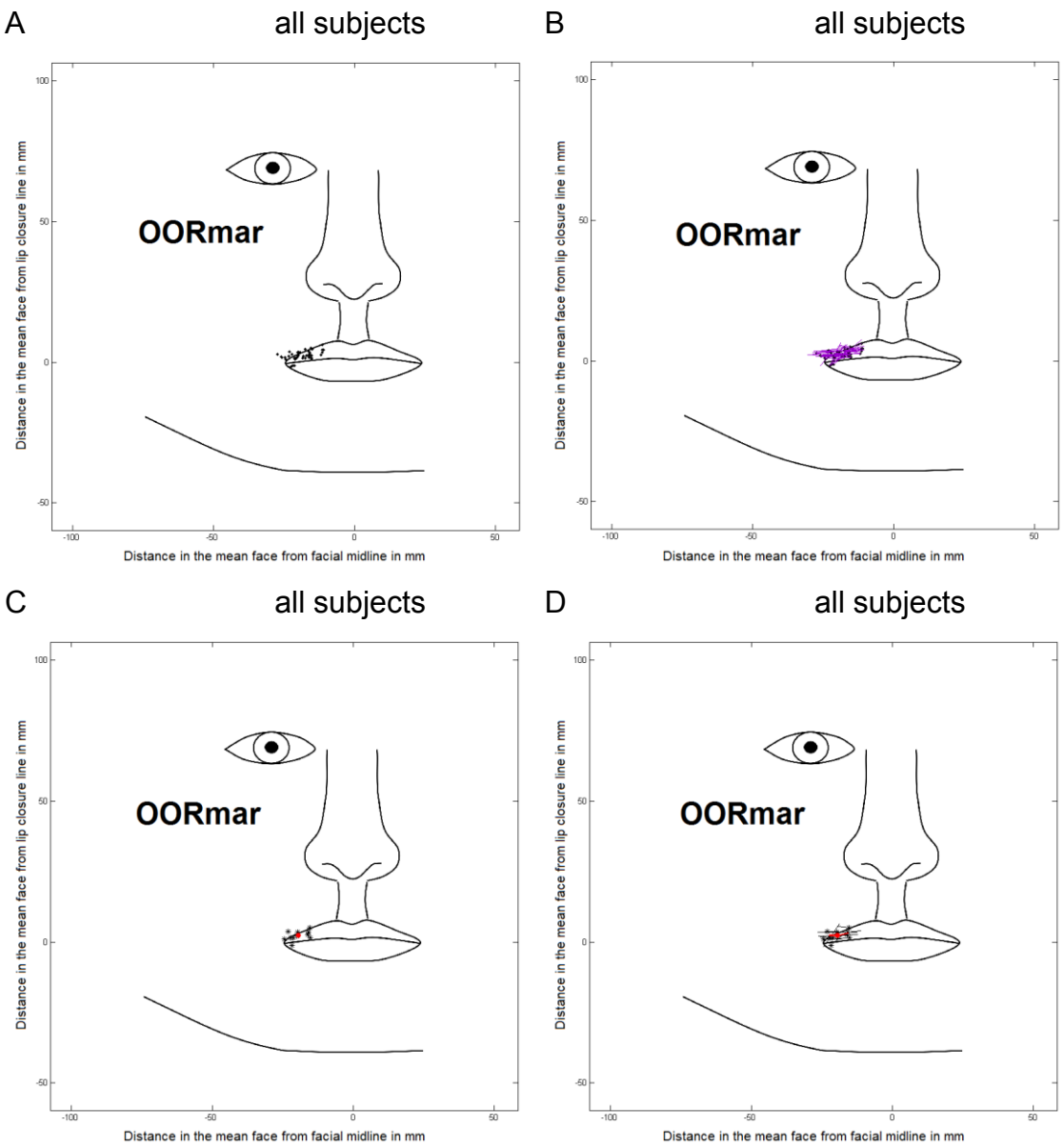


Figure 47: All subjects' orbicularis oris muscle pars marginalis (OORmar) motor units without (A) and with (B) fiber orientation in the normalized face. All median orbicularis oris muscle pars marginalis motor units (*) and mean of the median values (red) in the normalized face without (C) and with (D) fiber orientation. Note the schematic representation of the lip closure line in the normalized face, i.e. the display of the OORmar MU in the lower lip in A-D.
High-density surface electromyography (HDsEMG) measurements of the midfacial muscles. Department of orthodontics, Ulm University, 2014.

3.4.10 Orbicularis oris muscle pars peripheralis

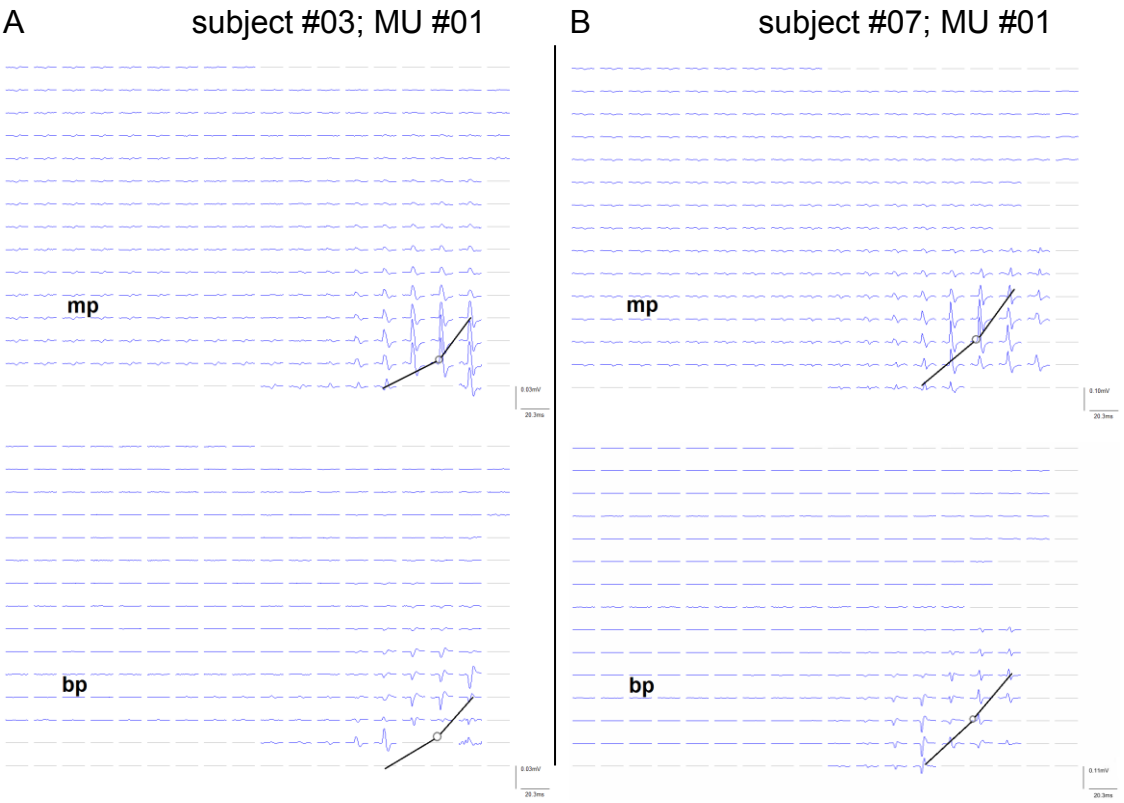
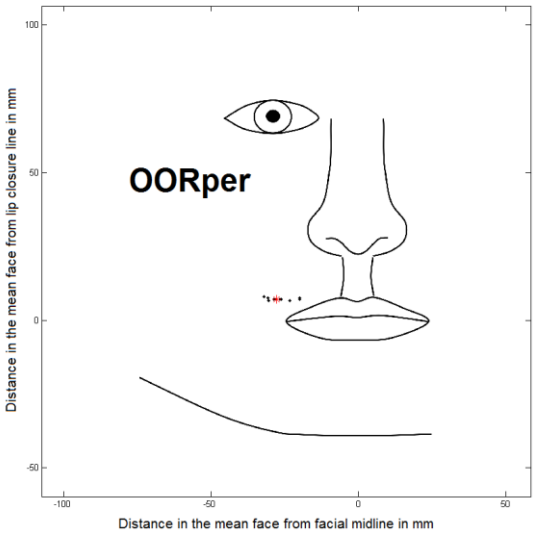


Figure 48: Two representative motor units of orbicularis oris pars peripheralis muscle in monopolar (mp) and bipolar-vertical (A) or bipolar-horizontal (B) (bp) montage. The fast decline in amplitude in the monopolar templates indicates the muscle's superficial location. The position of signal phase reversal in the bipolar-vertical templates indicates the endplates' location. The lack of some motor unit action potentials refers to channels with bad connection that are omitted. Therefore the signal phase reversal in bipolar montage (B) is not visible.
High-density surface electromyography (HDsEMG) measurements of the midfacial muscles. Department of orthodontics, Ulm University, 2014.

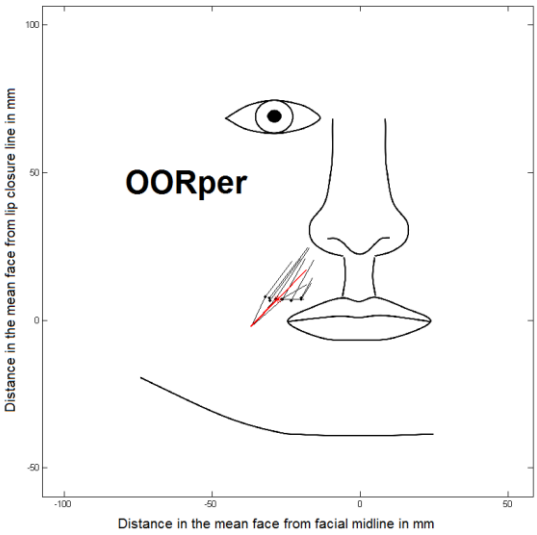
All subjects showed MUs belonging to OORper, most of which in contraction of OOR (Table 2).

Figure 48 shows two representative MUs of OORper in monopolar and bipolar-vertical (A) or bipolar-horizontal (B) montage. The fast decline in amplitude in the monopolar template indicates the MUs superficial location.

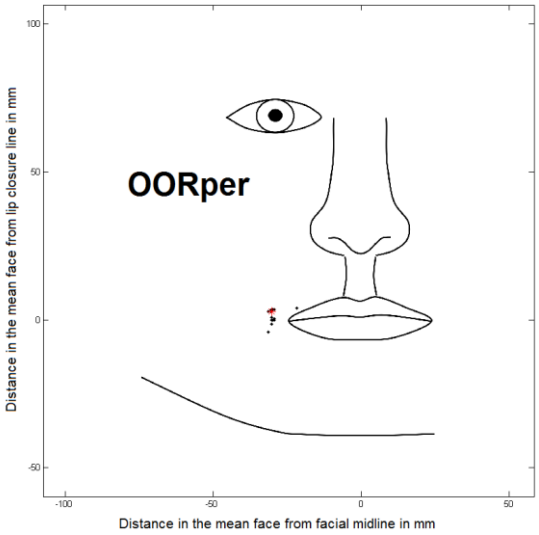
A1 subject #02



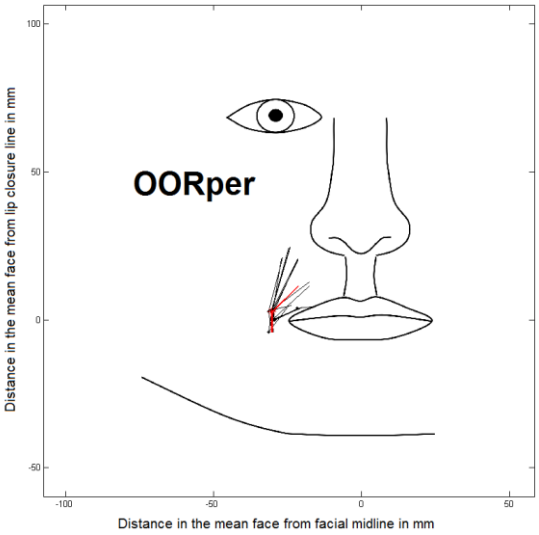
A2



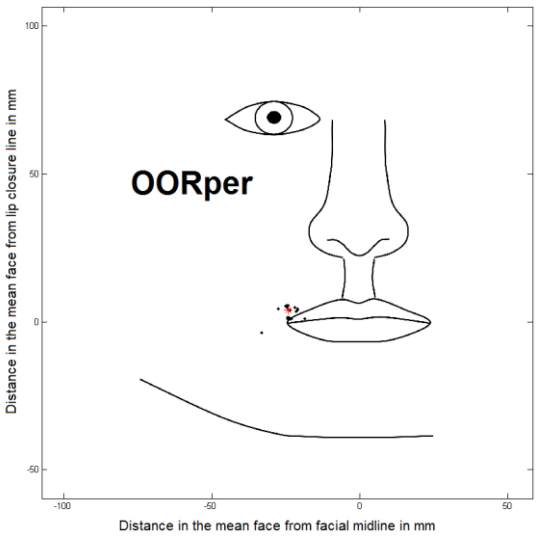
B1 subject #06



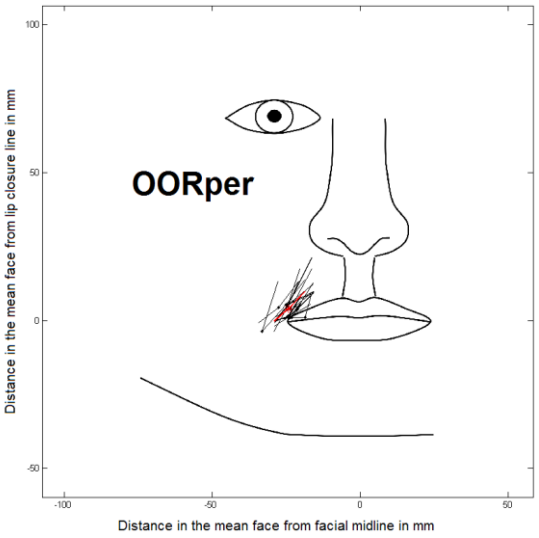
B2



C1 subject #07



C2



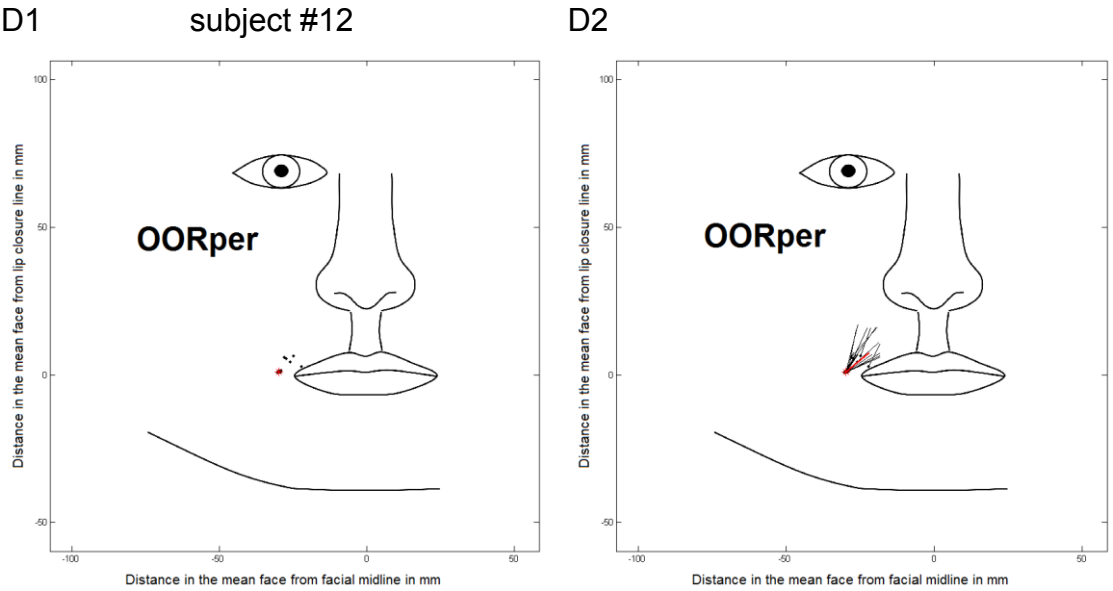


Figure 49: Representative subjects' total orbicularis oris muscle pars peripheralis (OORper) motor units (black) and median motor units (red) in the normalized face with (A2, B2, C2, D2) and without (A1, B1, C1, D1) fiber orientation.
High-density surface electromyography (HDsEMG) measurements of the midfacial muscles. Department of orthodontics, Ulm University, 2014.

Endplate location, number of fibers per endplate and fiber orientation show high inter-individual variability. Endplates are either arranged in a line (A), clustered in the area of the modiolus (B, D) or distributed over the muscle. Fibers run either parallel to the vermillion border in latero-caudal direction and converge towards the modiolus or fibers rise from the modiolus like a fan and run in medio-cranial direction. Due to the fibers' illustration as vectors, it is not possible to display the fibers curved course around the oral fissure as seen in the MUAP movies. However,

Figure 50 shows all OORper MUs and thereby OORper's dense network of fibers and the distribution of endplates over the muscle with a predominant cluster in the area of the modiolus.

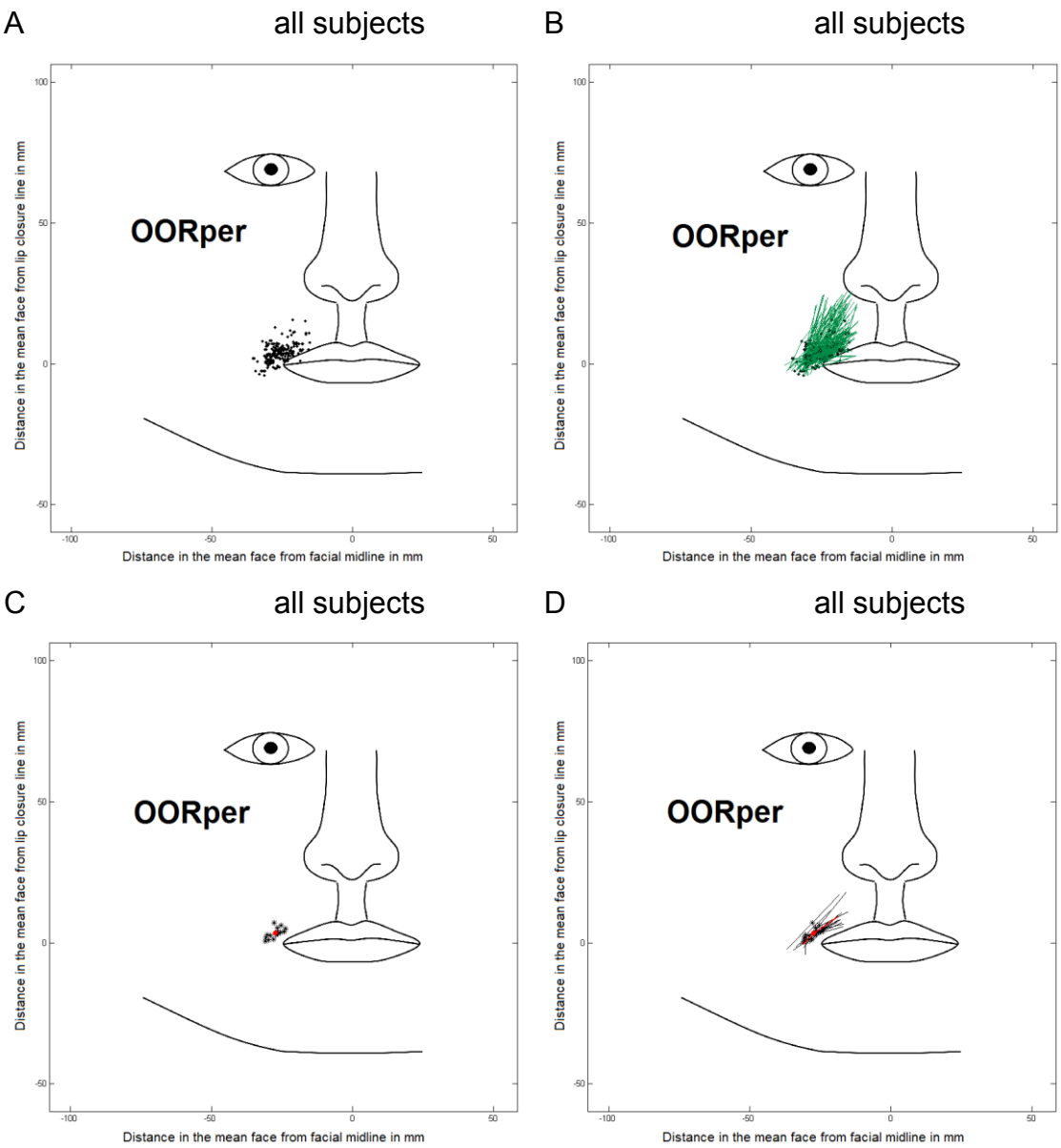


Figure 50: All subjects' orbicularis oris muscle pars peripheralis (OORper) motor units without (A) and with (B) fiber orientation. All median orbicularis oris muscle pars peripheralis motor units (*) and mean of the median values (red) in the normalized face without (C) and with (D) fiber orientation.
High-density surface electromyography (HDsEMG) measurements of the midfacial muscles. Department of orthodontics, Ulm University, 2014.

3.4.11 Orbicularis oris muscle pars tangentialis

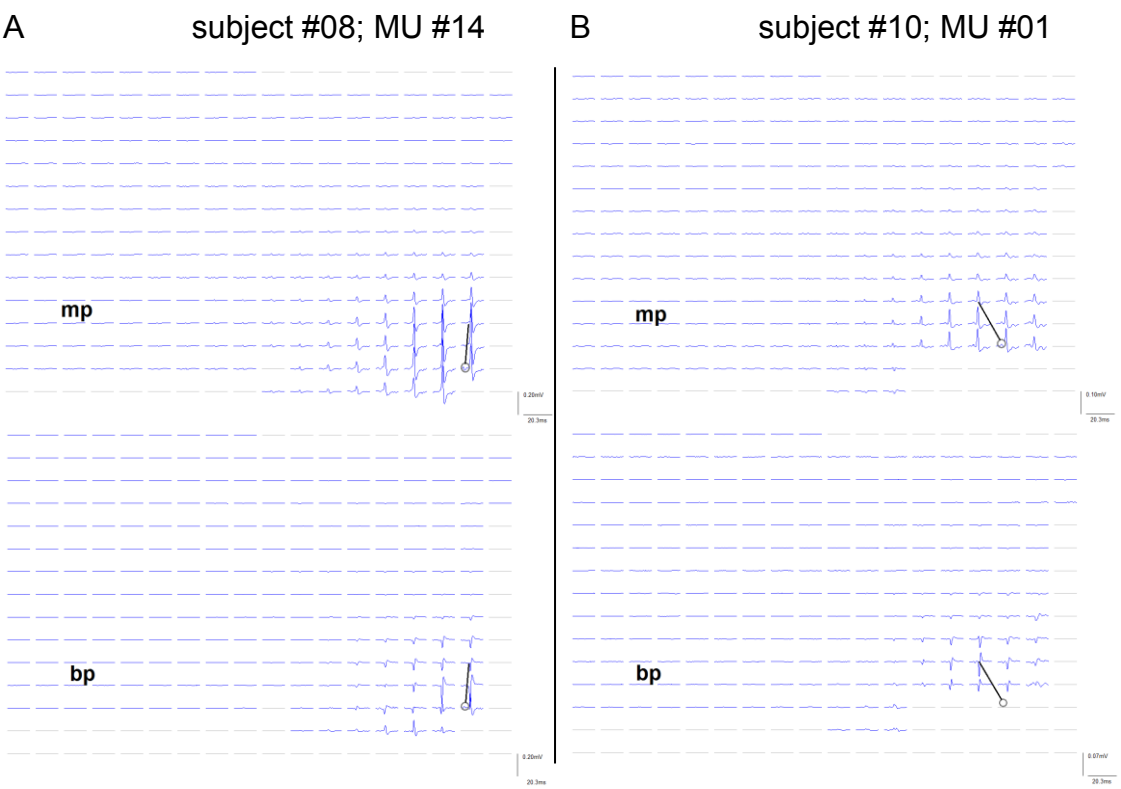


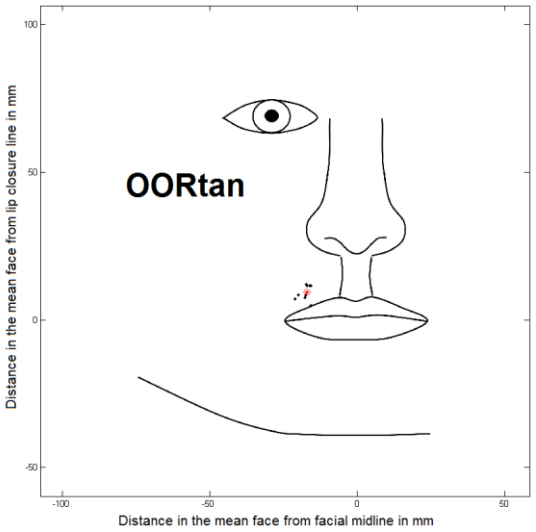
Figure 51: Representative templates of orbicularis oris muscle pars tangentialis motor units in monopolar (mp) and bipolar-vertical (bp) montage. The motor endplates are located in the lower medial corner of the electrode grid with fibers rising in medio-cranial (A) and latero-cranial (B) direction from the endplate zone.
High-density surface electromyography (HDsEMG) measurements of the midfacial muscles. Department of orthodontics, Ulm University, 2014.

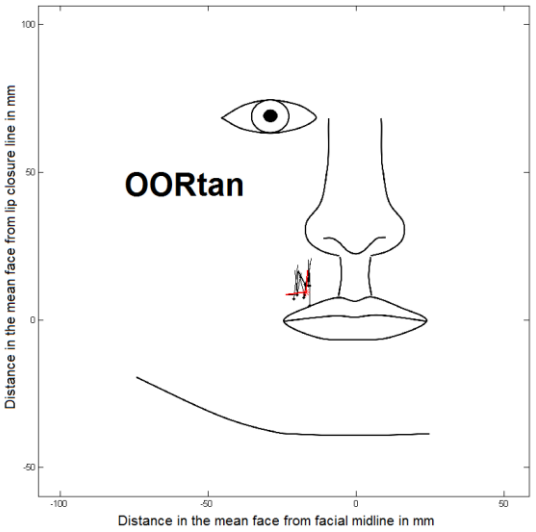
OORtan was identified in thirteen subjects. Corresponding MUs were found in all contractions, except for contractions of ZYGmaj. However, they were predominantly found in contraction of OOR (Table 2).

Figure 51 shows two representative templates of OORtan MUs in monopolar (mp) and bipolar-vertical (bp) montage. The fast decline in amplitude in the monopolar template indicates their superficial location. Fibers rise in latero-cranial (B) and medio-cranial (A) direction from the endplate zone.

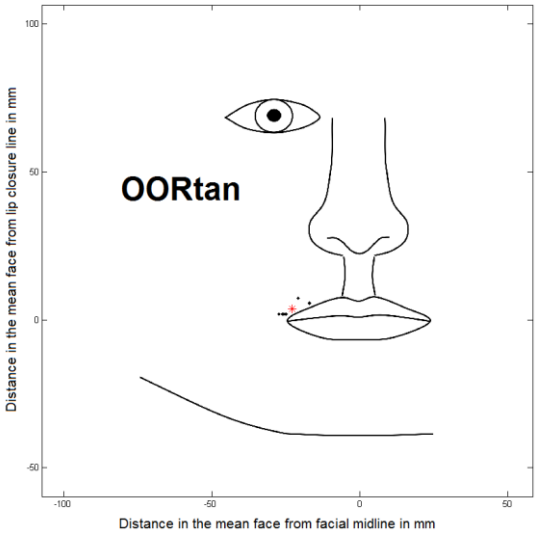
Figure 52 shows four subjects MUs of OORtan and illustrates again high inter-individual variability. Endplates are predominantly found in clusters, located halfway between the corner of the mouth and the philtral column with fibers in both latero-cranial and medio-cranial direction, i.e. perpendicular to OORper's fibers.

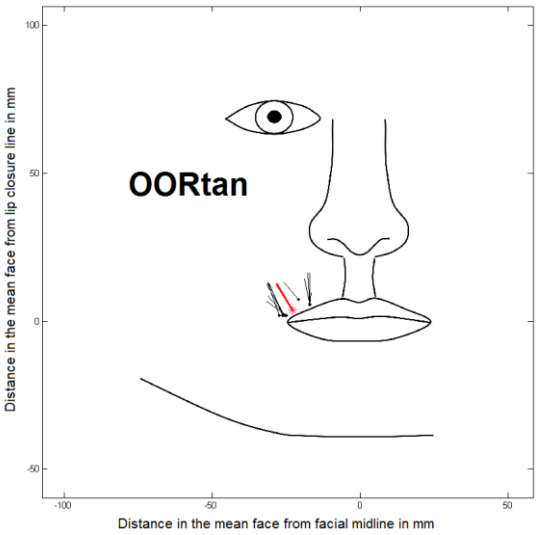
A1 subject #02 A2



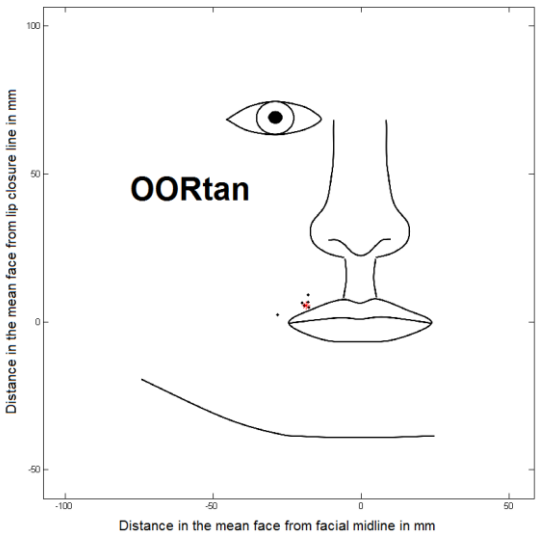


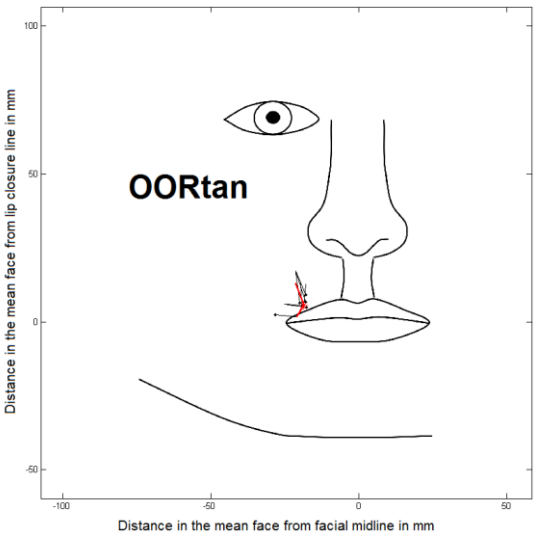
B1 subject #04 B2





C1 subject #08 C2





D1 subject #10 D2

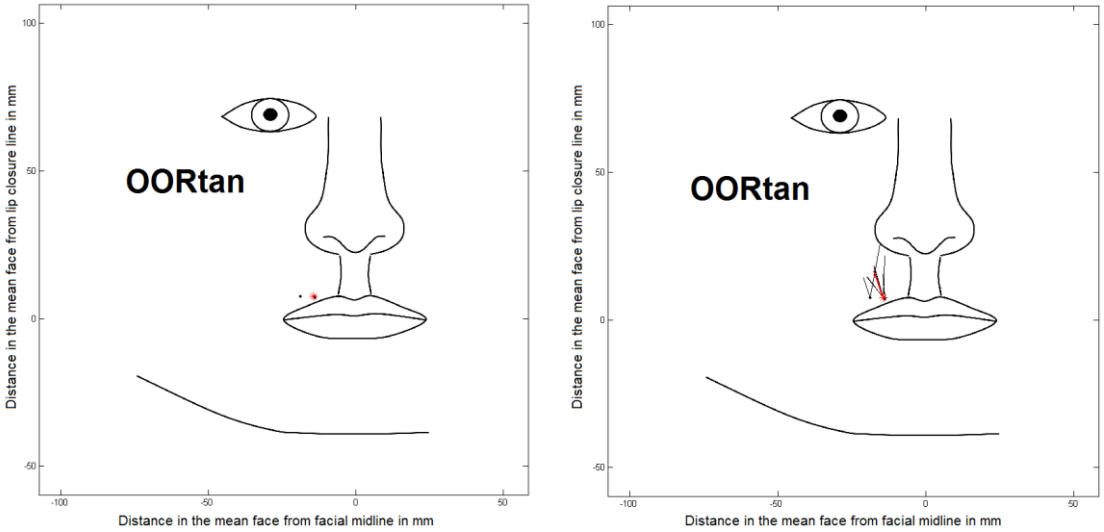


Figure 52: Representative subjects' total orbicularis oris muscle pars tangentialis (OORtan) motor units (black) and median motor units (red) in the normalized face without (A1, B1, C1, D1) and with (A2, B2, C2, D2) fiber orientation.
High-density surface electromyography (HDsEMG) measurements of the midfacial muscles. Department of orthodontics, Ulm University, 2014.

Figure 53 shows all OORtan MUs in the normalized face. The endplates are arranged in a line parallel to the vermillion border but predominantly clustered halfway between the corner of the mouth and the philtral column. Due to the schematic representation of the lip closure line in the normalized face, single MUs' fibers seem to cross the lip closure line, which can actually not occur.

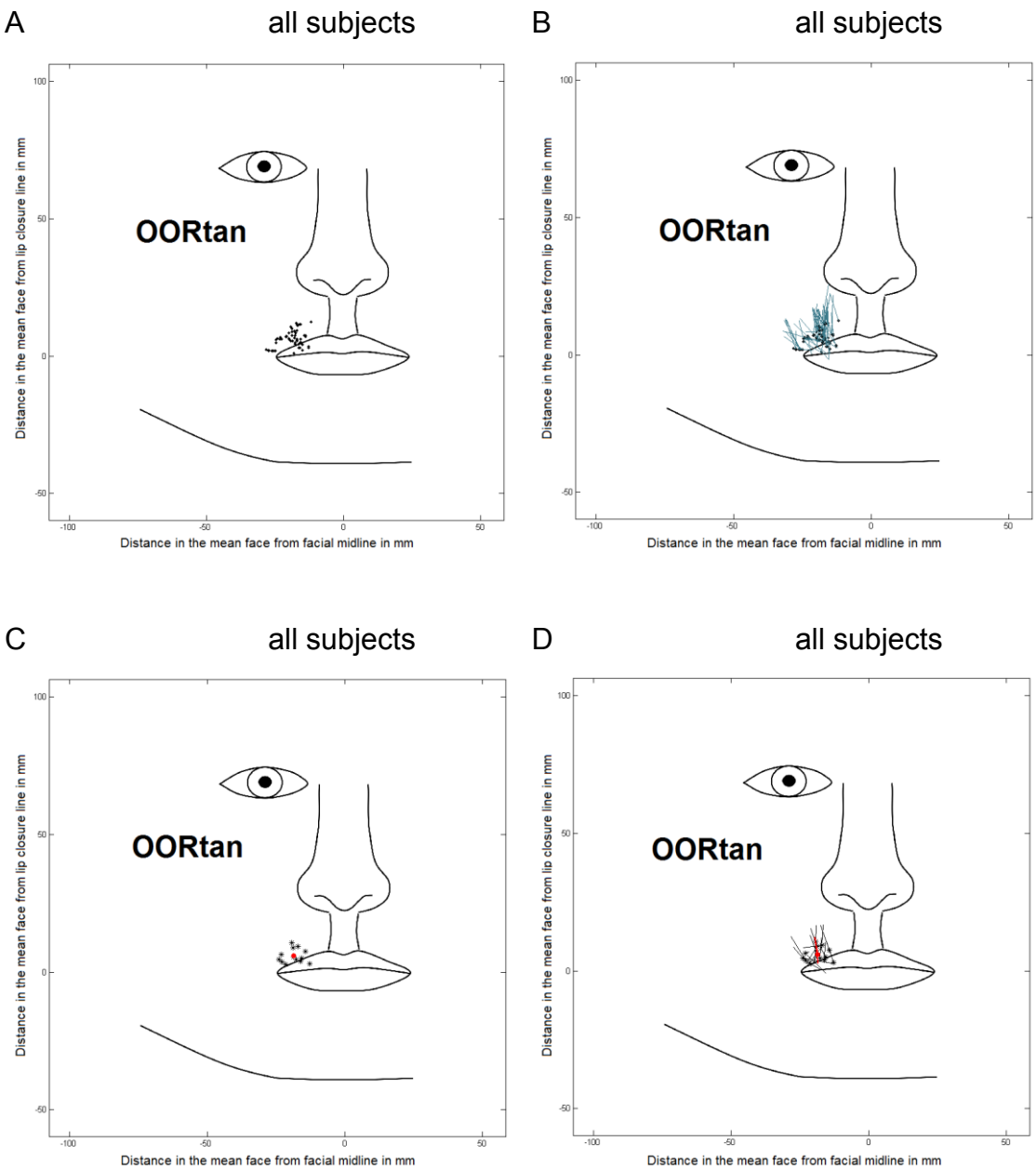


Figure 53: All subjects' orbicularis oris muscle pars tangentialis (OORtan) motor units without (A) and with (B) fiber orientation. All median orbicularis oculi muscle (OOC) motor units (*) and mean of the median values (red) in the normalized face without (C) and with (D) fiber orientation.
High-density surface electromyography (HDsEMG) measurements of the midfacial muscles. Department of orthodontics, Ulm University, 2014.

3.4.12 Nasalis muscle

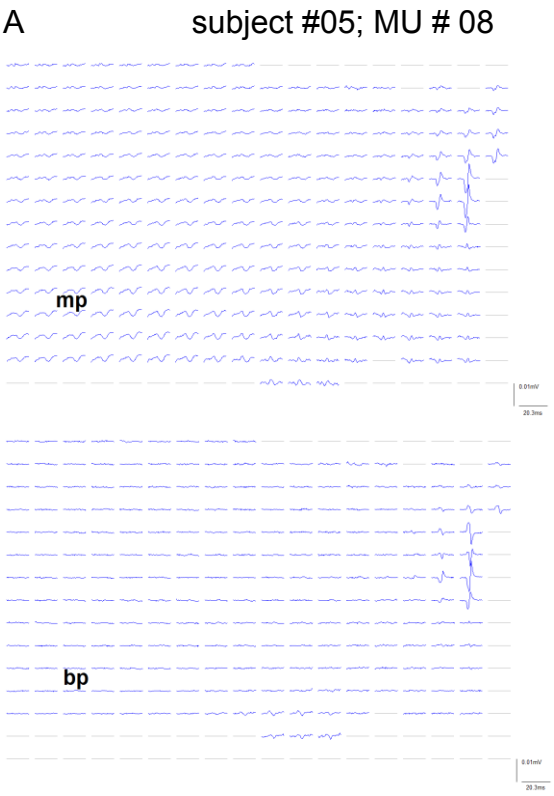


Figure 54: Characteristic template of a nasalis muscle motor unit in monopolar (mp) and bipolar (bp) montage.
High-density surface electromyography (HDsEMG) measurements of the midfacial muscles. Department of orthodontics, Ulm University, 2014.

In seven subjects a total of 17 propagating potentials were found that we assigned to NAS due to the potential's location and orientation. NAS was found in all contractions except for LLS and ZYGmaj (Table 2). Figure 54 shows a characteristic template of NAS in monopolar and bipolar montage. The monopolar template shows a conspicuous waveform with a large negative deflection and a fast decline in amplitude which reveals the potentials superficial location. No signal phase reversal can be determined in the bipolar template. Nevertheless, the potentials propagation could be followed from the second column from the right and the eighth row propagating towards the electrode grid's border at the very right column and third row. This corresponds to an area lateral to the ala of the nose up to the bridge of the nose.

3.5 Motor unit sizes

The MU electrical size was estimated by the area under the curve of the largest surface MUAP in a monopolar template

MU size estimation showed a large variability between units with many small MUs and some larger. Mean MU size of BUC and ZYGmaj were relatively large compared to the other muscles. The mean MU sizes of fiber groups of the OOR complex showed relatively high variability. No correlation between mean MU size and information about the depth acquired from anatomical textbooks could be observed.

Table 6: Mean motor unit (MU) size and range of MU size (minimum and maximum) determined as the area under the curve in the monopolar template for all examined muscles (Buccinator (BUC), incisivus (INC), levator anguli oris (LAO), orbicularis oculi (OOC), orbicularis oris pars marginalis (OORmar)/ pars peripheralis (OORper)/ pars tangentialis (OORtan), zygomaticus major (ZYGmaj), zygomaticus minor (ZYGmin) muscle). High-density surface electromyography (HDsEMG) measurements of the midfacial muscles. Department of orthodontics, Ulm University, 2014.

	MU size in mVms		
	Mean	Minimum	Maximum
BUC	0.563566	0.072693	3.723946
INC	0.271372	0.054177	1.29032
LAO	0.321868	0.028112	3.853854
LLS	0.185671	0.018178	0.6279804
LLSan	0.145008	0.035504	2.7411703
OOC	0.2306	0.032262	2.7139217
OORmar	0.456204	0.047269	2.4625368
OORper	0.330687	0.041411	3.0358061
OORtan	0.3001557	0.03909	0.9449565
ZYGmaj	0.7802949	0.062844	3.0154152
ZYGmin	0.231369	0.016123	0.6366474

4 Discussion

4.1 Recording technique

In this study, the technique of HDsEMG was successfully employed to topographically characterize the midfacial musculature. The highly flexible electrode grids were specially developed for the facial musculature. They proved good electrical connection of the single electrodes even on uneven facial contours and proved to withstand moisture, e.g. saliva, in most measurements. The electrode grids follow the skin movement without significantly hindering the performance of selective muscle contractions (Lapatki et al. 2006; Lapatki et al. 2004). A loss of electrical connection during the measurements in the area around the oral fissure in the present study may be explained by the presence of saliva which may have dissolved the adhesive together with the mechanical loading.

In order to cover the large area of the midfacial muscles and to obtain an adequate resolution in the spatial domain at the same time, a compromise concerning the IED and size of recording area was necessary. For examination of the motor endplate zone, the IED of small and superficial muscles should not exceed 3 mm, whereas for larger and deeper muscles an IED of 5 mm is sufficient (Blok et al. 2002). To achieve maximal coverage of the midfacial muscles, two rectangular electrode grids with an IED of 4 mm and a total of 256 electrodes were used for this study.

However, the IED of 4 mm seemed to be somewhat large for very short and superficial muscles such as OOR, which in turn may have led to an insufficient recording of the potentials' propagation.

To adapt the electrode grids to anatomical properties the best way possible, the medial grid was rotated by 180 degrees and the bottom seven electrodes of the most medial column were cut out for better adaption for the lateral contour of the nose. The carrier material lateral to the bottom three electrodes of the remaining medial column was then cut in to achieve additional flexibility. The medial electrode grid's lead wire irritated some individuals in terms of a reduction of the field of vision, despite the lead wire's caudal deflection.

The lateral grid was shifted one row cranially to ensure coverage of the subzygomatic fossa. All in all, complete coverage of LLS and ZYGmin was

achieved. Depending on anatomical properties, some muscles were not covered completely or just in parts. OOC was found on the electrode grid's cranial border, therefore not covering the corners of the eye. ZYGmaj was not entirely covered by the electrode grid in the area latero-cranial to the subzygomatic fossa; therefore the MUAP could not be followed to the extinction but only to the electrode grids border. Recording of LLSan was limited by the grid's coverage of the nose. BUC was often found on the electrode grid's caudal border. Likewise, fibers of the upper lip and LAO were incompletely covered due to the limitation that the vermillion could not be covered.

Electrode cream forms an electrically conductive film between the skin and the electrode, which in turn results in relatively low electrode-to-skin-impedances. Low impedance reduces the noise level contained in the signal, thus, raising the signal-to-noise ratio. Hence, the use of electrode cream guarantees high signal quality despite the minimal surface area each electrode provides (Lapatki et al. 2004; Radeke et al. 2014).

4.2 Data analysis

For the decomposition of the recorded interference signals, the CKC technique implemented in MATLAB (The Mathworks, Natick, MA) was used (Holobar et al. 2007). This method for fully automatic decomposition allows for identification of individual MUs' discharge patterns. It has been validated in various skeletal muscles with different anatomical characteristics and has proven to be highly resistant to MUAP superimposition, noise and MU discharge synchronization (Holobar et al. 2007; Holobar et al. 2009; Holobar et al. 2010; Radeke et al. 2014).
In the sequential observation of the MUAPS, i.e. the 'MUAP movie', the motor endplate's location is depicted as the electrode location with the maximal amplitude. The propagating MUAP from the endplate to its termination point corresponds to the motor unit's fiber orientation illustrated as a vector. A limitation of this illustration is the impossibility to display deflections or temporary attenuations in the muscle fiber course as well as the missing representation of the third dimension, which may result in inaccurate anatomical mapping. Further limitation is valid for MUs with fibers exceeding the electrode grid. In these cases, the muscle fiber's termination point was determined as the border of the grid. Individual muscles' results for those cases are discussed in the context of the individual muscle. Potentials propagating over the electrode grid but with a motor endplate outside the electrode grid were excluded from the data analysis.
Marking of characteristic facial landmarks such as the inferior orbital margin or the subzygomatic fossa and the 3D structured-light face scans were the basis for the normalized face's dimensions. The 3D scan's accurate coordinates of facial landmarks and the electrode grid enabled exact reproduction of every subject's electrode grid position relative to facial landmarks in the normalized face. However, the fact that the nose, the vermillion border and the lip closure line were not individualized in the schematic average face proved to be suboptimal for the results' presentation.

4.3 Discussion of results

Although subjects were trained beforehand in selectively contracting midfacial muscles, no completely selective contraction was achieved. However, this was expected and has been reported in a previous study of the midfacial muscles (Matt 2013). This study was necessary to gain again more topographical information of the midfacial musculature, as the previous study's setup (cf. Matt 2013) did not sufficiently record the midfacial muscles.

The characteristic spatial profile allowed the decomposed MUAPs to be assigned to certain facial muscle subcomponents. The results of this study agreed with descriptions and drawings in anatomical textbooks in terms of muscle position and fiber orientation, which was also found in previous studies of the facial musculature (Matt 2013; Lapatki et al. 2006). Hence, the results' discussion is in the context of macro- and micro anatomical knowledge (Schünke et al. 2009; Benninghoff et al. 2008; Standring et al. 2008; Aumüller et al. 2010).

16.7 % of all identified MUs were assigned to OOC, the majority thereof was found in selective OOC contraction. Due to the electrode grid's position and inter individual differences in the subjects' facial height it was only possible to cover parts of the lower OOC. The course of OOCs MUAP propagation agreed with the muscle fibers' elliptic course around the eye as described in anatomical textbooks. However due to our method of evaluation, it was only possible to display the elliptic course in the MUAP movies but not to illustrate them in the normalized faces. Dissection studies found the pretarsal and preseptal OOC to be innervated by five to seven terminal twigs of the zygomatic branches of the facial nerve. The middle portion of the lower OOC was innervated by two to three twigs of the zygomatic branch and the medial portion was innervated by one to two terminal twigs of the buccal branch (Happak et al. 1997; Hwang et al. 2001). Our study found OOC's MUs to be distributed over the muscle with coexistent MU clusters. Although no strict pattern of cluster distribution could be identified, a noticeable amount of subjects showed endplate clusters under the lateral canthus and under the pupil. Neubert (2016) applied the technique of HDsEMG to the upper face. OOC motor endplates were found to be spread over the entire muscle but the appearance of clusters, e.g. lateral to the outer canthus, was described as well.

Matt (2013) found predominant endplate localization in the nasal third of the lower OOC using HDsEMG and therefore concluded the existence of numerous endplate clusters to be more likely. These HDsEMG studies' findings disagree with the histological study of (Happak et al. 1997), which found OOCs motor endplates to be evenly spread over the muscle.

Selective contraction of ZYGmaj was relatively easy for the subjects, which resulted in the fact that 66.2% of the total number of ZYGmaj MUs was found in selective contraction. ZYGmaj is innervated from its deep surface by two to four branches of the zygomatic arch of the facial nerve (Happak et al. 1997). In a dissection study a point halfway from the root of the helix and the lateral commisure of the mouth was defined to reliably find the zygomatic branch of the facial nerve, which innervates the ZYGmaj (Dorafshar et al. 2013). ZYGmaj's endplates were clustered or arranged in a narrow band perpendicular to muscle fiber direction and some subjects showed additional discrete MUs medio-caudally to the main MU cluster. In relation to anatomical landmarks, the MU cluster was located slightly below a point that was two-thirds from the corner of the mouth on a connection line from the corner of the mouth to the subzygomatic fossa. These findings conform to a histological study that found ZYGmaj to have a predominant motor zone located near the origin in the proximal third of the muscle and two to three additional small motor zones in eccentric position in the proximal and distal third of the muscle (Happak et al. 1997). ZYGmaj fiber orientation matches descriptions in anatomical textbooks. The superior fibers run from their endplates in latero-cranial direction towards the subzygomatic fossa, which was determined to be a reliable landmark for the identification of ZYGmaj (Miller et al. 2007). The inferior fibers run in medio-caudal direction towards the modiolus. One subject's results (subject #02) for the inferior fibers indicates the anatomical variation of a bidif ZYGmaj with the inferior fibers splitting in two muscle fibers bands at the infrazygomatic region (Hur et al. 2010).

ZYGmin was found in four subjects, each of which also showing MUs of ZYGmaj. The small number of subjects showing ZYGmin may on the one hand be due to difficulty to selectively contract this muscle. On the other hand, this finding conforms to various studies, which show the inconstancy of ZYGmin's occurrence

(Pessa et al. 1998a). Just as ZYGmaj, ZYGmin is innervated from its deep surface by two to four branches of the zygomatic arch of the facial nerve. It is also described to have a predominant motor zone near its origin in the proximal third of the muscle and additional small motor zones in eccentric position in the proximal and distal third of the muscle (Happak et al. 1997). Our study found the majority of ZYGmin's MUs located at the lateral canthus at a level above the ala of the nose, which corresponds to the muscle's cranial third. These MUs' fibers ran in latero-cranial direction towards the subzygomatic fossa and in medio-caudal direction towards the upper lip. This agrees with Happak et al. (1997) and Matt (2013), who found similar endplate locations and fiber orientations. Furthermore one subject's ZYGmin MUs were located in the area of the subzygomatic fossa with its superior fibers in latero-cranial direction going beyond the subzygomatic fossa, which may reflect ZYGmin to emanate from OOC (Aumüller et al. 2010). The inferior fibers were shorter than the other ZYGmin MUs' inferior fibers, however, showed a similar orientation.

Selective contraction of LLS and LLSan was easy for the subjects, yet only 12 subjects showed LLS and 13 subjects showed LLSan. Fiber orientation of LLS and LLSan agreed with descriptions and drawings in anatomical textbooks (Schünke et al. 2009; Benninghoff et al. 2008; Standring et al. 2008; Aumüller et al. 2010). However, LLSan's MUAPs in medio-cranial direction onto the bridge of the nose could only be traced to electrode grid's border. Consequently, it is likely that more endplates can be found on the nose and MUAPs may run further onto the bridge of the nose than depicted in this study. Both muscles' endplates were found as clusters lateral to the nose, whereas LLS MUs were located more lateral than LLSan MUs, which reached up to the nose. This confirms the assumption of medial located endplates of LLS and LLSan and a vertical fiber orientation from a previous study examining the midface (Matt 2013). An occurrence of two to four large motor zones per muscle distributed over the muscle in eccentric position as described in a histological study could not be confirmed in our study (Happak et al. 1997).

LAO was found in all subjects. It showed high inter-individual variability in terms of endplate location and fiber direction. Endplates appeared either in one cluster

latero-cranial to the corner of the mouth or loosely distributed over the muscle or in a combination of clusters and additional eccentric endplates. Matt (2013) found LAO's endplates to be distributed in a vertical direction over the muscle. These findings of both electrophyiological studies do not agree with a histological study which found LAO's endplates in two to four large motor zones distributed over the muscle in eccentric position (Happak et al. 1997). Due to insufficient coverage of LAO in the area of the modiolus, it is likely for LAO fibers to reach further in direction of the modiolus. LAO's templates often showed activity in the area of BUC and vice versa. This can be a sign of cross-talk but also shows BUC's and LAO's large MU size.

In the majority of cases BUC MUs were found on the caudal border of the lateral electrode grid. Therefore the existence of further MUs caudal to the position of the electrode grid is very likely. BUC MUs mainly appeared as clusters in the individual subjects' data. Due to the limited coverage of BUC with the electrode grid, all subjects' data showed a distribution of BUC endplates along the caudal border of the electrode grid. This corresponds to an area lateral to the eye and in a vertical dimension between the corner of the mouth and the philtrum. This does not agree with Matt (2013) and Happak et al. (1997), who found BUC endplates to be evenly distributed over the muscle. BUCs fibers running both towards the modiolus and in latero-cranial direction to its origin as found in this study agree with descriptions and drawings in anatomical textbooks (Schünke et al. 2009; Benninghoff et al. 2008; Standring et al. 2008; Aumüller et al. 2010). However, BUC could neither be depicted as the broad muscle plate as described in a histological study nor could a crossing of fibers on their way to the modiolus be observed (Matt 2013; Happak et al. 1997). These two characteristics may be revealed by better coverage of BUC, i.e. a more caudal electrode grid position.

The OOR is a highly complex muscle and consists of four quadrants, each of which anatomically subdivided in a marginal part located within the lip red, a peripheral part around the lips and a tangential part perpendicular to the marginal and peripheral parts. Depending on the subjects' facial heights it was possible to cover more or less of the lip vermillion. Furthermore, examination of the OORmar was often limited by the loss of electrical contact during the measurements in the

area around the oral fissure, due to the presence of saliva. OORmar and OORper were investigated in co-contraction with OORtan as selective contraction of OOR's subcomponents is difficult. Histological and anatomical studies found OOR to be innervated from its lateral side by terminal nerve branches of the facial nerve, i.e. the zygomatic, buccal and mandibular branch (Mitsukawa et al. 2014). The endplates were found to be evenly spread over the muscle either as isolated endplates or in a great number of small motor endplate zones (Matt 2013; Happak et al. 1997). In agreement with these previous data, all of OOR's subcomponents endplates were found to be spread over the muscle. However, examination of OOR's individual subcomponents reveals a predominant endplate distribution for every subcomponent. In the case of OORmar, an even distribution over the lip vermillion was observed, though few individuals showed an endplate cluster near the corner of the mouth. OORmar's fibers were found to be very short and due to the electrode grid's position they could not be observed up to the facial midline. OORper showed high inter-individual differences in terms of endplate distribution. The individual subjects' data show both clustering in the area of the corner of the mouth and discrete endplates. Regarding all subjects endplates, a large main cluster cranial to the corner of the mouth and further single endplates distributed over the muscle could be observed. OORper has long fibers that run vertical but as well as parallel to the vermillion zone, which could again not be observed up to the facial midline. Just as the other subcomponents MUs, OORtan MUs were evenly distributed over the muscle. Moreover, a large main cluster halfway between the corner of the mouth and the philtral column could be observed. In the individual subjects, the occurrence of motor zones parallel to the vermillion border was found. OORtan fibers are arranged perpendicular to OORper and OORmar fibers and run in cranial direction up to where the retractors of the upper lip insert into the muscular substance of the upper lip. This supports the assumption that OORtan fibers belong in functional respects to the retractors of the upper lip (Blair 1986).

Another part of the upper lips' fiber group is INC, which is rarely mentioned in literature. This might be due to its existence as a part of the OOR complex. INC has bony attachment and intermingles with fibers of the OORper in its course to the modiolus. Matt (2013) found INC's endplates to be distributed over the entire OOR. In our study INCs endplates were found clustered in a vertical line on the

medial border of the electrode grid, which renders the existence of more endplates located further medial not only possible but very likely. INC's decline in amplitude in monopolar templates showed INC to be located deeper than OORper. INCs fibers appeared long and ran towards the modiolus which argues for its intermixture with OORper fibers.

In summary, the small territories and distinct muscle fiber orientations reflect OOR's complicated fiber architecture in the upper lip as observed before in the lower OOR (Lapatki et al. 2006). From all these electrophysiological, anatomical and histological data, especially in terms of the high inter-individual variability, it can be concluded that the MU architecture of OOR in the upper lip is highly developed and very complex. Therefore it requires further electrophysiological and histological investigation, especially with regard to the fibers' architecture in the area of the facial midline and the lip vermillion.

RIS could not be found in this study. A possible reason might be its high variability in both occurrence in individuals and its shape, which ranges from one or more slender fasciles to a wide fan (Pessa et al. 1998a; Waller et al. 2008; Ewart et al. 2005). Another possible reason might be a more caudal location of the muscle than the electrode grid's position in this study, which in turn did not allow for RIS to be detected.

Potentials in the area of the ala of the nose, which showed no clear endplate but a propagation of the potential, were assigned to NAS. The fact that no clear endplate could be detected but the propagation of a potential might present a limitation of the two-dimensional method used for investigation of the three-dimensional muscle system.

The electrical MU size determined in this study does not include 'depth correction'. On the one hand, the facial muscles' depth could not be determined in this study. On the other hand, depth correction was only carried out for the biceps brachii muscle so far (Roeleveld et al. 1997b). Due to differences in anatomical characteristics of skeletal and facial muscles, the depth correction method for biceps brachii muscle has not been validated for facial muscles and could therefore not be applied for the facial muscles in this study. Still, the values in Table 3 may approximate the MU sizes well as most facial muscles are located more or less superficially underneath the facial skin. BUC and LAO are an

exception due to their very deep location and OORmar for its very superficial location. This has to be considered in these muscles' MU size interpretation. Due to the fact that the electrical MU size is proportional to a MUs' number of muscle fibers, ZYGmaj and BUC comprise a higher-than-average number of muscle fibers per MU when compared to the other facial muscles. This characteristic may play an important role in the consideration of cross-talk and may explain the appearance of BUC activity in LAO recordings and vice versa.

4.4 Conclusion

Application of the HDsEMG to the midfacial muscles represents a non-invasive method to achieve topographical and physiological information. In this electrophysiological study, the position and distribution of MU endplates, muscle fiber orientations and MU sizes of the midfacial muscles have been mapped and quantitatively determined using 245 individual electrodes with an IED of 4 mm. The collected data add to the basic neuro-physiologic and anatomical knowledge of the midfacial musculature. Moreover, the results obtained in this study can be seen as a basis for improving accuracy, electrode positioning, and reproducibility (Lapatki et al. 2006). The non-invasive tool of facial sEMG has proven of value in numerous research and clinical applications, e.g. in psychophysiology in order to detect emotions by application of facial EMG, e.g. to the zygomaticus major muscle (Huang et al.2009) or pathophysiology. Furthermore, this study's results disclosure new prospects in the clinical application of BoNT. It has already been demonstrated that endplate targeted injections with minimal doses optimize the effect of BoNT (Lapatki et al. 2011). In respect thereof, BoNT might be an alternative to hitherto existing therapies as for example it is already the case in the treatment of gummy smiles (Polo 2008; Sucupira et al. 2012; Mazzuco et al. 2010). Knowledge of midfacial muscles' topographical characteristics can thereby contribute to an improved electrode placement for various applications.

5 Summary

This study's aim was to gain topographical information of the midfacial musculature on a motor unit level. By means of high-density surface electromyography, motor units' endplate positions, fiber orientations, and sizes were examined. Sixteen specially trained, healthy subjects performed selective contraction of ten midfacial muscles (buccinator muscle, incisivus labii superioris muscle, levator anguli oris muscle, levator labii superioris and levator labii superioris alaeque nasi muscle, orbicularis oculi muscle, orbicularis oris muscle pars marginalis/ peripheralis/ tangentialis, zygomaticus major muscle and zygomaticus minor muscle). Signals were recorded using high-density surface electromyography grids (245 channels). The raw surface electromyography data was decomposed into the contributions of single motor units by application of the CKC-method (convolution kernel compensation). The decomposed motor unit action potentials were represented in templates, which are topographically unique for every motor unit ('motor unit fingerprint'). Analysing the motor units as amplitude maps sequences revealed the motor unit's locations and fiber orientations. The results were illustrated in a mean face, which was created by averaging the subjects' 3D face scan data.

Motor units (MUs) of all ten selectively contracted muscles were found and characterized.

Orbicularis oculi muscle and the marginal part of orbicularis oris muscle showed widely distributed endplates on the muscle. A clustering of endplates within individuals but with great variation of the location of clusters between individuals was found for buccinator muscle, levator anguli oris muscle, the peripheral and tangential part of orbicularis oris muscle and zygomaticus minor muscle. A clustering of endplates with similar cluster locations among individuals was found for incisivus muscle, levator labii superioris muscle, levator labii superioris alaeque nasi muscle and zygomaticus major muscle.

The MUs' muscle fiber orientations generally conform well to descriptions and drawings in anatomical textbooks and literature. However, the electrode grid's size and its inter-electrode distance were limitations in the recording, as the gain of topographical information was only possible with the simultaneous loss of selectivity, which is especially true for the fiber length and orientation of short

muscle fibers. This fact has to be taken into account in the evaluation of every muscle's result.

This study's results contribute to the basic anatomical and neurophysiologic knowledge of the facial, especially the midfacial musculature. They can contribute to establish objective electrode placement guidelines or to advance examination methods and (non-)surgical therapies.

6 **Bibliography**

1. Aumüller G, Aust G, Doll A, Engele J, Kirsch J, Mense S, Reißig D, Salvetter J, Schmidt, W., Schmitz F, Schulte E, Spanel-Borowski K, Wolff W, Wurzinger L J, Zilch H : Mimische Muskulatur. In: Aumüller G, Aust G, Doll A, Engele J, Kirsch J, Mense S, Reißig D, Salvetter J, Schmidt, W., Schmitz F, Schulte E, Spanel-Borowski K, Wolff W, Wurzinger L J, Zilch H (Hrsg) : Anatomie, 2. Auflage, Georg Thieme Verlag KG, Stuttgart, S. 870-874 (2010)

2. Bae J H, Lee J H, Youn K H, Hur M S, Hu K S, Tansatit T, Kim H J: Surgical consideration of the anatomic origin of the risorius in relation to facial planes. Aesthet.Surg.J., 34: 43-9 (2014)

3. Benninghoff A, Drenckhahn D: Skelett- und Muskelsystem. In: Benninghoff A, Drenckhahn D: Anatomie. Makroskopische Anatomie, Histologie, Embryologie, Zellbiologie, Bd 1, 17. Auflage, Urban & Fischer Verlag/Elsevier GmbH, München, Jena, S. 524-530 (2008)

4. Blair C: Interdigitating muscle fibers throughout orbicularis oris inferior: preliminary observations. J.Speech Hear.Res., 29: 266-269 (1986)

5. Blok J H, van Dijk J P, Drost G, Zwarts M J, Stegeman D F: A high-density multichannel surface electromyography system for the characterization of single motor units. Rev.Sci.Instrum., 73: 1887-1897 (2002)

6. Broman H, Bilotto G, De Luca C J: A note on the noninvasive estimation of muscle fiber conduction velocity. IEEE Trans.Biomed.Eng., 32: 341-344 (1985)

7. Dayakar M M, Gupta S, Shivananda H: Lip repositioning: An alternative cosmetic treatment for gummy smile. J.Indian.Soc.Periodontol., 18: 520-523 (2014)

8. Disselhorst-Klug C, Silny J, Rau G: Improvement of spatial resolution in surface-EMG: a theoretical and experimental comparison of different spatial filters. IEEE Trans.Biomed.Eng., 44: 567-574 (1997)

9. Dorafshar A H, Borsuk D E, Bojovic B, Brown E N, Manktelow R T, Zuker R M, Rodriguez E D, Redett R J: Surface anatomy of the middle division of the facial nerve: Zuker's point. Plast.Reconstr.Surg., 131: 253-257 (2013)

10. Ewart C J, Jaworski N B, Rekito A J, Gamboa M G: Levator anguli oris: a cadaver study implicating its role in perioral rejuvenation. Ann.Plast.Surg., 54: 260-3; discussion 263 (2005)

11. Farina D, Fortunato E, Merletti R: Noninvasive estimation of motor unit conduction velocity distribution using linear electrode arrays. IEEE Trans.Biomed.Eng., 47: 380-388 (2000)

12. Freilinger G, Happak W, Burggasser G, Gruber H: Histochemical mapping and fiber size analysis of mimic muscles. Plast.Reconstr.Surg., 86: 422-428 (1990)

13. Garber D A, Salama M A: The aesthetic smile: diagnosis and treatment. Periodontol.2000, 11: 18-28 (1996)

14. Happak W, Liu J, Burggasser G, Flowers A, Gruber H, Freilinger G: Human facial muscles: dimensions, motor endplate distribution, and presence of muscle fibers with multiple motor endplates. Anat.Rec., 249: 276-284 (1997)

15. Holobar A, Farina D, Gazzoni M, Merletti R, Zazula D: Estimating motor unit discharge patterns from high-density surface electromyogram. Clin.Neurophysiol., 120: 551-562 (2009)

16. Holobar A, Minetto M A, Botter A, Negro F, Farina D: Experimental analysis of accuracy in the identification of motor unit spike trains from high-density surface EMG. IEEE Trans.Neural Syst.Rehabil.Eng., 18: 221-229 (2010)

17. Holobar A, Zazula D: Multichannel Blind Source Separation Using Convolution Kernel Compensation. IEEE Transactions on Signal Processing, 55: 4487-4496 (2007)

18. Hu K S, Jin G C, Youn K H, Kwak H H, Koh K S, Fontaine C, Kim H J: An anatomic study of the bifid zygomaticus major muscle. J.Craniofac.Surg., 19: 534-536 (2008)

19. Huang H Y, Hu S: Sex differences found in facial EMG activity provoked by viewing pleasant and unpleasant photographs. Percept.Mot.Skills, 109: 371-381 (2009)

20. Hur M S, Hu K S, Park J T, Youn K H, Kim H J: New anatomical insight of the levator labii superioris alaeque nasi and the transverse part of the nasalis. Surg.Radiol.Anat., 32: 753-756 (2010)

21. Hwang K: Surgical anatomy of the facial nerve relating to facial rejuvenation surgery. J.Craniofac.Surg., 25: 1476-1481 (2014)

22. Hwang K, Kim D J, Hwang S H: Musculature of the pars marginalis of the upper orbicularis oris muscle. J.Craniofac.Surg., 18: 151-154 (2007)

23. Hwang K, Lee D K, Lee E J, Chung I H, Lee S I: Innervation of the lower eyelid in relation to blepharoplasty and midface lift: clinical observation and cadaveric study. Ann.Plast.Surg., 47: 1-5; discussion 5-7 (2001)

24. Hwang W S, Hur M S, Hu K S, Song W C, Koh K S, Baik H S, Kim S T, Kim H J, Lee K J: Surface anatomy of the lip elevator muscles for the treatment of gummy smile using botulinum toxin. Angle Orthod., 79: 70-77 (2009)

25. Imhof M, Podda M, Sommer B: Leitlinie der Deutschen Dermatologischen Gesellschaft. S1-Leitlinie: Ästhetische Botulinumtoxin-Therapie. http://www.awmf.org/uploads/tx_szleitlinien/013-

077l_S1_%C3%84sthetische_Botulinumtoxin_Therapie_2012-11.pdf, AWMF online, (2012) date of download: 03.10.2014

26. Ito J, Moriyama H, Shimada K: Morphological evaluation of the human facial muscles. Okajimas Folia Anat.Jpn., 83: 7-14 (2006)

27. Kleine B U, Blok J H, Oostenveld R, Praamstra P, Stegeman D F: Magnetic stimulation-induced modulations of motor unit firings extracted from multi-channel surface EMG. Muscle Nerve, 23: 1005-1015 (2000)

28. Lapatki B G, Stegeman D F, Zwarts MJ: Visual Examination of facial muscle contractions. In: Lapatki B G (Hrsg): The Facial Musculature. Characterisation at a Motor Unit Level, Donders series, Netherlands, S. 27-37 (2010)

29. Lapatki B G, Oostenveld R, Van Dijk J P, Jonas I E, Zwarts M J, Stegeman D F: Topographical characteristics of motor units of the lower facial musculature revealed by means of high-density surface EMG. J.Neurophysiol., 95: 342-354 (2006)

30. Lapatki B G, Van Dijk J P, Jonas I E, Zwarts M J, Stegeman D F: A thin, flexible multielectrode grid for high-density surface EMG. J.Appl.Physiol.(1985), 96: 327-336 (2004)

31. Lapatki B G, van Dijk J P, van de Warrenburg B P, Zwarts M J: Botulinum toxin has an increased effect when targeted toward the muscle's endplate zone: a high-density surface EMG guided study. Clin.Neurophysiol., 122: 1611-1616 (2011)

32. Marateb H R, McGill K C, Holobar A, Lateva Z C, Mansourian M, Merletti R: Accuracy assessment of CKC high-density surface EMG decomposition in biceps femoris muscle. J.Neural Eng., 8: 066002-2560/8/6/066002. Epub 2011 Oct 6 (2011)

33. Masuda T, Sadoyama T: The propagation of single motor unit action potentials detected by a surface electrode array. Electroencephalogr.Clin.Neurophysiol., 63: 590-598 (1986)

34. Matt F: Topographische Charakterisierung der Mittelgesichtsmuskulatur auf Ebene der motorischen Einheiten. Med Dissertation, Univeristät Ulm Klinik für Zahn-, Mund- und Kieferheilkunde Abteilung Kieferorthopädie (2013)

35. May M, Schaitkin B M: The Facial Nerve. 2nd edition, Thieme, Stuttgart, (1999)

36. Mazzuco R, Hexsel D: Gummy smile and botulinum toxin: a new approach based on the gingival exposure area. J.Am.Acad.Dermatol., 63: 1042-1051 (2010)

37. Merletti R, Lo Conte L, Avignone E, Guglielminotti P: Modeling of surface myoelectric signals--Part I: Model implementation. IEEE Trans.Biomed.Eng., 46: 810-820 (1999)

38. Metting van Rijn A C, Peper A, Grimbergen C A: High-quality recording of bioelectric events. Part 1. Interference reduction, theory and practice. Med.Biol.Eng.Comput., 28: 389-397 (1990)

39. Miller P J, Smith S, Shah A: The subzygomatic fossa: a practical landmark in identifying the zygomaticus major muscle. Arch.Facial Plast.Surg., 9: 271-274 (2007)

40. Mitsukawa N, Moriyama H, Shiozawa K, Satoh K: Study on distribution of terminal branches of the facial nerve in mimetic muscles (orbicularis oculi muscle and orbicularis oris muscle). Ann.Plast.Surg., 72: 71-74 (2014)

41. Neubert J: Topographical Characterization of the Upper Facial Musculature Revealed by Mean of High-density Surface Electromyography. Med Dissertation, Univeristät Ulm Klinik für Zahn-, Mund- und Kieferheilkunde Abteilung Kieferorthopädie (2016)

42. Pessa J E, Zadoo V P, Adrian E K,Jr, Yuan C H, Aydelotte J, Garza J R: Variability of the midfacial muscles: analysis of 50 hemifacial cadaver dissections. Plast.Reconstr.Surg., 102: 1888-1893 (1998a)

43. Pessa J E, Zadoo V P, Garza P A, Adrian E K,Jr, Dewitt A I, Garza J R: Double or bifid zygomaticus major muscle: anatomy, incidence, and clinical correlation. Clin.Anat., 11: 310-313 (1998b)

44. Polo M: A simplified method for smile enhancement: botulinum toxin injection for gummy smile. Plast.Reconstr.Surg., 131: 934e-935e (2013)

45. Polo M: Botulinum toxin type A (Botox) for the neuromuscular correction of excessive gingival display on smiling (gummy smile). Am.J.Orthod.Dentofacial Orthop., 133: 195-203 (2008)

46. Polo M: Botulinum toxin type A in the treatment of excessive gingival display. Am.J.Orthod.Dentofacial Orthop., 127: 214-8; quiz 261 (2005)

47. Radeke J, van Dijk J P, Holobar A, Lapatki B G: Electrophysiological method to examine muscle fiber architecture in the upper lip in cleft-lip patients. J.Orofac.Orthop., 75: 51-61 (2014)

48. Roeleveld K, Sandberg A, Stalberg E V, Stegeman D F: Motor unit size estimation of enlarged motor units with surface electromyography. Muscle Nerve, 21: 878-886 (1998)

49. Roeleveld K, Stegeman D F: What do we learn from motor unit action potentials in surface electromyography?. Muscle Nerve Suppl., 11: S92-7 (2002)

50. Roeleveld K, Stegeman D, Falck B, Stalberg E: Motor unit size estimation: confrontation of surface EMG with macro EMG. Electroencephalogr Clin Neurophysiol.1997 Jun;105(3):181-8., (1997a)

51. Roeleveld K, Stegeman D F, Vingerhoets H M, Van Oosterom A: The motor unit potential distribution over the skin surface and its use in estimating the motor unit location. Acta Physiol.Scand., 161: 465-472 (1997b)

52. Rossi G, Cortesina G: Morphological Study of the Laryngeal Muscles in Man. Insertions and Courses of the Muscle Fibres, Motor End-Plates and Proprioceptors. Acta Otolaryngol., 59: 575-592 (1965)

53. Schünke M, Schulte E, Schumacher U: Systematik der Muskulatur. In: Schünke M, Schulte E and Schumacher U (Hrsg) Prometheus: Lernatlas der Anatomie: Kopf, Hals und Neuroanatomie, 2., Georg Thieme Verlag, Stuttgart, S. 62-65 (2009)

54. Shim K S, Hu K S, Kwak H H, Youn K H, Koh K S, Fontaine C, Kim H J: An anatomical study of the insertion of the zygomaticus major muscle in humans focused on the muscle arrangement at the corner of the mouth. Plast.Reconstr.Surg., 121: 466-473; (2008)

55. Shinohara H, Kominami R, Yasutaka S, Taniguchi Y: The anatomy of the lacrimal portion of the orbicularis oculi muscle (tensor tarsi or Horner's muscle). Okajimas Folia Anat.Jpn., 77: 225-232 (2001)

56. Speckmann E , Hescheler J, Köhling R: Quergestreifte Muskulatur. In: Speckmann E , Hescheler J and Köhling R (Hrsg) Physiologie, 5. Auflage, Urban & Fischer Verlag/Elsevier GmbH, München, S. 175-195 (2008)

57. Stal P, Eriksson P O, Eriksson A, Thornell L E: Enzyme-histochemical and morphological characteristics of muscle fibre types in the human buccinator and orbicularis oris. Arch.Oral Biol., 35: 449-458 (1990)

58. Standring S: Functional Anatomy of the Musculoskeletal System; Face and Scalp. In: Standring S (Hrsg): Gray's Anatomy: The Anatomical Basis of Clinical Practice, 40 ed., Elsevier, Churchill Livingstone, S. 103-549 (2008)

59. Storrer C L, Valverde F K, Santos F R, Deliberador T M: Treatment of gummy smile: Gingival recontouring with the containment of the elevator muscle of the upper lip and wing of nose. A surgery innovation technique. J.Indian.Soc.Periodontol., 18: 656-660 (2014)

60. Suber J S, Dinh T P, Prince M D, Smith P D: OnabotulinumtoxinA for the treatment of a "gummy smile". Aesthet.Surg.J., 34: 432-437 (2014)

61. Sucupira E, Abramovitz A: A simplified method for smile enhancement: botulinum toxin injection for gummy smile. Plast.Reconstr.Surg., 130: 726-728 (2012)

62. Van Vugt J P, van Dijk J G: A convenient method to reduce crosstalk in surface EMG. Cobb Award-winning article, 2001 Clin.Neurophysiol., 112: 583-592 (2001)

63. Waller B M, Cray J J, Burrows A M: Selection for universal facial emotion. Emotion, 8: 435-439 (2008)

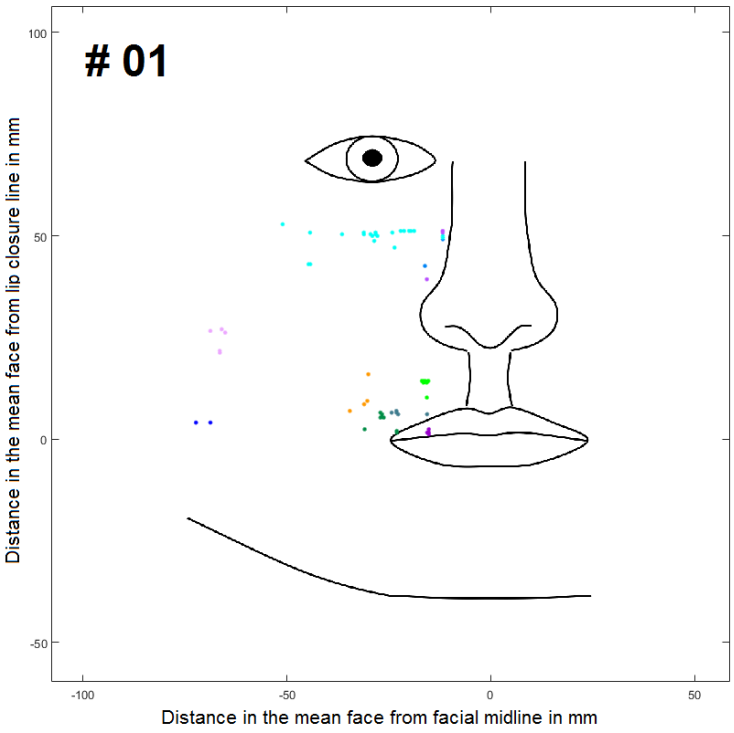
64. Zwarts M J, Lapatki B G, Kleine B U, Stegeman D F: Surface EMG: how far can you go?. Suppl.Clin.Neurophysiol., 57: 111-119 (2004)

65. Zwarts M J, Stegeman D F: Multichannel surface EMG: basic aspects and clinical utility. Muscle Nerve, 28: 1-17 (2003)

Appendix

Individual subjects' results in the mean face

A



B

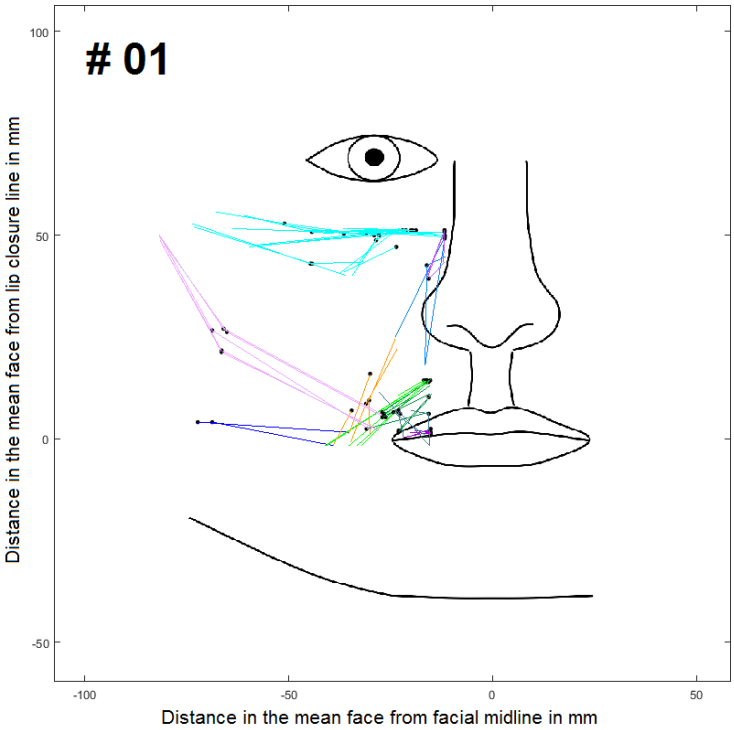
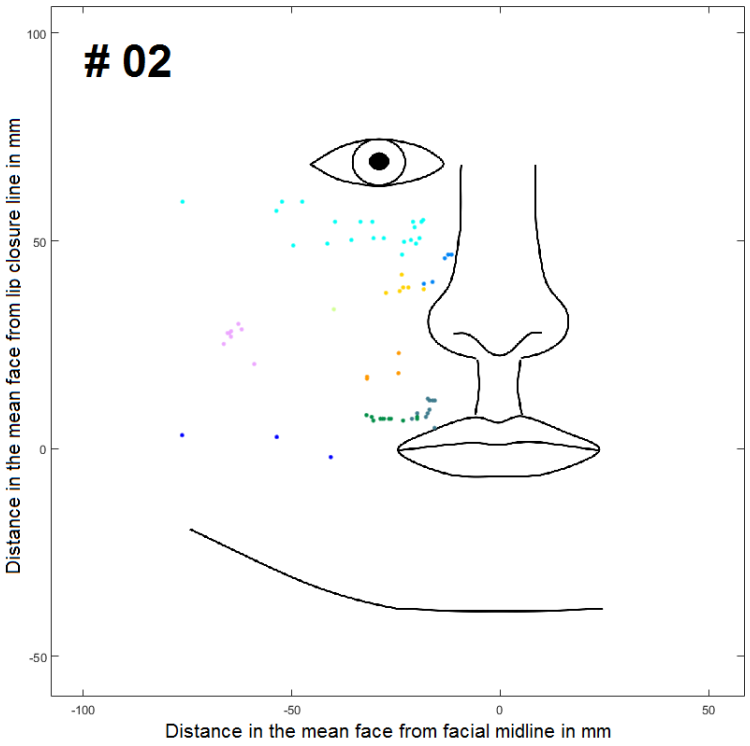


Figure 55: Subject # 01: normalized motor units without (A) and with (B) fiber orientation projected on the averaged face: OOC (turquois), ZYGmaj (light purple), ZYGmin (light green), BUC (dark blue), LAO (orange), LLS (yellow), LLSan (light blue), OORper (dark green), OORmar (dark purple), OORtan (grey), INC (light green) and NAS (pink).
High-density surface electromyography (HDsEMG) measurements of the midfacial muscles. Department of orthodontics, Ulm University, 2014.

A



B

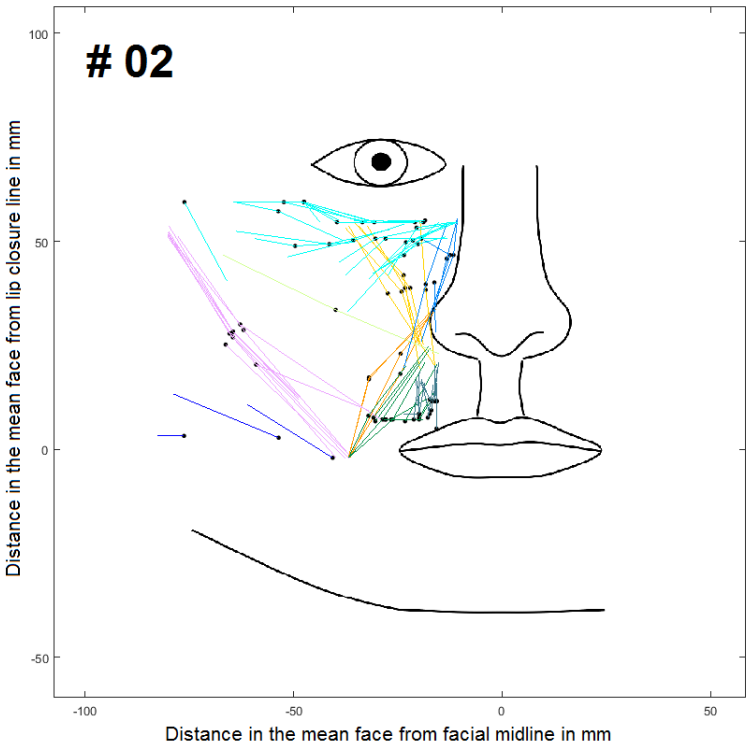
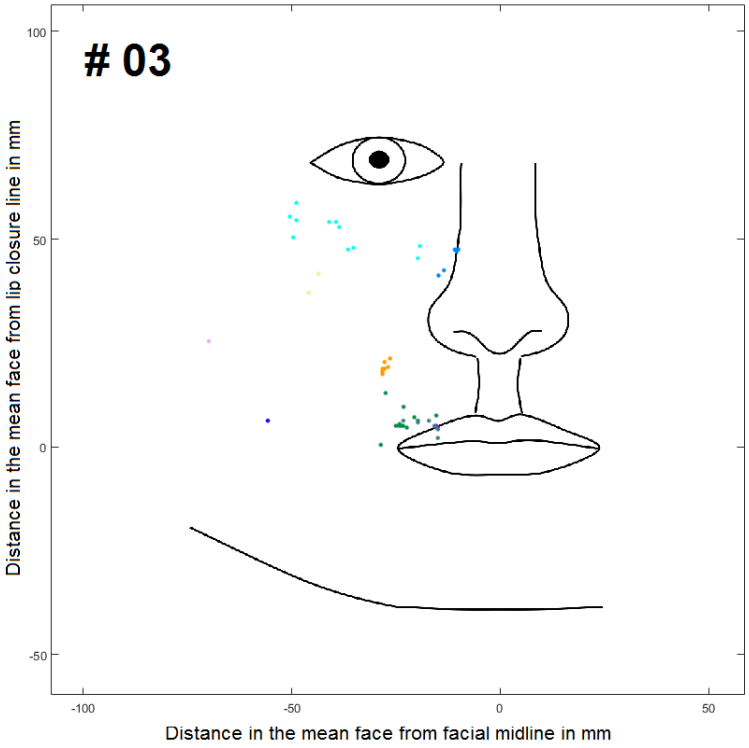


Figure 56: Subject # 02: normalized motor units without (A) and with (B) fiber orientation projected on the averaged face: OOC (turquois), ZYGmaj (light purple), ZYGmin (light green), BUC (dark blue), LAO (orange), LLS (yellow), LLSan (light blue), OORper (dark green), OORmar (dark purple), OORtan (grey), INC (light green) and NAS (pink).
High-density surface electromyography (HDsEMG) measurements of the midfacial muscles. Department of orthodontics, Ulm University, 2014.

A



B

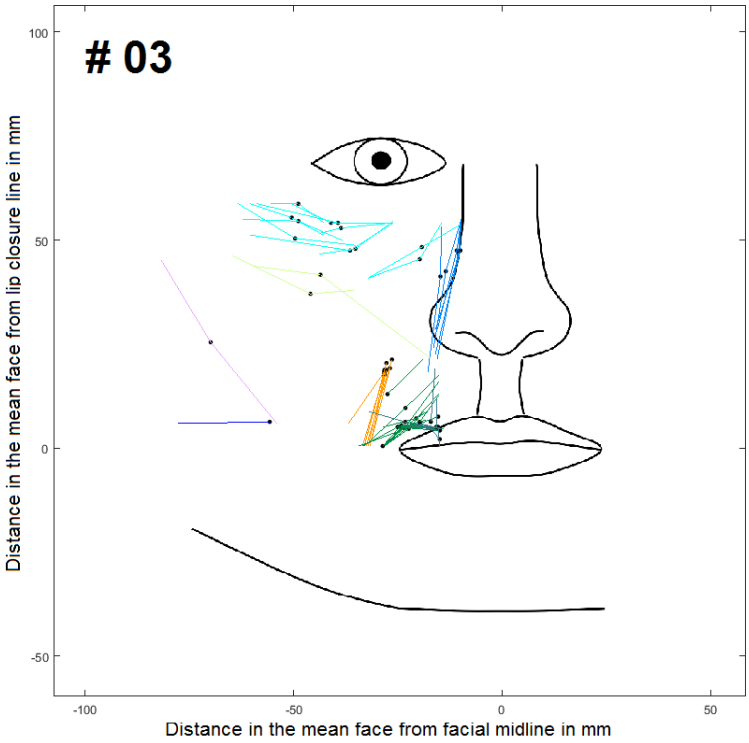
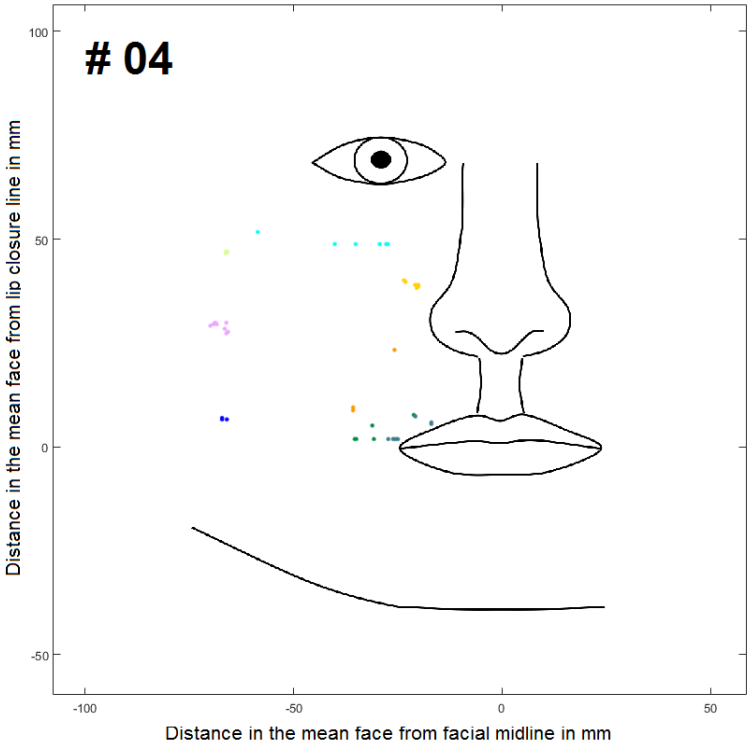


Figure 57: Subject # 03: normalized motor units without (A) and with (B) fiber orientation projected on the averaged face: OOC (turquois), ZYGmaj (light purple), ZYGmin (light green), BUC (dark blue), LAO (orange), LLS (yellow), LLSan (light blue), OORper (dark green), OORmar (dark purple), OORtan (grey), INC (light green) and NAS (pink).
High-density surface electromyography (HDsEMG) measurements of the midfacial muscles. Department of orthodontics, Ulm University, 2014.

A



B

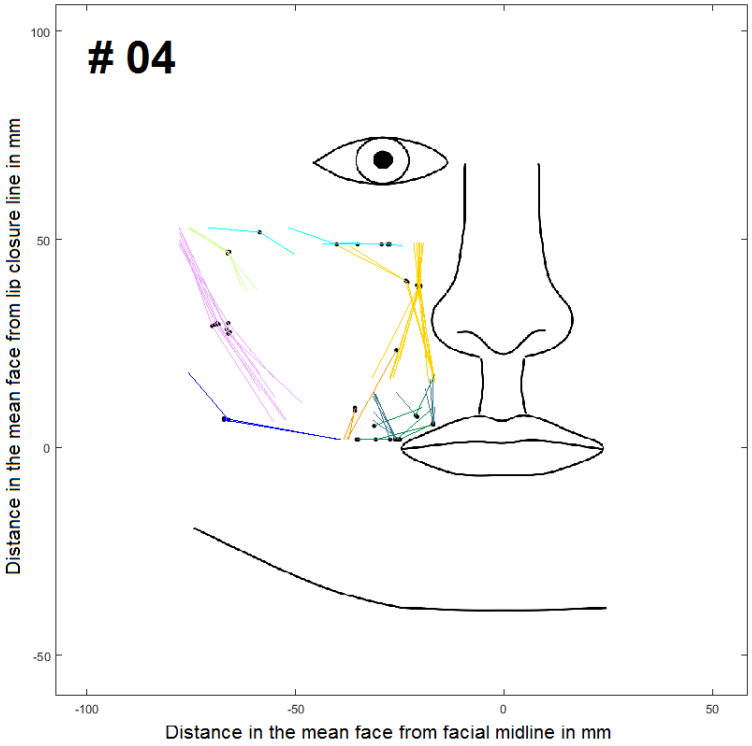
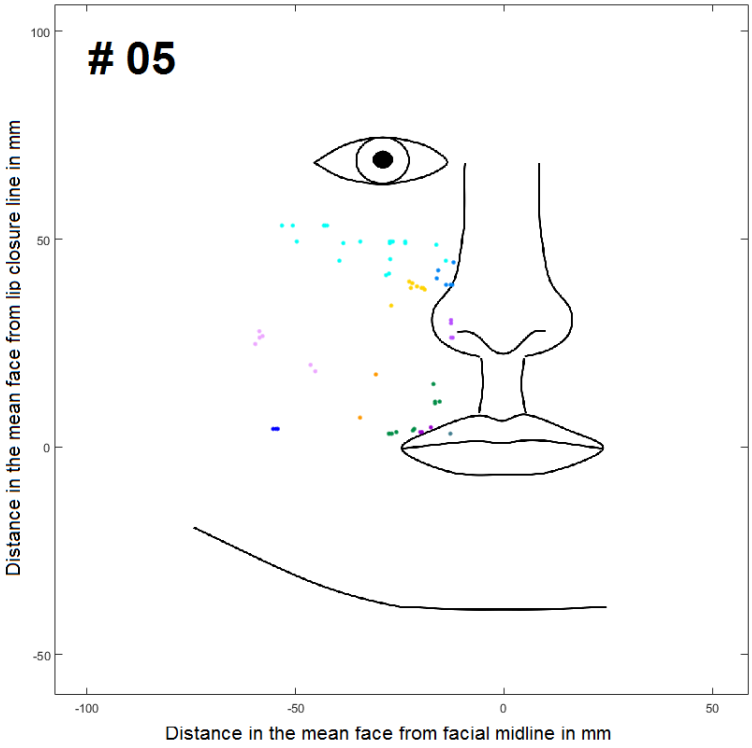


Figure 58: Subject # 04: normalized motor units without (A) and with (B) fiber orientation projected on the averaged face: OOC (turquois), ZYGmaj (light purple), ZYGmin (light green), BUC (dark blue), LAO (orange), LLS (yellow), LLSan (light blue), OORper (dark green), OORmar (dark purple), OORtan (grey), INC (light green) and NAS (pink).
High-density surface electromyography (HDsEMG) measurements of the midfacial muscles. Department of orthodontics, Ulm University, 2014.

A



B

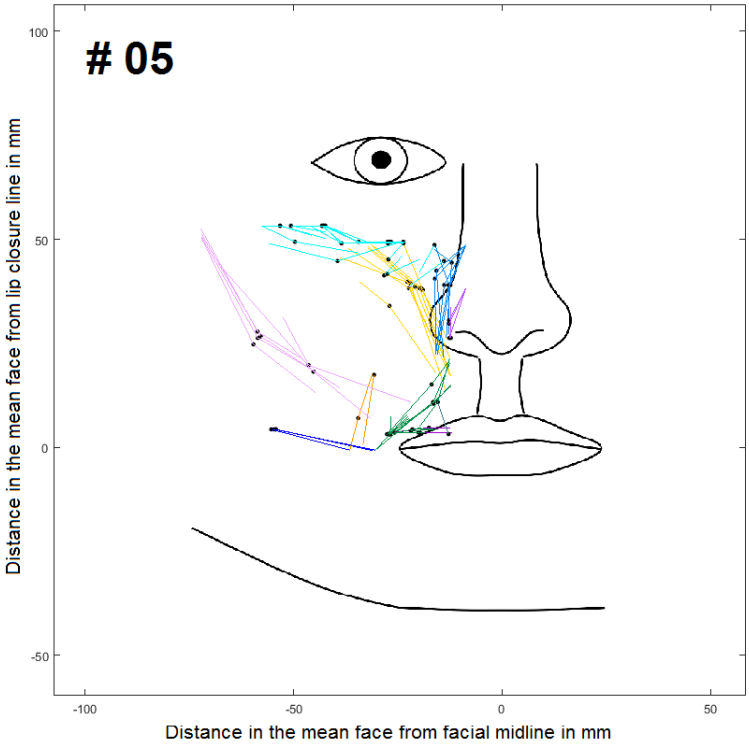
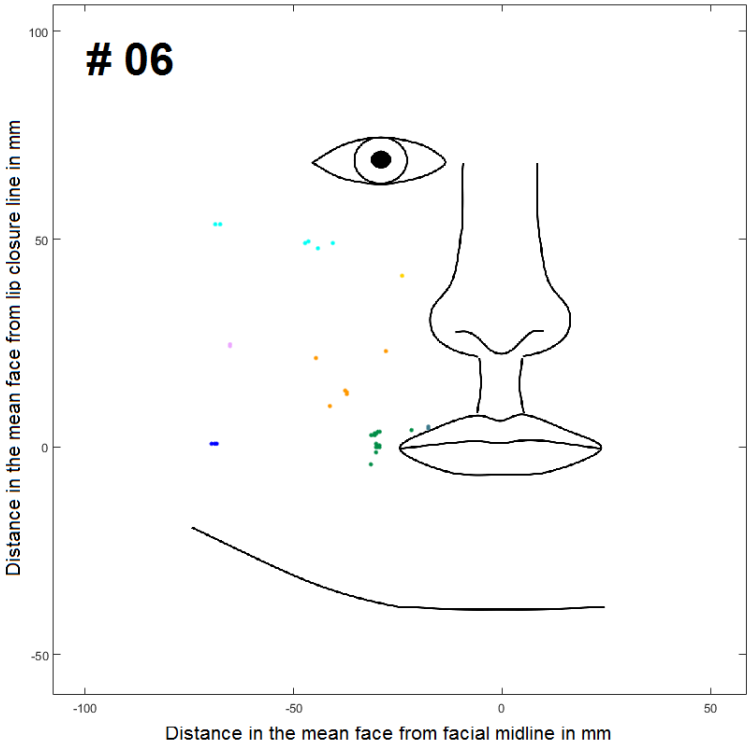


Figure 59: Subject # 05: normalized motor units without (A) and with (B) fiber orientation projected on the averaged face: OOC (turquois), ZYGmaj (light purple), ZYGmin (light green), BUC (dark blue), LAO (orange), LLS (yellow), LLSan (light blue), OORper (dark green), OORmar (dark purple), OORtan (grey), INC (light green) and NAS (pink).
High-density surface electromyography (HDsEMG) measurements of the midfacial muscles. Department of orthodontics, Ulm University, 2014.

A



B

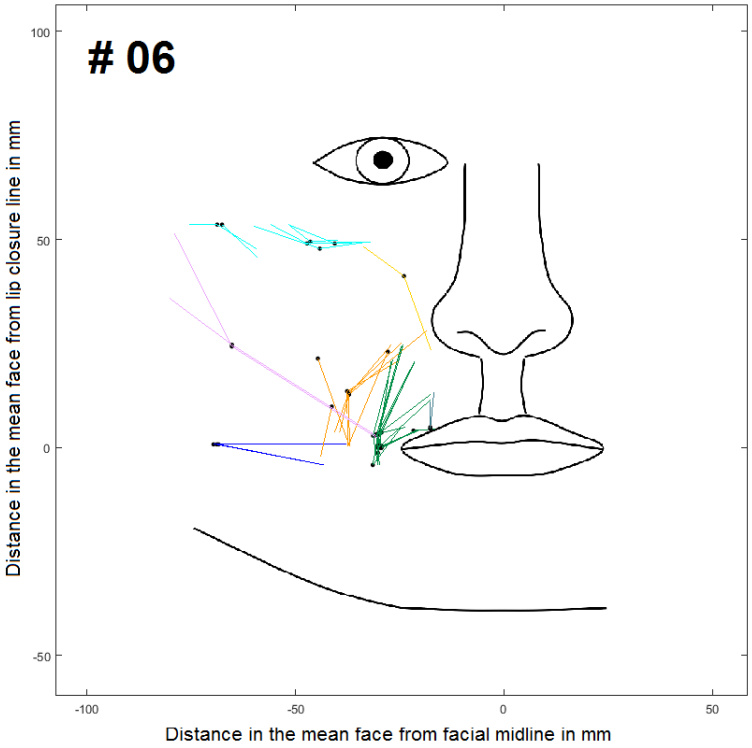
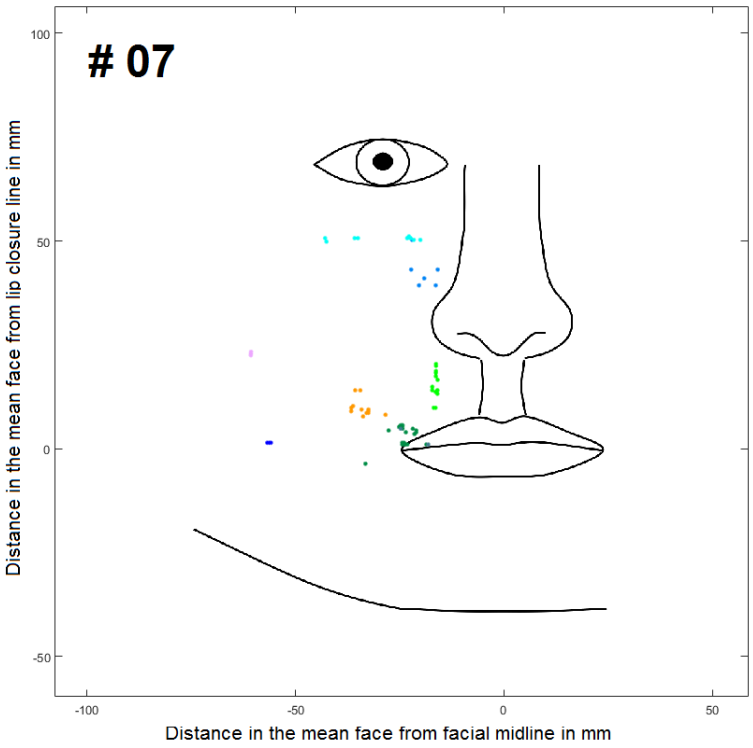


Figure 60: Subject # 06: normalized motor units without (A) and with (B) fiber orientation projected on the averaged face: OOC (turquois), ZYGmaj (light purple), ZYGmin (light green), BUC (dark blue), LAO (orange), LLS (yellow), LLSan (light blue), OORper (dark green), OORmar (dark purple), OORtan (grey), INC (light green) and NAS (pink).
High-density surface electromyography (HDsEMG) measurements of the midfacial muscles. Department of orthodontics, Ulm University, 2014.

A



B

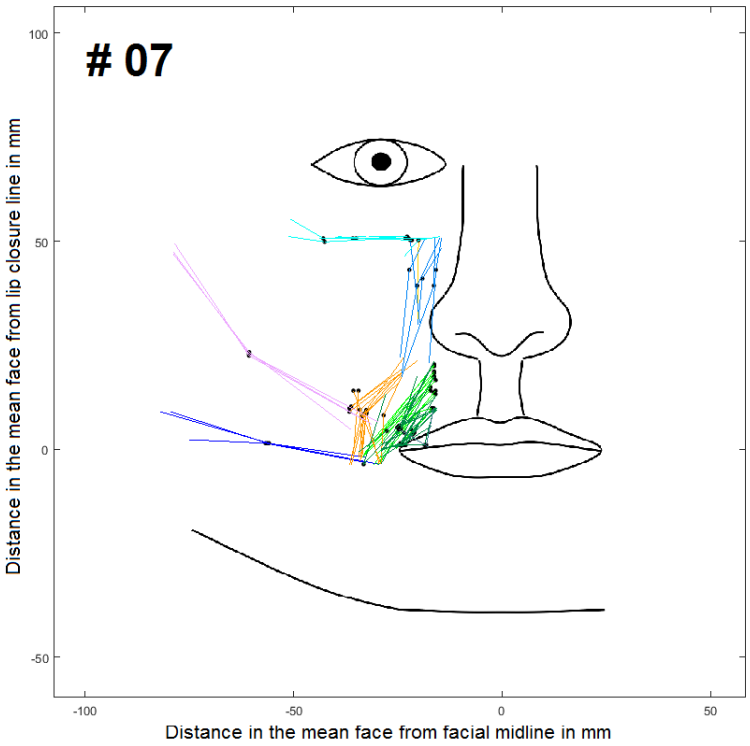
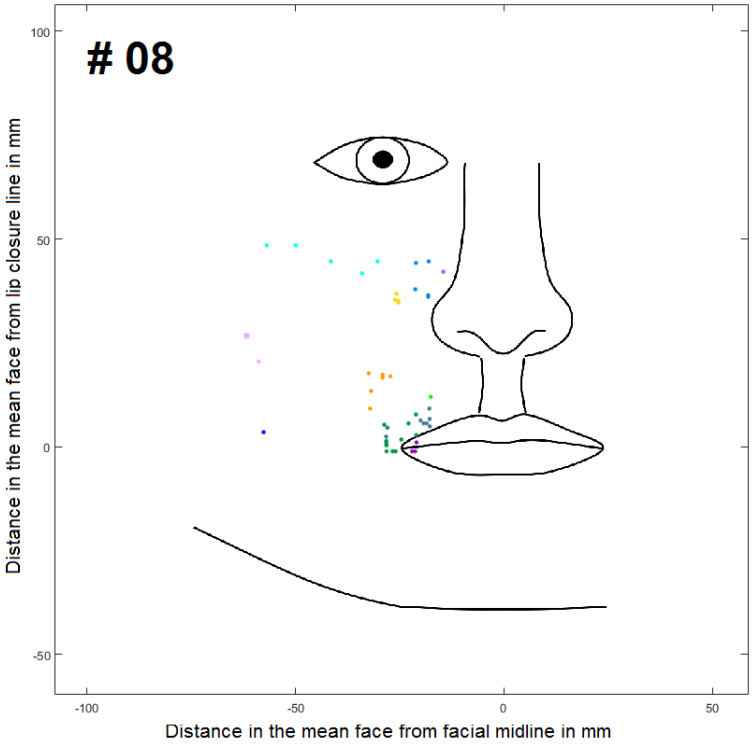


Figure 61: Subject # 07: normalized motor units without (A) and with (B) fiber orientation projected on the averaged face: OOC (turquois), ZYGmaj (light purple), ZYGmin (light green), BUC (dark blue), LAO (orange), LLS (yellow), LLSan (light blue), OORper (dark green), OORmar (dark purple), OORtan (grey), INC (light green) and NAS (pink).
High-density surface electromyography (HDsEMG) measurements of the midfacial muscles. Department of orthodontics, Ulm University, 2014.

A



B

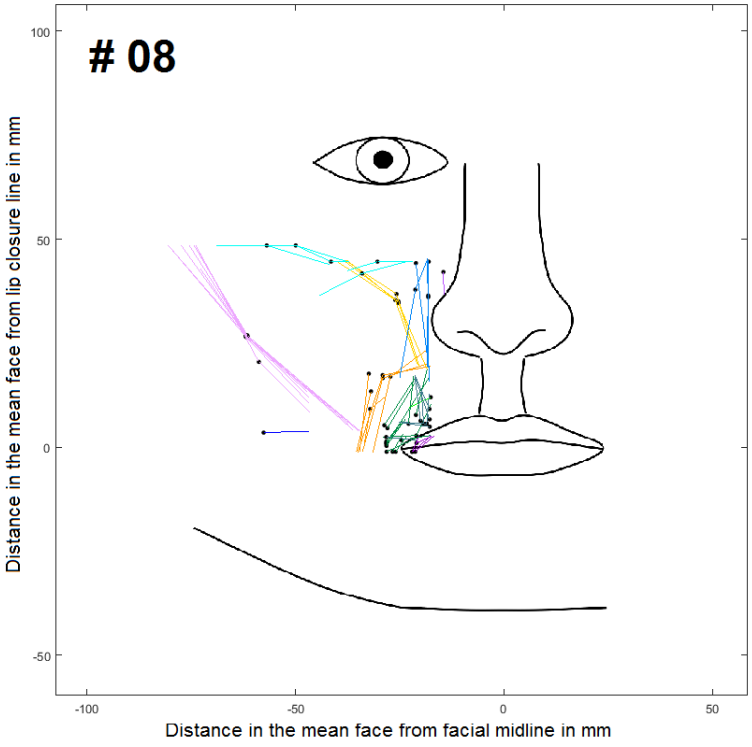
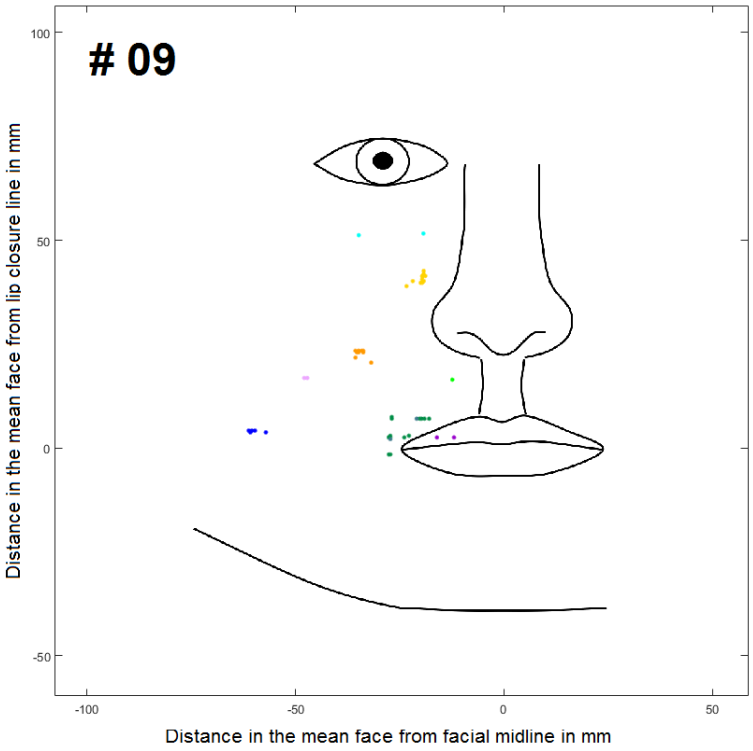


Figure 62: Subject # 08 normalized motor units without (A) and with (B) fiber orientation projected on the averaged face: OOC (turquois), ZYGmaj (light purple), ZYGmin (light green), BUC (dark blue), LAO (orange), LLS (yellow), LLSan (light blue), OORper (dark green), OORmar (dark purple), OORtan (grey), INC (light green) and NAS (pink).
High-density surface electromyography (HDsEMG) measurements of the midfacial muscles. Department of orthodontics, Ulm University, 2014.

A



B

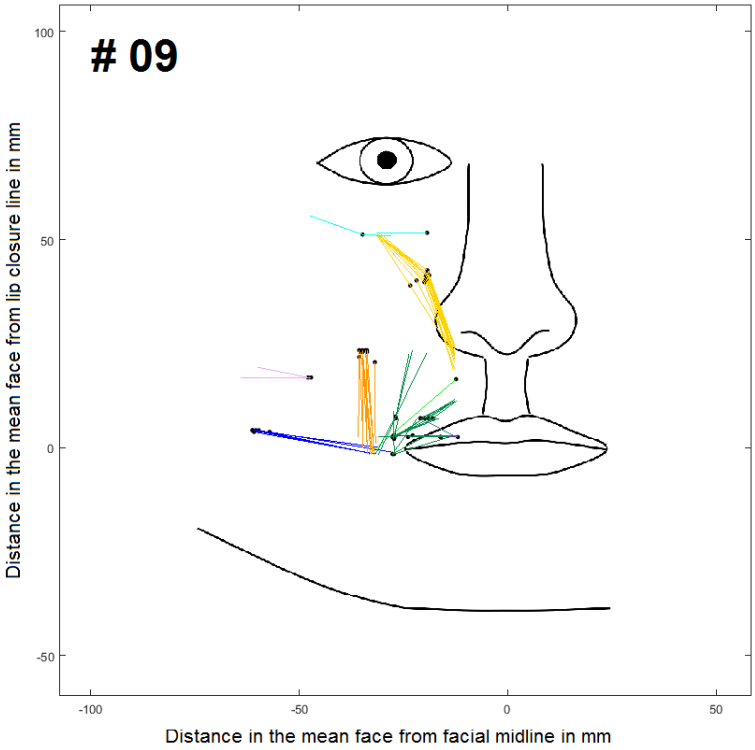
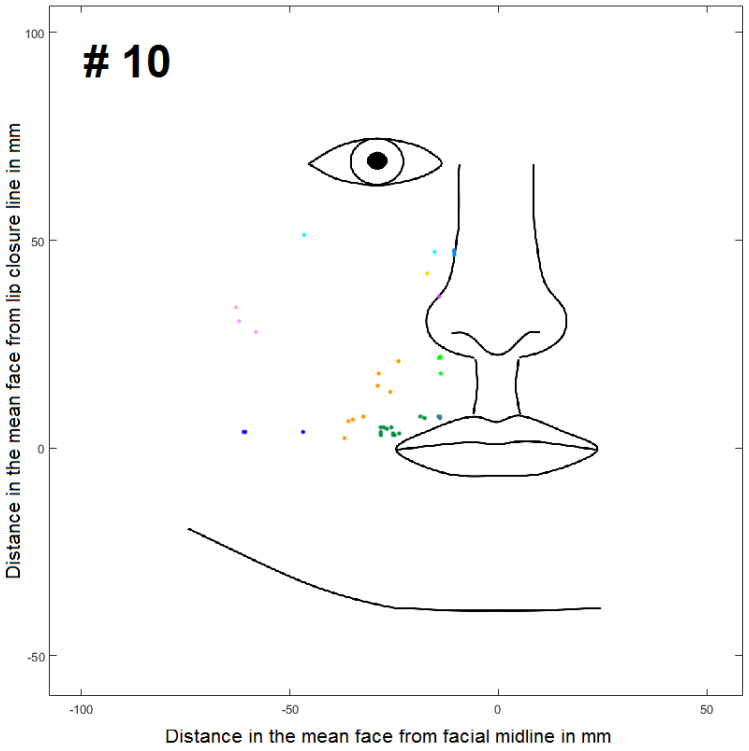


Figure 63: Subject # 09: normalized motor units without (A) and with (B) fiber orientation projected on the averaged face: OOC (turquois), ZYGmaj (light purple), ZYGmin (light green), BUC (dark blue), LAO (orange), LLS (yellow), LLSan (light blue), OORper (dark green), OORmar (dark purple), OORtan (grey), INC (light green) and NAS (pink).
High-density surface electromyography (HDsEMG) measurements of the midfacial muscles. Department of orthodontics, Ulm University, 2014.

A



B

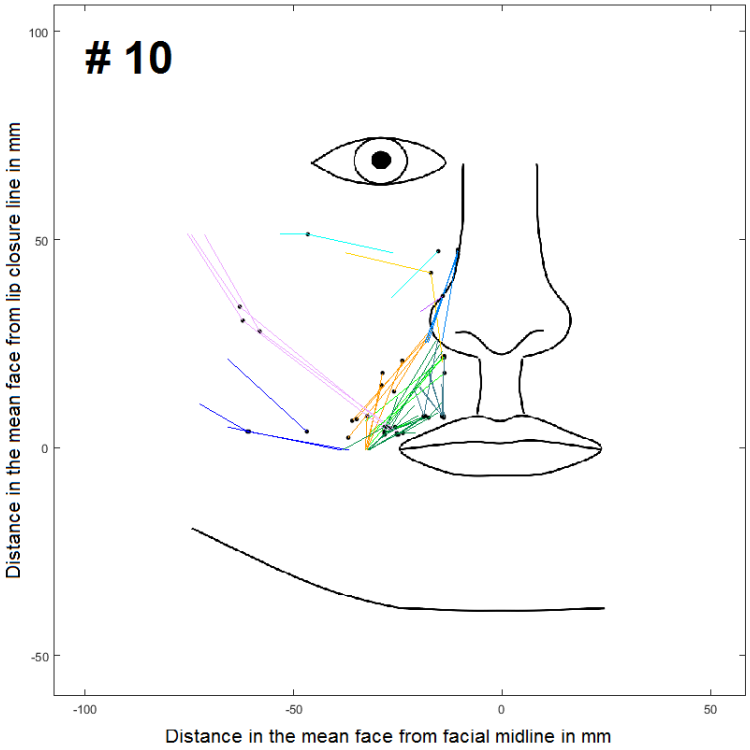
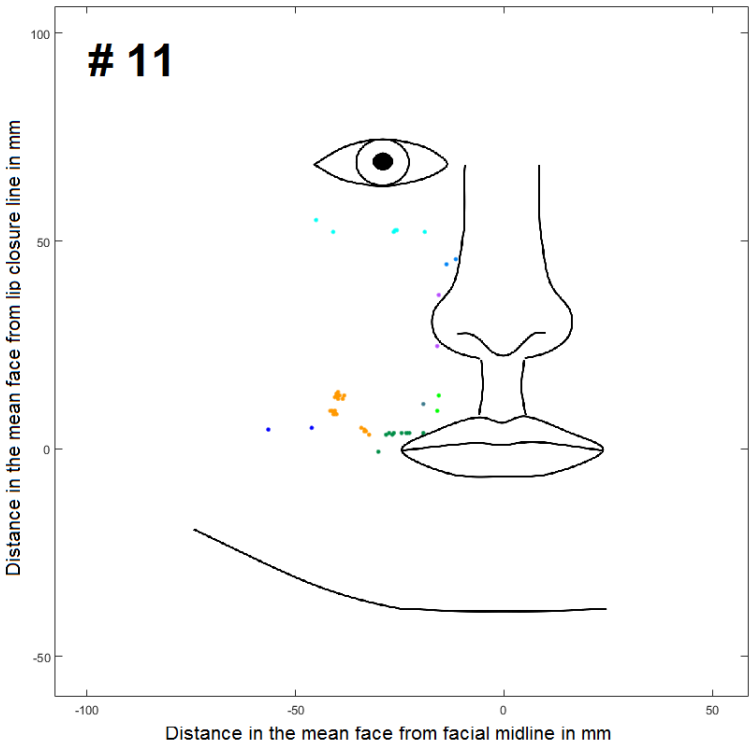


Figure 64: Subject # 10: normalized motor units without (A) and with (B) fiber orientation projected on the averaged face: OOC (turquois), ZYGmaj (light purple), ZYGmin (light green), BUC (dark blue), LAO (orange), LLS (yellow), LLSan (light blue), OORper (dark green), OORmar (dark purple), OORtan (grey), INC (light green) and NAS (pink).
High-density surface electromyography (HDsEMG) measurements of the midfacial muscles. Department of orthodontics, Ulm University, 2014.

A



B

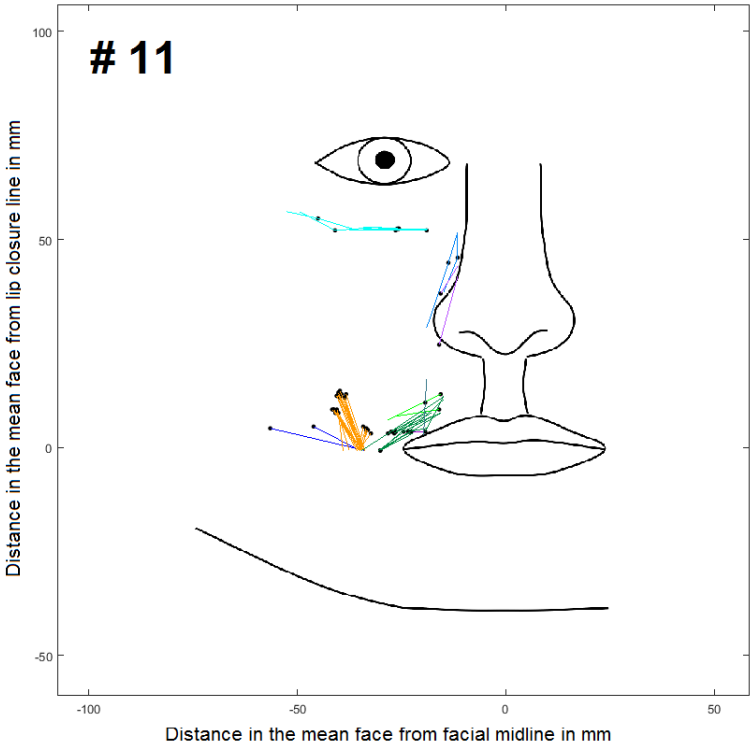
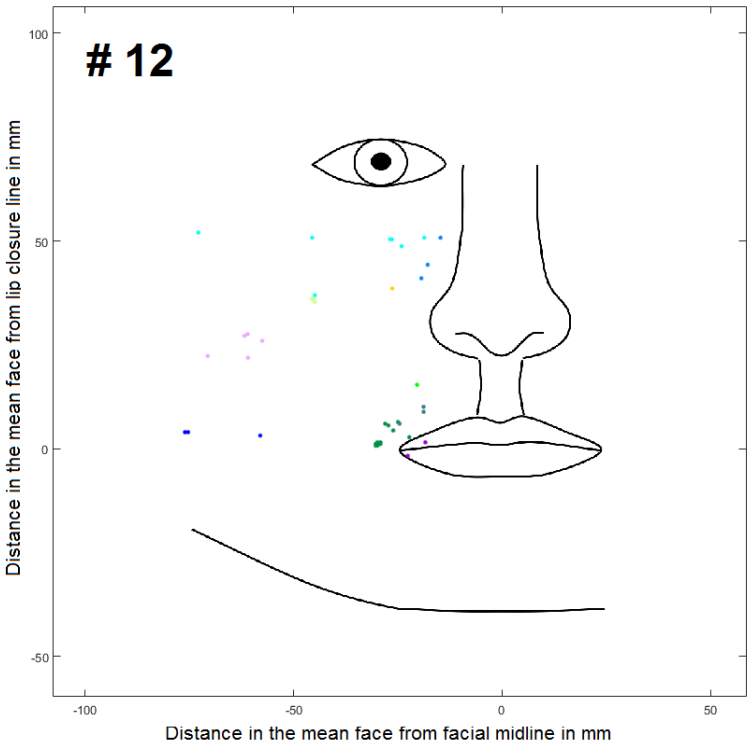


Figure 65: Subject # 11: normalized motor units without (A) and with (B) fiber orientation projected on the averaged face: OOC (turquois), ZYGmaj (light purple), ZYGmin (light green), BUC (dark blue), LAO (orange), LLS (yellow), LLSan (light blue), OORper (dark green), OORmar (dark purple), OORtan (grey), INC (light green) and NAS (pink).
High-density surface electromyography (HDsEMG) measurements of the midfacial muscles. Department of orthodontics, Ulm University, 2014.

A



B

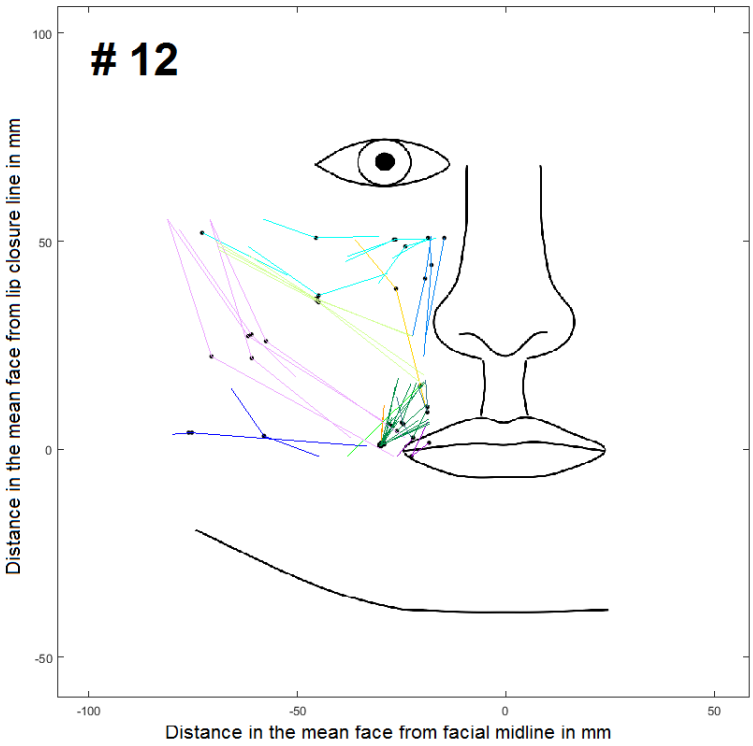
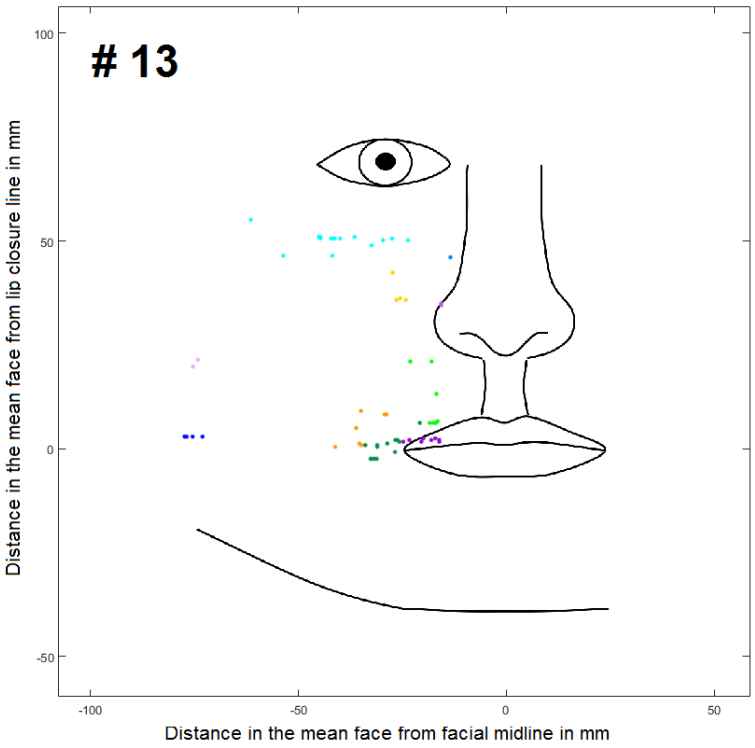


Figure 66: Subject # 12: normalized motor units without (A) and with (B) fiber orientation projected on the averaged face: OOC (turquois), ZYGmaj (light purple), ZYGmin (light green), BUC (dark blue), LAO (orange), LLS (yellow), LLSan (light blue), OORper (dark green), OORmar (dark purple), OORtan (grey), INC (light green) and NAS (pink).
High-density surface electromyography (HDsEMG) measurements of the midfacial muscles. Department of orthodontics, Ulm University, 2014.

A



B

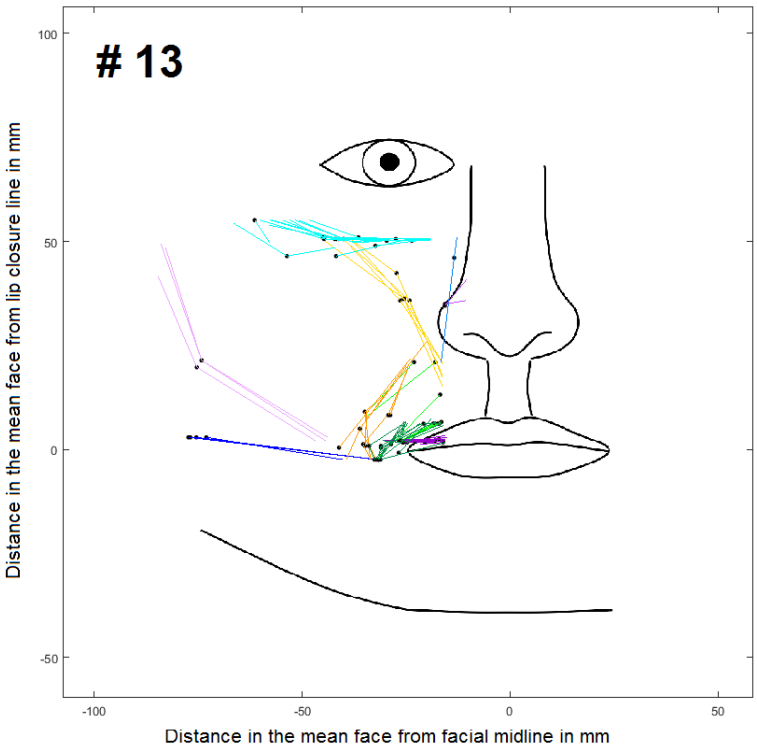
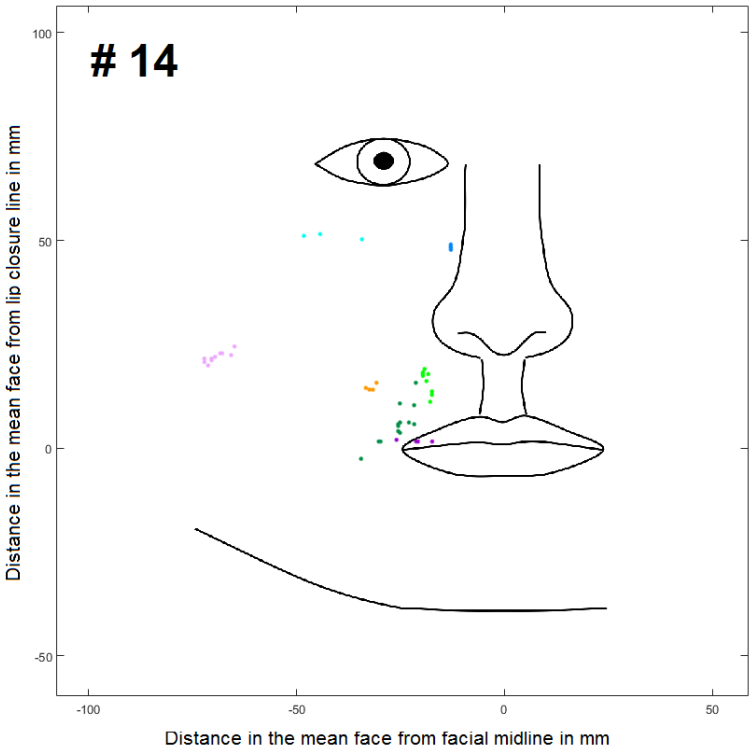


Figure 67: Subject # 13: normalized motor units without (A) and with (B) fiber orientation projected on the averaged face: OOC (turquois), ZYGmaj (light purple), ZYGmin (light green), BUC (dark blue), LAO (orange), LLS (yellow), LLSan (light blue), OORper (dark green), OORmar (dark purple), OORtan (grey), INC (light green) and NAS (pink).
High-density surface electromyography (HDsEMG) measurements of the midfacial muscles. Department of orthodontics, Ulm University, 2014.

A



B

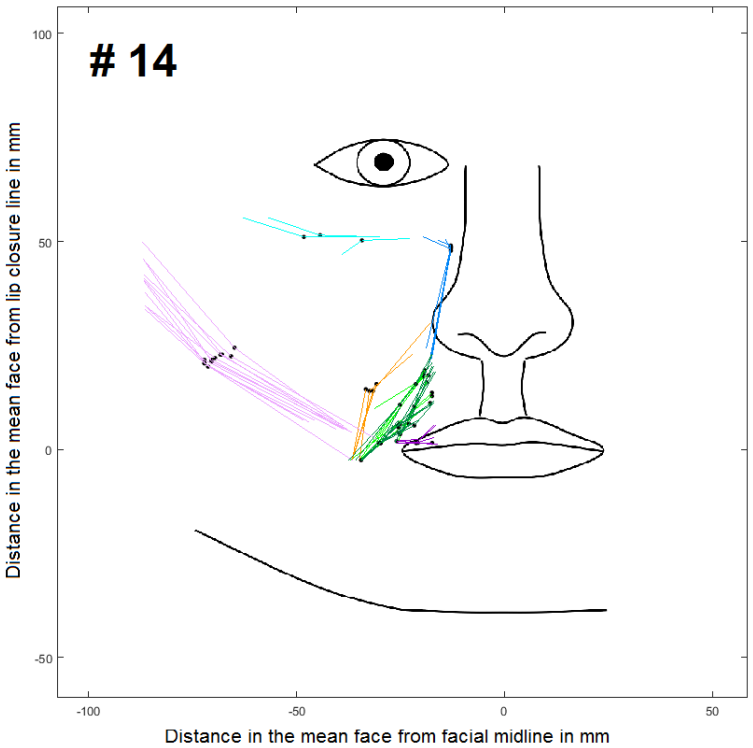
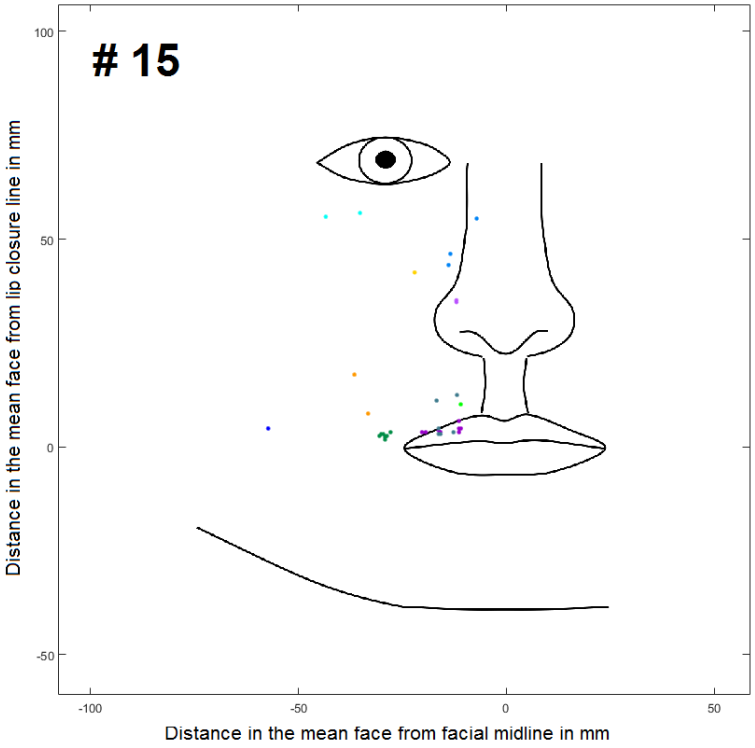


Figure 68: Subject # 14: normalized motor units without (A) and with (B) fiber orientation projected on the averaged face: OOC (turquois), ZYGmaj (light purple), ZYGmin (light green), BUC (dark blue), LAO (orange), LLS (yellow), LLSan (light blue), OORper (dark green), OORmar (dark purple), OORtan (grey), INC (light green) and NAS (pink).
High-density surface electromyography (HDsEMG) measurements of the midfacial muscles. Department of orthodontics, Ulm University, 2014.

A



B

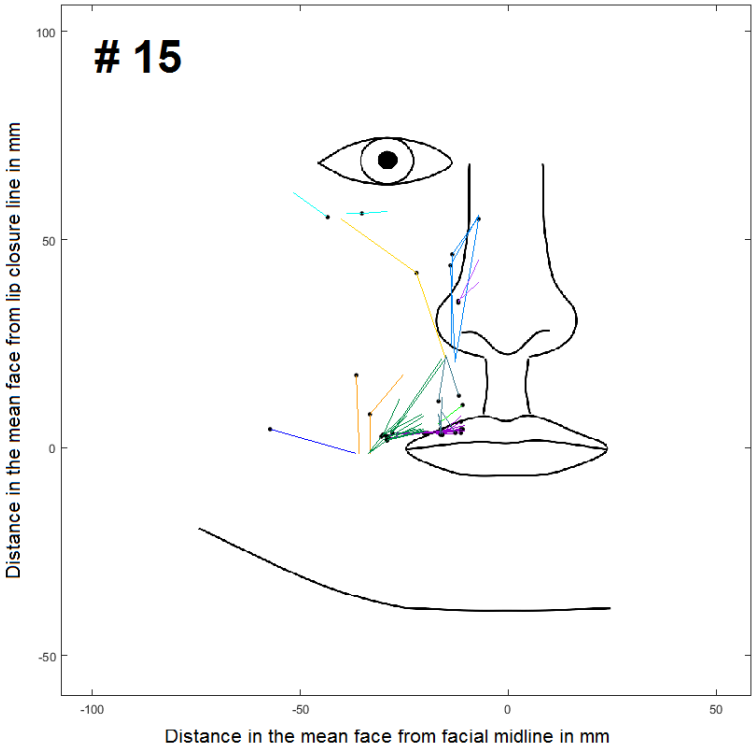
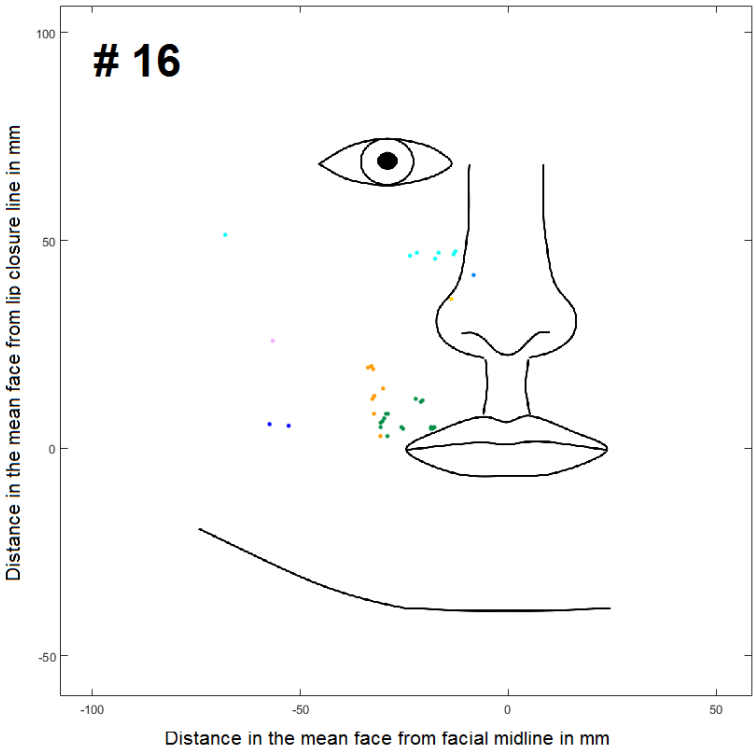


Figure 69: Subject # 15: normalized motor units without (A) and with (B) fiber orientation projected on the averaged face: OOC (turquois), ZYGmaj (light purple), ZYGmin (light green), BUC (dark blue), LAO (orange), LLS (yellow), LLSan (light blue), OORper (dark green), OORmar (dark purple), OORtan (grey), INC (light green) and NAS (pink).
High-density surface electromyography (HDsEMG) measurements of the midfacial muscles. Department of orthodontics, Ulm University, 2014.

A



B

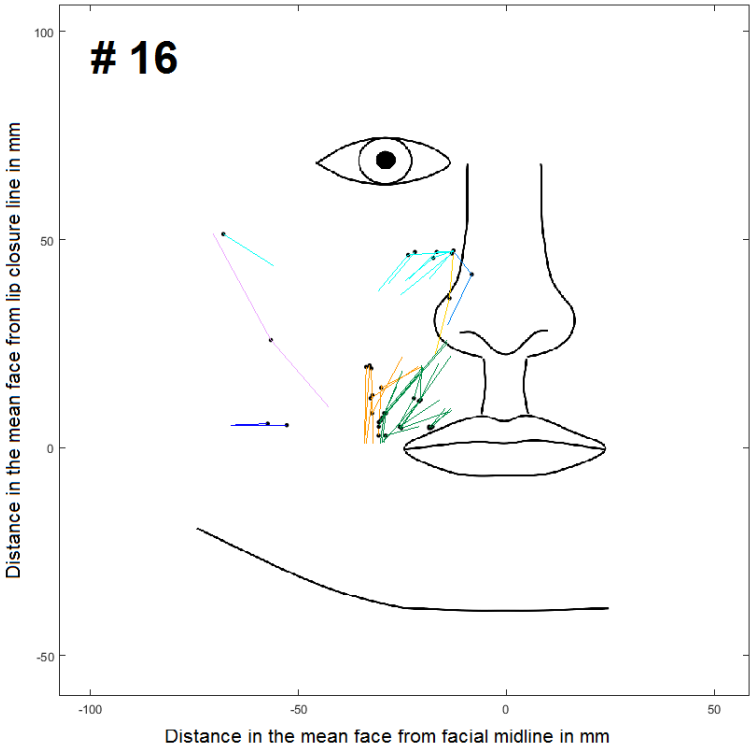


Figure 70: Subject # 16: normalized motor units without (A) and with (B) fiber orientation projected on the averaged face: OOC (turquois), ZYGmaj (light purple), ZYGmin (light green), BUC (dark blue), LAO (orange), LLS (yellow), LLSan (light blue), OORper (dark green), OORmar (dark purple), OORtan (grey), INC (light green) and NAS (pink).
High-density surface electromyography (HDsEMG) measurements of the midfacial muscles. Department of orthodontics, Ulm University, 2014.

Curriculum vitae

Der Lebenslauf wurde aus Gründen des Datenschutzes entfernt.